UNIVERSITÀ DEGLI STUDI DI NAPOLI "FEDERICO II"

PhD Thesis

"Angiogenesis and innervation during the integration of engineered skin substitutes"

Coordinator	Author	Tutor	Co-tutor
Prof Giuseppe Cringoli	Dr Isabella Mavaro	Prof Rosita Diana	Prof Chiara Attanasio

To rise up stronger than before.

Contents

Contents

Acknowledgments

I wish to express my deepest gratitude to my co-tutor, Professor Chiara Attanasio for support, guidance, patience. She taught me how to overcome difficulties in all research and non-research related challenges and she has been so precious to me for pushing me not to give up.

I am also grateful to Professor Paolo de Girolamo for his guidance since the very beginning of my PhD.

I'm truly thankful to Dr Antonio Palladino who in addition to being an important point of reference who has patiently helped me to learn numerous laboratory techniques he has been a precious friend. I'm also thankful to Carmela Pizzoleo for her support, for her so kindly way to welcome me into the new group and also for all our coffee-moments to find serenity and calm.

My PhD experience would not have been so enriching and meaningful without the constant support and encouragement of Claudia Mazio. With her incredible kindness, patience and helpfulness she has guided me until the end of this long experience.

I'm thankful to Professor Paolo Antonio Netti for hosting me in the IIT of Naples with his extreme kindness and helpfulness.

I'm grateful to Professor Andrea Banfi for giving me the opportunity to follow the activities of his research group of the Department of Biomedicine in the University of Basilea.

I'm also thankful to the research group guided by Luigia Cristino of the CNR of Pozzuoli where I started my PhD experience.

Thanks to my friends and colleagues Lea Tunisi and Alba Clara Fernandez with whom I have shared many crazy moments, I wanted to share also more time with you.

Acknowledgments

Thanks to my friends for having believed in me and above all for having supported me especially in this last period.

I'm so grateful to my family for supporting me and for making possible the realization of my entire study path. I hope to make you always proud of me. And thanks to my brother Alessandro, you give me incredible strength in every day of my life, through your big blue eyes.

I want to thank my half Gennaro. Thank you for your constant encouragement, love, comprehension, support.

Eleonora Maria, I'm so grateful to you for all the somersaults you do in my belly while I'm writing these aknowledgments. I love you and can't wait to meet you.

Abbreviations

ADSCs Adipose-derived stromal cells

ANG Angiogenin

ASCs Adipose-derived stem cells

BDNF Brain derived neurotrophic factor

CEA Cultured Epidermal Autograft

CGRP Calcitonin gene–related peptide

CSS Cultured Skin Substitutes

DEJ Dermal epidermal junction

DRGs Dorsal Root Ganglia

ECM Extracellular matrix

FGF Fibroblast Growth Factor

GDNF Glial-derived neurotrophic factor

HDE Human dermis equivalent

HDFs Human dermal fibrblasts

HDMEC Human dermal microvascular endothelial cells

HIF-1A Hypoxia inducible factor 1-alpha

HUVECs Human umbilical vein endothelial cells

Abbreviations

MCs	Meissner corpuscles
MMPs	Metalloproteinases
NGF	Nerve growth factor
NIRS	Near Infrared Spectroscopy
NT3	Neurotrophin 3
NTs	Neurotrophins
OCT	Optical Coherence Tomography...
PDGF	Platelet-derived growth factor
PVD	Pre-Vascularized Dermis
SP	Substance P
SVF	Stromal vascular fraction
TE	Tissue Engineering
TGFα	Trasforming growth factor α
TGFβ	Trasforming growth factor β
TGN	Trans-Golgi network
TRPV1	Vanilloid thermoreceptors
VEGF	Vascular Endothelial Growth Factor

Abbreviations

VWF	von Willebrand factor
SHG	Second harmonic generation
MMP	Multiphoton microscopy

Figures

Figures

Tables

Abstract

Numerous advances have been made in the field of skin tissue engineering in recent years to overcome skin injuries, burns and pathologies. Most of skin substitutes are exogenous matrices requiring the contribution of both host fibroblasts and endothelial cells and, therefore, a long time to become functional after implantation. In view of this, here we investigate the potential of a specific pre-vascularized dermis (PVD) obtained by seeding freshly isolated fibroblasts onto gelatin microbeads and adding, at a certain culture time, endothelial cells (HUVECs) [1]. More in detail, we implanted our engineered skin on the back of nu/nu mice in a full thickness skin defect model which, respect to the subcutaneous pocket we previously experienced, is more functional for both general and wound healing applications.

At different timepoints (3, 7, 14, 21 and 42 days) we retrieved our skin biohybrids and analysed them by histology and immunofluorescence. Animal studies were performed following the guidelines of EU (2010/63/EU).

Our main objective is to study the behaviour and the degree of integration of our skin substitute in the host organism. First of all, an appreciable integration of a pre-vascularized substitute with host tissue results in a fast anastomosis between the two vascular networks. However, since integration is a complex process there are other aspects which have to be considered. For example, a major limitation of skin substitutes in clinical application is to mimic the physiological sensitivity of the host skin.

Regarding vascularization, we looked for the expression of the lectins Griffonia Semplicifolia and Ulex Europaeus Agglutinin I (UEA I) to mark murine and human vessels, respectively. We noticed, starting from day 14

onwards, the onset of numerous anastomosis between the two vascular networks (human and murine). Afterwards, from the innervation standpoint, we looked at the expression of Neurofilament-M, PGP9.5, NGF and BDNF along with the corresponding receptors TrkA and TrkB. Interestingly, we noticed a partial reinnervation of our skin substitutes already 42 days after implantation through the appreciable expression of PGP9.5, a promising result in comparison with other skin substitutes where the reinnervation is observed not earlier than after 8 weeks of implantation [2]. Therefore, since neurotrophins guide fibroblasts differentiation into myofibroblasts, also increasing skin tensile strength, we analysed the variation of the Young Modulus of our samples via indentation test. Moreover, to better frame the expression of our markers we performed a quantitative analysis through PCR.

In conclusion, our skin substitute, when implanted in a full thickness skin defect model, shows an earlier vascularization and innervation time compared to other substitutes described in the literature leading us to investigate the connection between vascularization and innervation during tissue development and maturation.

During the last decades, several studies have been carried out aiming to produce an adequate engineered skin substitute. Tissue engineering (TE) is a precious alternative to the standard therapeutic approaches in solving significant issues linked to wound healing and organ repair (Pattanaik et al., 2019).

Skin substitutes are also involved in the replacement of damaged skin after burns, surgery or in case of pathologies (Sharma, 2019).

The skin is the largest organ of the body, with an area of around 2 m^2 in humans, which accomplishes different essential roles such as protection of the underlying tissues from pathogens and mechanical shocks, thermal tactile and dolorific sensitivity, lipid reserve and site of D^3 vitamin synthesis (Przekora, 2020).

The application of tissue engineering principles in the field of skin substitutes have changed over time. Already in 2004, complex constructs made of different layers of cells have been produced starting from simple epidermal sheets (Auger et al., 2004).

Focusing on physiological processes such as vascularization and innervation is of basic importance to improve the quality of the most important features of engineered skin (Biedermann et al., 2016).

Therefore, the first skin substitutes were representative only of the epidermal component and were obtained from cultures of keratinocytes after enzymatic separation of epidermis from dermis. Epithelial substitutes have been widely used in the clinical field but for the replacement of full-thickness injuries it is necessary to replace both the epidermal and the dermal components. On the other hand, to limit scar formation and wound contraction at the site of implantation the addition of the dermal compartment to the epidermis engineered tissue is essential (Shevchenco et al., 2010; Groeber et al., 2011).

Also, it has to be considered that “bioengineered skins” can be both cellular and acellular. For example, Integra® Dermal Regeneration Template (Integra Life Science Corporation, Plainsboro, NJ, USA) is an acellular construct consisting in a double-layer membrane system for skin replacement designed for the treatment of full-thickness lesions in a two-step procedure. More in detail, a temporary epidermis made of a thin layer

of silicone controls the loss of moisture from the wound on the top of the matrix which is composed of cross-linked fibres. The inner layer is a scaffold able to stimulate the regeneration of dermal skin fibroblasts. When the dermal compartment has regenerated the silicon outer layer is replaced with an epidermal skin sheet (Shahrokhi et al., 2014).

Apligraf® (Organogenesis, Canton, MA) is a good example of cellular and allogenic skin substitute being composed of human foreskin fibroblasts and keratinocytes cultured in a matrix of bovine collagen. Apligraf was the first skin substitute applied to promote tissue recovery in case of ulcers (Eaglstein et al., 1995). Unfortunately, these construct present numerous limitations like reduced vascularization, improper scarring, failure to integrate with the host tissue, low mechanical resistance and immune rejection (Shevchenco et al., 2010; Shaghayegh et al., 2020).

The main concern related to full-thickness skin substitutes is the lack of vascularization. To overcome the long time needed for the constructs to be vascularized in vivo, different potential solutions can be applied: 1) the pre-treatment of the tissue with growth factors; 2) the design of the tissue with specific architectures able to guide angiogenesis; 3) the creation of a pre-vascularized tissue (Brudno et al., 2013; Mastrullo et al.,2020). This latter solution implies the *in vitro* co-culture of endothelial cells with stromal cells within a 3D matrix to obtain a capillary network. In 2005 Tremblay and co-workers demonstrated that some pre-vascularized constructs were able to show anastomosis with the host vasculature in only four days (Tremblay et al., 2005) while a non pre-vascularized construct needed longer times to be vascularized *de novo*. The majority of skin substitutes presents exogenous matrices, like those of animal origin, which are able to degrade over the time. Mazio et al., in 2019 obtained a Pre-Vascularized Dermis (PVD) starting from a human dermis equivalent (HDE), strengthened by the presence of a collagen-rich matrix self-produced by primary dermal fibroblasts and, therefore, totally endogenous. After observing the *in vitro* capillary network formation, the authors implanted the construct in a mouse subcutaneous pocket model showing the onset of functional anastomosis between the implanted skin and the host vasculature in a single week (Mazio

et al, 2019). However, although these significant advances, the loss of sensitivity in the injured areas still remains an unsolved, crucial issue.

Skin is innervated by long axons originating from cell bodies located in the dorsal root ganglia (DRGs). These free nerve fibers end near blood vessels, sweat glands and hair follicles (Hendrix et al, 2008; Peters et al, 2006) innervating the dermis and the base of the epidermis (Misery, 2005; Misery, 2007). Dermis, through the cell-cell and cell-extracellular matrix (ECM) cross-talks, guides these axons to the sensory system of the epidermis represented especially by Merkel cells (Denda, 2003; Martorina et al, 2017). Roggenkamp et al., in 2013 produced a construct composed of dermal fibroblasts and neurons seeded in two different collagen gels covered by air-exposed keratinocytes mimicking the epidermis. After 12 days, the authors observed the free fibres within the dermis as well as into the basal layer of the epidermis (Roggenkamp et al, 2013).

In 2019, Martorina et al. also developed an *in vitro* model of engineered skin seeded with cells isolated from the DRGs. Beyond the finding of a positive signal for the Neurofilament-M both in the dermis and in the basal layer of the epidermis the authors demonstrated the sensitivity of their construct by a topical administration of capsaicin on the top of the epidermis. Since a nervous stimulus involves a change in intracellular calcium concentration, they quantified the calcium currents obtained from the different Ca++ concentrations in their model DRGs (Martorina et al, 2019). Moving on to in vivo reinnervation of skin substitutes, some authors focused their research on the invasion of the engineered construct by host nervous fibres after implantation.

The most common hindrance reported in the studies performed over the last decades is the very long time required for innervation. In general, in the skin, there are many unmyelinated fibres devoted to the slow conduction of pain signals respect to the myelinated ones devoted to the fast conduction of thermal sensation and mechanotransduction (Julius and Basbaum, 2001; Biedermann et al, 2016).

Biedermann et al., in 2013 demonstrated in a rat full thickness skin defect model, an appreciable reinnervation of their skin substitute in 8-10 weeks (Biedermann et al, 2013; Biedermann et al, 2016).

Despite these significant advances, the main focus remains to obtain a relatively fast reinnervation of the skin substitute which would ensure the almost total recovery of tissue sensitivity in skin implanted patients.

Arasteh S, Khanjani S, Golshahi H, Mobini S, Jahed MT, Heidari-Vala H, Edalatkhah H, Kazemnejad S, 2020. Efficient Wound Healing Using a Synthetic Nanofibrous Bilayer Skin Substitute in Murine Model. journal of surgical research (245) 31-44.

Auger FA, Berthod F, Moulin V, Pouliot R, Germain L, 2004. Tissue-engineered skin substitutes: from in vitro constructs to in vivo applications. Biotechnol. Appl. Biochem. 39, 263–275.

Biedermann T, Bo¨ttcher-Haberzeth S, Klar AS, Pontiggia L, Schiestl C, Meuli-Simmen C, Reichmann E, Meuli M, 2013. Rebuild, restore, reinnervate: do human tissue engineered dermo-epidermal skin analogs attract host nerve fibers for innervation? Pediatr Surg Int 29:71–78.

Biedermann T, Klar AS, Bo¨ttcher-Haberzeth S, Reichmann E, Meuli M, 2016. Myelinated and unmyelinated nerve fibers reinnervate tissue engineered dermo-epidermal human skin analogs in an in vivo model. Pediatr Surg Int.

Brudno Y, Ennett-Sheparda AB, Chena RR, Aizenbergb M, Mooneya DJ, 2013. Enhancing Microvascular Formation And Vessel Maturation Through Temporal Control Over Multiple Pro-Angiogenic And Pro-Maturation Factors. Biomaterials 34(36).

Denda M, Tomitaka A, Akamatsu H, Matsunaga K, 2003. Altered distribution of calcium in facial epidermis of aged adults. J Invest Dermatol 121(6):1557-8.

Eaglstein WH, Iriondo M, Laszlo K, 1995. A composite skin substitute (graftskin) for surgical wounds. A clinical experience. Dermatol Surg 21(10):839-43.

Groeber F, Holeiter M, Hampel M, Hinderer S, Schenke-Layland K, 2011. Skin tissue engineering — In vivo and in vitro applications. Advanced Drug Delivery Reviews 128, 352–366.

Hendrix S, Picker B, Liezmann C, Peters EMJ, 2008. Skin and hair follicle innervation in experimental models: a guide for the exact and reproducible evaluation of neuronal plasticity. Exp Dermatol 17(3):214-27.

Julius D, Basbaum AI, 2001. Molecular mechanisms of nociception. Nature 413(6852):203-10.

Martorina F, Casale C, Urciuolo F, Netti PA, Imparato G, 2017. In vitro activation of the neuro-transduction mechanism in sensitive organotypic human skin model. Biomaterials 113:217-229.

Mastrullo V, Cathery W, Velliou E, Madeddu P, Campagnolo P, 2020. Angiogenesis in Tissue Engineering: As Nature Intended? Front Bioeng Biotechnol. 20; 8:188.

Mazio C, Casale C, Imparato G, Urciuolo F, Attanasio C, De Gregorio M, Rescigno F, Netti PA, 2019. Pre-vascularized dermis model for fast and functional anastomosis with host vasculature. Biomaterials 192:159-170.

Misery L, 2005. The interactions between skin and nervous system. Giornale Italiano di Dermatologia e Venereologia 140, 677-684.

Misery L, 2007. Innervazione cutanea. EMC - Medicina Riabilitativa 14, 1-4.

Pattanaik S, Arbra C, Bainbridge H, Dennis SG, Fann SA, Yost MJ, 2019. Vascular Tissue Engineering Using Scaffold-Free Prevascular Endothelial–Fibroblast Constructs. BioResearch 8.1.

Peters EMJ, Arck PC, Paus R, 2005. Hair growth inhibition by psychoemotional stress: a mouse model for neural mechanisms in hair growth control. Exp Dermatol 15(1):1-13.

Przekora A, 2020. A Concise Review on Tissue Engineered Artificial Skin Grafts for Chronic Wound Treatment: Can We Reconstruct Functional Skin Tissue In Vitro? Cells, 9, 1622.

Roggenkamp D, Köpnick S, Stäb F, Wenck H, Schmelz M, Neufang G, 2013. Epidermal nerve fibers modulate keratinocyte growth via neuropeptide signaling in an innervated skin modelJ Invest Dermatol. 133(6):1620-8.

Shahrokhi S, Anna A, Jeschke MG, 2014. The Use of Dermal Substitutes in Burn Surgery: Acute Phase. Wound Repair Regen. 22(1).

Sharma P, Kumar P, Sharma R, Bhatt VD, Dhot PS, 2019. Tissue Engineering; Current Status & Futuristic Scope. Journal of Medicine and Life 12, 225–229.

Shevchenko RV, James SL James SE, 2010. A review of tissue-engineered skin bioconstructs available for skin reconstruction. J. R. Soc. Interface 7, 229–258.

Tremblay P, Hudon V, Berthod F, Germain L, Auger FA, 2005. Inosculation of Tissue-Engineered Capillaries with the Host's Vasculature in a Reconstructed Skin Transplanted on Mice. Am J Transplant 5(5):1002-10.

Chapter 1

Engineered skin substitutes
State of the art and models

1.1 The skin

From the top to the bottom, the skin is composed by an epithelium, the epidermis, and by the underlying connective tissue formed by elastic and collagen fibres, the dermis. The subcutaneous tissue, the hypodermis, consists predominantly of adipose tissue. Within the dermis there are the skin appendages, nails, hairs and glands, along with vessels and nerves. The epidermis is composed of several layers: stratum basale, stratum spinosum, stratum granulosum, stratum lucidum, and stratum corneum. Through the process of keratinization, keratin filaments are formed inside the keratinocytes as they rise to the surface, until they reach the stratum corneum, where we find only dead keratinocytes, mainly consisting in keratin filaments. The dermis is anchored to the epidermis through the dermo-epidermal junction (DEJ). In the dermis two portions are distinguished: the most superficial adventitia, consisting mainly of cells and the reticular part which is the deepest portion made of fibers. From a histological point of view, the cellular component is represented by fibroblasts responsible for the synthesis of the various fibrillary components and the amorphous substance. In addition to these, however, we find other cells such as mastcells, lymphocytes and macrophages; these cells are necessary for the immune and inflammatory response that is activated when harmful conditions occur. In addition, the copious blood circulation allows immediate reinforcement by circulating cells. The basic substance is composed mainly of glucosaminoglycoglycans, glycoproteins that are intended to retain a lot of water forming a gel able to provide the characteristic turgor to the skin. The two main glucosaminoglycans are heparin and hyaluronic acid. Fibers, instead, are mainly represented by collagen (70% of total skin proteins) a protein with supporting function produced by fibroblasts and arranged to form a thick ed structure resistant to traction. Further, there is elastin which, as the name itself indicates, provides elasticity to the tissue. Skin is the largest organ of the integumentary apparatus, with an area of around 2 square meters in humans, which accomplishes different essential roles such as protection of the underlying tissues from pathogens and mechanical shocks, thermal tactile

and dolorific sensitivity, lipid reserve and site of D^3 vitamin synthesis (Przekora, 2020).

Therefore, although in many cases the skin is able to self-renew, when the damage is serious the tissue cannot regenerate by its own (Fig. 1.1).

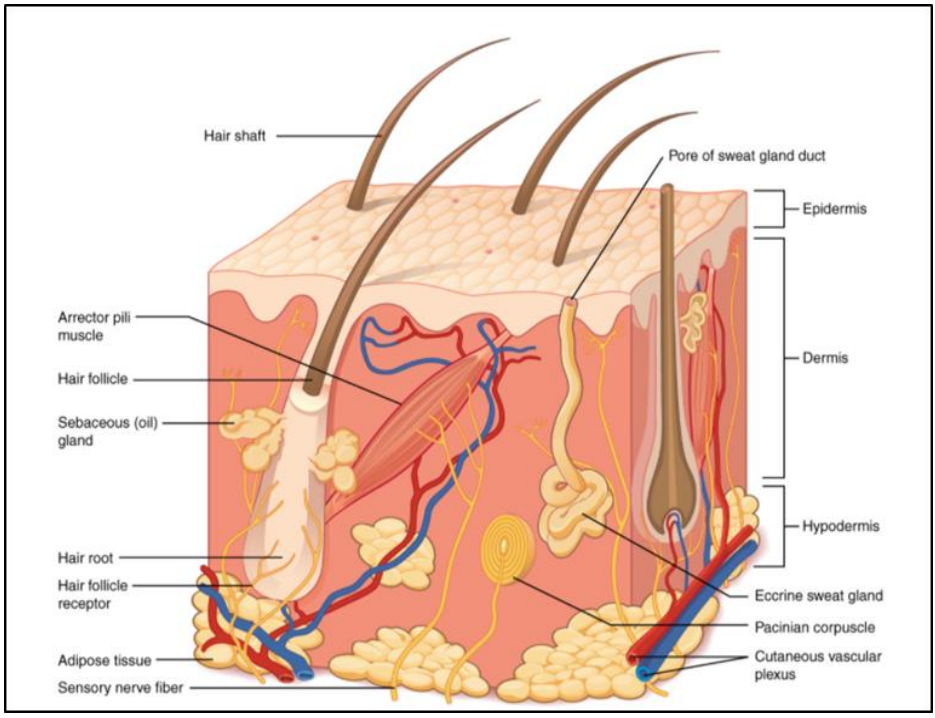

Fig. 1.1 | Skin structure (Anatomy and Physiology, The Integumentary System. https://courses.lumenlearning.com/wmopen-biology2/chapter/structure-and-function-of-skin)

1.1.1 Skin microenvironment

Epidermis and dermis are interfaced through the DEJ. Skin is a tissue with an undulate shape consisting of epidermal protrusions into the dermis and dermal projections into the epidermis (dermal papilla). Therefore, it consists both in a diaphragm and a means of biochemical communication between the two compartments (Jeong et al., 2020). Epidermis is attached to a basement membrane mainly consisting of two *laminae*, the basal and the reticular. The components of the basal lamina are secreted by epithelial cells. The lamina appears as an electron-dense layer 20-100 μm thick located immediately below the epidermis. The components of the reticular lamina, instead, are secreted by fibroblasts and the lamina is directly connected to the underlying connective tissue. Extracellular matrix is reach of collagen IV, perlecan, laminin and integrins acting as cell and tissue support (Le Bleau et al., 2007).

Dermis is predominantly composed by ECM along with collagen and elastin fibers strength and elasticity to the compartment. Within the matrix vessels ensures oxygen and nutrient supplies to the cells like fibroblasts, endothelial cells, smooth muscle cells and mast cells (Chua et al., 2016). ECM is a non-cellular compartment and is composed of a large number of proteins including collagens, glycoproteins (GP), and ECM-associated proteins showing a diversity of biochemical and biophysical functions (Levi et al., 2020). Strength and elasticity in the skin are sustained through the maintenance of extracellular matrix molecules by mesenchymal cells. Indeed, a disordered organization of ECM leads to impaired tissue function (Shook et al., 2018). ECM molecules guide cells for movement, attachment, migration, differentiation and proliferation. In view of this, ECM provides the integrity of tissue structure regulating cell-cell and cell-ECM interactions through specific molecules such as cytokines and growth factors.

1.1.2 Skin microcirculation

Microcirculation is defined as the blood flow through arterioles, capillaries and venules, which are the smallest vessels in the vasculature included within organs and tissues. The microcirculation provides tissue perfusion,

fluid homeostasis, and delivery of oxygen and nutrients also contributing to control temperature and to initiate the inflammatory response (Bentov and Reed, 2015).

Cutaneous microcirculation is organized in two different plexuses of arterioles and venules extended in the dermis. One of these plexuses is positioned in the deep portion of the dermis, at the interface between dermis and subcutaneous tissue, while the other one is located into the superficial part of the dermis, next to the epidermis, originating the nutritive capillary loops of the dermal papillae. The two plexuses are connected forming a lateral network for the nourishment of sweat glands and hair bulbs (Braverman, 1989). The micro-vessels in the papillary dermis vary in diameter from 10 to 35 μm whereas in the lower dermis diameters are wider, reaching a value of about 50 μm. Finally, microcirculation is essential to guarantee the exchange of nutrients and metabolites between blood and tissue, to protect the tissue against significant fluctuations in hydrostatic pressure in the capillary network and to decrease peripheral vascular resistance (Fig.1.2) (Neubauer-Geryk et al., 2019).

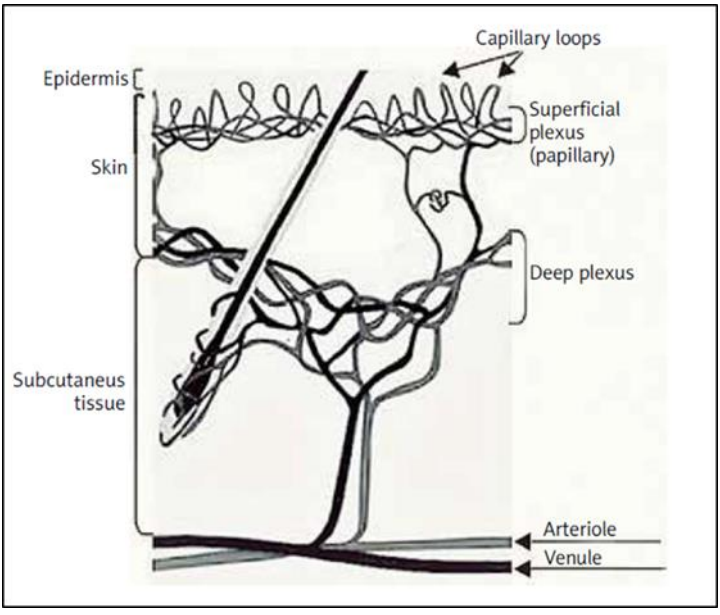

Fig. 1.2 | Skin microcirculation (Neubauer-Geryk et al., 2019)

1.1.3 Skin innervation

Skin is the center of perception of numerous stimuli from the external environment. From the dorsal root ganglia originate nerve fibers that reach the dermis and then penetrate the basement membrane innervating epidermal cells or remaining as free endings (Boulais and Misery, 2008).
All epidermal cells (keratinocytes, melanocytes, Langerhans cells and Merkel cells) express sensor proteins and neuropeptides regulating the neuro-immuno-cutaneous system. Especially Langerhans cells and mast cells strengthen the communication between neuroendocrine and immune systems (Misery, 1998; Hsieh, et al., 1997; Ashrafi et al., 2016; Blake et al., 2019).

1.2 Engineered skin substitute models

Numerous advances have been recently made in the field of skin tissue engineering to overcome skin injuries, burns and pathologies.
Tissue engineering is an interdisciplinary biomedical research field aimed to developl solutions to replace patient damaged tissues (Lalan et al., 2001). Depending on the different type of wound one type of graft is recommended instead of another. For example, is preferable to use an autograft when the wound is deep and is charachterized by the loss of keratynocites (not available for the re-epitelization). The autograft consists of wound replacement with a thin layer of donor skin composed by the whole epidermis and a portion of dermis (known as split-thickness graft). This kind of graft, since origins directly from the donor, does not risk being rejected (Majewsky and Jablonska, 1997; Clendenning and Van Scott, 1965). Skin allografts overcome donor tissue limitation. These grafts were used since the Second world war and are obtained from both corpses and living donors. Allografts can be revascularized as autografts and promote angiogenesis through grow factors and cytokines for wound healing (Halim et al., 2010). Finally, xenografts are surgical grafts from one species to another dissimilar species. These grafts, obtained from animals, can be used as temporary for

human wounds (Nathoo et al., 2014). Xenografts and allografts showed immediately limitations linked to immunological rejection, after grafting. Instead, autografts were not able to replace large wound areas for the reduced availability of healthy skin from the patient (Oualla-Bachiri et al., 2020).

1.2.1 Tissue Engineering

To overcome the various limitations of autografts, allografts and xenografts, in 1985 Mangoldt obtained syntetic grafts through the "epithelial cell seeding" technique (Leigh et al., 1995). Since then, skin replacement undergone major changes leading to the birth and development of Tissue Engineering. In 1981 autologous sheets were created by cultured epithelium from keratinocytes cell expansion from two burned patients (O'Connor et al., 1981). Since the difficulties to use a sheet made only of keratynocytes in clinical application, Burke et al. in 1981 created a dermal substitute (Burke et al., 1981). Therefore, the first apparition of a skin substitute made of both keratinocytes and fibroblasts was performed in 1990s by Cuono et al. (Hickerson et al., 1994). In addition to clinical applications, skin substitutes were also used to test pharmaceutical substances and to study skin pathological models *in vitro* (Vig et al., 2017). Many engineered skin substitutes for wound healing are on the market, however the majority of them are still in a pre-clinical testing phase. The properties of engineered tissue can be very different and depend on several factors such as the composition, the fabrication method, the number of layers, the presence/absence of cells, the type of biomaterial used. As skin substitutes, they should provide the patient with a barrier, which is fundamental to ensure protection against microorganisms but also to reduce pain, thus enabling a correct wound healing. Therefore, to improve the success for wound healing applications a full-layer vascularized skin substitute able to accelerate the process is promising to ameliorate patient quality of life.

1.3 Wound healing

Millions of people every year develop scars in response to skin injuries after surgery, trauma, or burns with significant undesired physical and psychological effects (Monavarian et al., 2019). According to the World Health Organization, more than 11 million burn injuries requiring medical attention are annually reported worldwide (World Health Organization. Burns. 2019). Burn injuries are an under- appreciated trauma that can be caused by many factors like friction, cold, heat, radiation, chemical or electric sources, however the majority of burn injuries are caused by heat from hot liquids, solids or fire (Jescke et al., 2020).

Wound treatment is carried out by fast closing of the wound to limit the damage caused by the loss of the skin barrier function and to prevent infections. Within the skin the first activators of wound healing are fibroblasts that start to create an initial tissue matrix, followed by inflammation and re-epithelization performed by keratinocytes. Afterwards, revascularization and ECM deposition occur to complete the healing process. However, some wounds are characterized by scar formation or by the unsuccessful healing which leads to the phenomenon of chronic wound (Powers et al., 2017). This latter is the consequence of vascular insufficiency, local-pressure effects, and pathological conditions like diabetes mellitus, along with compromised nutritional or immunological status. Therefore, also patient age can be a cause of impaired wound healing.

More specifically, during wound healing, skin reaction is organized in three phases: inflammation, proliferation, and maturation (Fig.1.3) (Reinke and Sorg, 2012). During the first four days the inflammatory phase takes place starting with blood coagulation in the damaged area to provide a protecting blood clot against pathogen access. Further, it starts the increase of blood flow in the wound area to carry the inflammatory mediators. These agents, like activated complement, lead to plasma extravasation and generation of a fibrin matrix. Then, immunocompetent cells are involved into the removal of dead tissue and the monitoring of the possible infection (Rodrigues et al., 2019). From the fifth to the twentieth day, the proliferation of endothelial cells and fibroblasts promoted by inflammatory cells take place (Werner and

Grose, 2003). Fibroblasts produce collagen that replace fibrin matrix and differentiate in myofibroblasts leading to the wound contraction. Afterwards, it starts the angiogenesis process resulting in the formation of granulation tissue. This tissue is so called because of its high density in cells: fibroblasts, granulocytes, macrophages, capillaries and loosely organized collagen bundles (Reinke and Sorg, 2012). It replaces the fibrin-fibronectin matrix also producing scar by maturation which consists of re-epithelialization of the wound along with the re-establishment of skin tensile strength.

The phenotype of macrophages evolves during the process of wound healing. In the inflammation phase they act as pro-inflammatory macrophages cleaning the wound from bacteria, in the proliferation phase are pro-wound healing inducing the proliferation of fibroblasts, keratinocytes and endothelial cells and finally in the remodeling phase are pro-resolving macrophages secreting MMPs for matrix remodeling (Fig.1.4). Therefore, macrophages are strictly related to the angiogenensis because during this process they position themselves next to new forming blood vessels contributing to their stabilization and fusion (Krzyszczyk P. et al., 2018).

Moreover, the lymphatic vasculature plays vital roles in tissue fluid balance, drenage, immune defense, metabolism and cancer metastasis. In adults, lymphatic vessel formation and remodeling occur primarily during inflammation and wound healing as well as in tumor growth. However, the functional roles of lymphatics in these processes are not fully understood (Kesler et al., 2013; Güç et al., 2017).

In addition to their traditional role as a route for the transport of fluid and immune cells, increasing evidence suggests that lymphatics are important tissue-specific players in crucial physiological and pathophysiological processes. The master transcription factor Prox1 and Vegfc/Vegfr3 signaling are key regulators of early lymphatic endothelial cell (LEC) fate and developmental lymphangiogenesis (Ma et al., 2021).

The use of EC in skin substitutes can accelerate blood and lymphatic capillary formation in the dermis both directly after integration to the graft

and indirectly by stimulating angiogenesis (Tremblay et al., 2005; Marino et al., 2014).

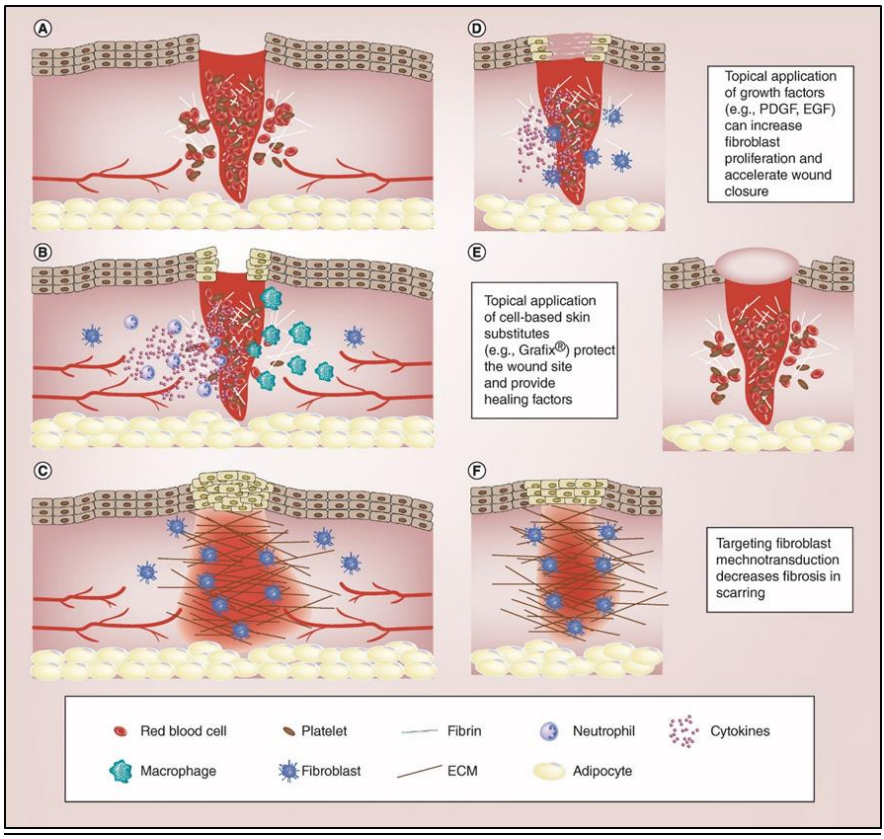

Fig. 1.3 | Wound healing pathophysiology and novel therapeutics for wound healing. An overview of cutaneous wound healing pathophysiology with a summary of recent wound healing therapeutics of note (A–C) (A) Platelets are recruited to the open wound and deposit fibrin (which serves as a preliminary extracellular matrix) to arrest bleeding. (B) Immune cells including neutrophils followed by macrophages are recruited to the wound and new blood vessels sprout around the site. Fibroblasts are recruited to the site and keratinocytes begin to migrate to cover the cutaneous wound surface. (C) Finally, the keratinocytes have covered the site. Below the fibroblasts deposit new extracellular matrix replacing the fibrin plug, which is then remodeled to form the final scar. New blood vessels are pruned, and nerves begin to regenerate to the site. (D) Growth factors such as PDGFs can be provided directly to the wound to stimulate fibroblast proliferation and accelerate wound closure. (E) Cell-based skin substitutes (e.g., Grafix R, Osiris Therapeutics, MD, USA) can be applied directly to the wound site to protect it and directly provide factors including cells involved in wound healing. (F) Fibroblast mechanotransduction plays a role in stimulating scar production. (desJardins-Park et al., 2018).

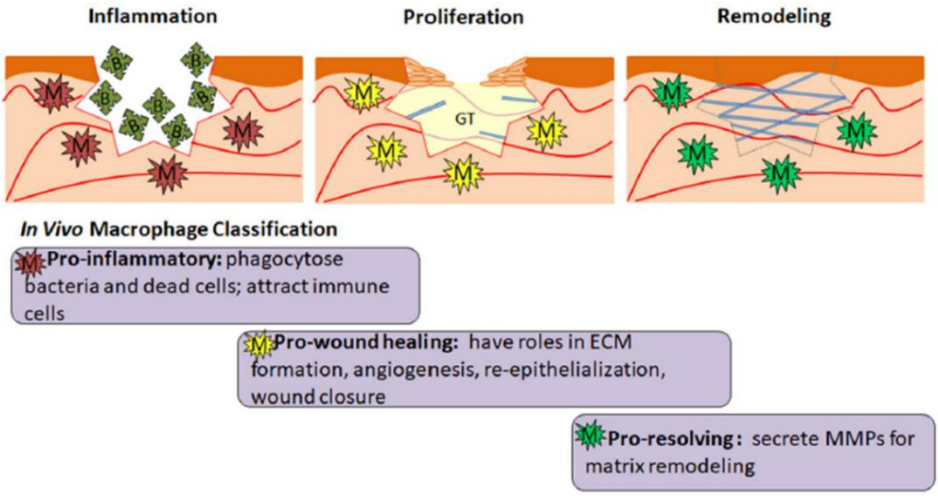

Fig.1.4 | The Role of Macrophage Phenotypes in Wound Healing. This process progresses through inflammation, proliferation and remodeling phases.
In inflammation, pro-inflammatory macrophages destroy dead cells and bacteria and prepare the wound for healing. During proliferation, pro-wound healing macrophages secrete factors boosting angiogenesis, formation of granulation tissue, collagen deposition, andreepithelialization. In remodeling, pro-resolving macrophages produce MMPs for matrix remodeling strengthening newly regenerated skin (Krzyszczyk P. et al., 2018).

1.4 Skin substitute features

An appreciable skin substitute should have some features like sterility, relatively low cost, reliability meaning that it must not cause toxicity or high inflammatory response (MacNeil 2007), at the same time it should protect from infectious agents such as bacteria, parasites, or fungus (D'Avignon et al., 2010; Mann et al., 2012; Han and Ceilley 2017). Further, skin substitutes should be easy to handle and to prepare, fast in adhering to the wound surface, also if this is irregular, and should promote angiogenesis. Therefore, if the skin substitute is temporary, it should be easily removed from the wound after its use and, when composed by cells, it should quickly adhere to the wound to facilitate their differentiation (Meuli et al., 2019). Some skin substitutes are created on the basis of biomaterials which should be

biodegradable, repairable, non-toxic, non-immunogenic, and non-inflammatory with low risk of disease transmission (Varkey et al., 2015). Choosing the right biomaterial is essential for the success of the engineered tissue. Different approaches have been adopted to develop engineered tissues, such as synthetic membranes for mono- or multi-layered cultures and 3D matrices for full-thickness models (Metcalfe and Ferguson, 2007). When a skin substitute is composed by cells, these should proliferate and differentiate in a similar manner as it happens in physiological conditions (Bacakova et al., 2019). Therefore, it is necessary to avoid the loss and the accumulation of water through the implanted constructs, since it is known that many burned patients die for dehydration (Namdar et al., 2010). Another essential feature is the capacity to be resistant to mechanical stresses considering in virtue of their tensile strength (Shimizu and Nonomura, 2018). Finally, in a burn injury, especially in case of use of cellular skin substitutes, the grafts should be resistant to hypoxia, although a burn wound area is naturally not well oxygenated. The graft also has to be flexible and robust enough to be surgically handled.

1.5 Different types of skin substitutes

Skin substitutes can be generally distinguished based on their anatomical features (epidermal, dermal or composite), composition (cellular or acellular), duration (permanent, semi-permanent or temporary), type of biomaterial (biological or synthetic), number of layers (one, two or three layers) (Fig.1.5).

Starting from acellular skin substitutes, their principal function is a temporary replacement of the damaged tissue during which they must avoid fluid loss and microbiological contamination. Therefore, these constructs are the favourite choice to cover superficial or partial full thickness wounds and burns (Vig et al., 2017). They usually consist of a nylon mesh or collagen, acting as a “dermis” and a silicon membrane acting as an “epidermis”. There are three kinds of acellular skin substitutes commercially available: Biobrane® (Mylan Bertek Pharmaceuticals, USA), Integra®

(DRT dermal regeneration template, LifeSciences Corp., USA), and Alloderm (LifeCell Inc., Branchburg, NJ, USA) (Hyland et al., 2018; Chang et al., 2019; Taufique et al., 2019).

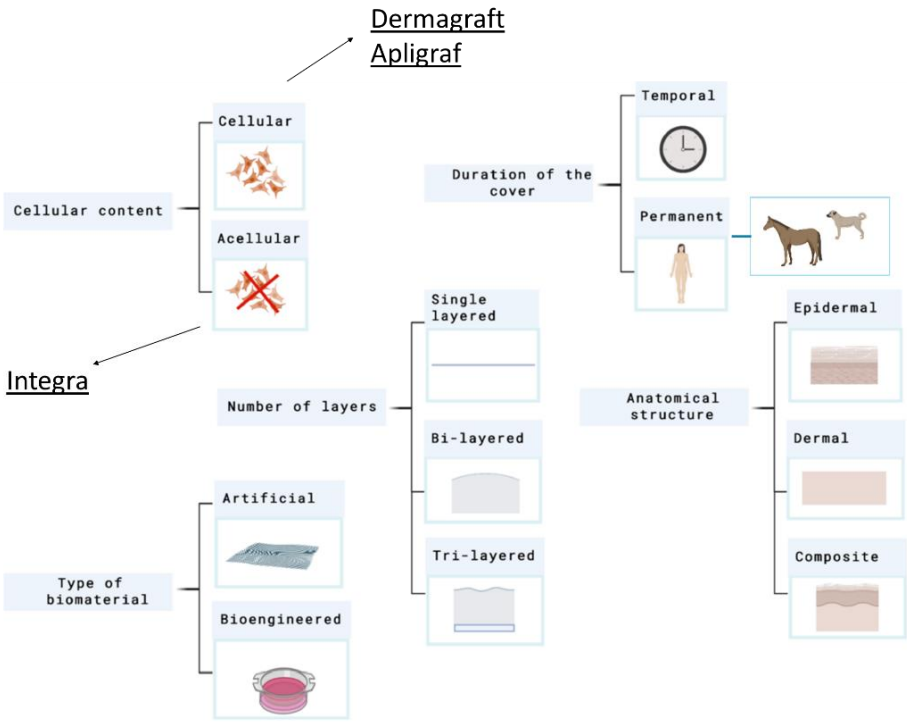

Fig. 1.5 | Principal parameters used to classify skin substitutes. Created with BioRender.com. (Oualla-Bachiri et al., 2020).

For example, Integra® dermal portion is represented by a matrix of bovine collagen and chondroitin-6-sulfate GAG while the epidermal compartment is made of a layer of the silicone polymer polysiloxane (Chang et al., 2019; Nicoli et al., 2016). Therefore, Integra® gives an appreciable aestetic result but is expensive and easily exposed to infection (Gonzalez et al., 2020). Biobrane® dermal compartment, instead, is made of a nylon mesh while the epidermal one is made of silicone in a matrix of porcine collagen. Cellular

skin substitutes are divided into allogenic and autologous. Allogenic grafts, like Dermagraft® (Advanced BioHealing, Inc., USA) and Apligraf® (Organogenesis, Canton, MA), are generally produced using neonatal foreskin fibroblasts with a mesh matrix. Indeed, Dermagraft® is a sterile, bioabsorbable polygalactin mesh scaffold seeded with human neonatal dermal fibroblasts (Hart et al., 2012). It is easy to handle but it does not show a well-represented extracellular matrixand is, in addition, particularly subjected to infections. Apligraf® is a bi-layered bioengineered skin substitute used for the first time to heal ulcers in 1998. In this constructs, human foreskin-derived neonatal fibroblasts and neonatal epidermal keratinocytes are cultured on a bovine type I collagen matrix (Zaulyanov and Kirsner, 2007). The mixture of fibroblasts and collagen is further exposed to heat to produce a loose matrix, which develops a dermal fibrous network (Curran and Plosker, 2002). It is still used mainly for the healing of leg ulcers and diabetic foot ulcers (Langer and Rogowski 2009). Finally, Apligraf® is expensive and difficult to store.

Both in the case of Dermagraft® and Apligraf® the skin substitute can produce cytokines and growth factors in a similarly to what happens in the human skin in physiological conditions (Varkey et al., 2015). There are two types of cellular autologous skin substitutes: Cultured Epidermal Autograft (CEA) and Cultured Skin Substitutes (CSS). CEA includes only keratinocytes obtained from the patient and is not able to heal full-thickness wounds. Therefore, due to a dermal-epidermal junction which is not formed correctly it is possible to have abnormal scars and hyperkeratosis (Supp and Boyce, 2005; Matsumura et al., 2019). Unlike CEA, CSS provides both epidermal and dermal components which make it suitable for permanent full thickness skin wound coverage, proving ideal cosmetic results (Boyce et al., 2002; Horch et al., 2005). Another category of skin substitutes is represented by xenografts an example of which is Matriderm® (Dr Suwelack Skin and HealthCare AG, Germany). It consists of a highly porous membrane composed of three-dimensionally coupled collagen and elastin. The collagen of the matrix is obtained from the bovine dermis while elastin derives from the hydrolysis of the bovine nuchal ligament. During the healing process Matriderm® resorbs while fibroblasts deposit the ECM

acting as a scaffold to restore the skin and modulate scar formation. Further, Matriderm thanks to its haemostatic properties, can reduce the risk of hematoma that may occur after skin grafting (Fig.1.6) (Min et al., 2014).

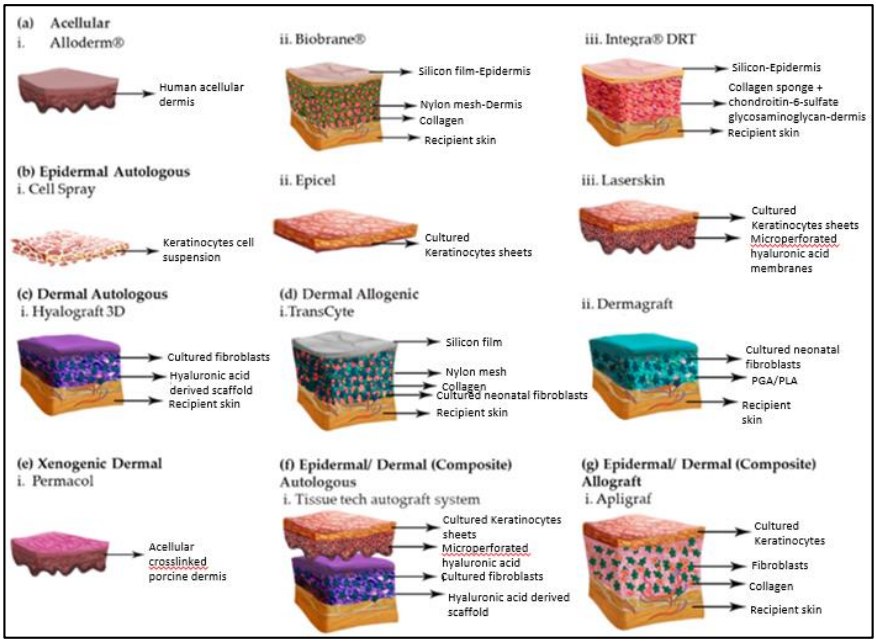

Fig. 1.6 | Tissue engineered skin substitutes. (a) Acellular: i. Karoderm ii. Biobrane iii. Integra (b) Epidermal Autologous: i. Cell Spray ii. Epicel iii. Laserskin (c) Dermal Autologous: i. Hyalograft 3D (d) Dermal Allogenic: i. TransCyte ii. Dermagraft (e) Dermal Xenogenic: i. Permacol (f) Epidermal/Dermal (Composite) Autologous i. Tissue tech Autograft system (g) Epidermal/Dermal (Composite) Allograft i. Apligraf. (Vig et al., 2017).

1.6 Skin substitute limitations

There are several limitations to the commercially available skin substitutes, in particular reduced vascularization, poor mechanical integrity, failure to integrate, scarring, and immune rejection are the most common (MacNeil 2007; Singer 2017). Therefore, it is still crucial to improve some aspects. For example, it might be interesting to introduce on the market skin

substitutes composed of a third layer representing the hypodermis. Indeed, a skin substitute representative of all the native skin compartments and of all the physiological skin features could be essential for the healing of deep full thickness wounds. Therefore, the lack of hypodermis results into reduced revascularization of the affected area. To overcome the limit linked to revascularization a good compromise is the pre-vascularized skin substitute however it is necessary to find solutions to speed up their fabrication process before grafting. Another limitation is the high cost of a skin substitute and the availability on a large scale. Currently, available skin substitutes mainly consist of fibroblasts and keratinocytes, thus lacking the ability to make differentiated structures, like hair and sweat glands (Oualla-Bachiri et al., 2020).

1.7 Skin substitutes in veterinary medicine

Skin wound healing is a complex and dynamic process that aims to restore lesioned tissues. Collagen-based skin substitutes are a promising treatment to promote wound healing by mimicking the native skin structure. In veterinary medicine this application is used for large and small animals (Melotti et al., 2021). Skin lesions are common events in the veterinary practice, regardless of sex or age, having different etiology such as trauma, burns, fights, and predation. In addition, these injuries can often result in loss of skin function due to extensive scarring or inability of the skin to close the wound (e.g., excessive loss of tissue after tumor resection or bite wounds). Indeed, the treatment of these kind of wounds, which might evolve into chronic or non-healing wounds, is a challenging and expensive issue to manage in the clinical practice of domestic animals (Melotti et al., 2021). Nowadays, the application of skin autografts to treat severe non-healing wounds is considered the gold standard (Theoret, 2005; Rothe et al., 2015). Autologous skin grafts are effective for the repair of large skin wounds, but the availability of large amounts of skin is often limited. Through bioengineering, several autologous skin substitutes have beendeveloped for use in human clinical practice. However, few skin substitutes are available for use in animals. In 2017, Ramió-Lluch and colleagues developed a canine

skin graft made of canine keratinocytes andfibroblasts that they implanted in two dogs with large, full-thickness skin wounds. They obtained a good degree of engraftment observing also a permanent epithelialisation in both dogs. They also showed complete differentiation and maturation of the epidermis while mature fibroblasts were embedded in a collagen matrix in the dermis **(**Ramió-Lluch et al., 2017).

Recently, Niimi and colleagues proposed a simple fixation method of a grafted skin substitute in a burned area by using polyurethane foam dressing (Allevyn Non-Adhesive, smith & nephew, UK) in a clinically relevant ovine burn wound model and they obtained that the grafted skin was completely integrated without any complications 7 days after implantation (Niimi, 2020) (Fig.1.7).

. In 2018, Kaasi and colleagues used acellular collagen biomembranes (Eva Scientific Ltd, São Paulo, Brazil) applied directly onto dog and cat wounds, and sutured them to the margins of the adjacent tissue. Both animal wounds healed fully without displaying any adverse effects while the healing rate in the two cases was comparable, maxing out at approximately 1 cm /day (Kaasi et al., 2018).

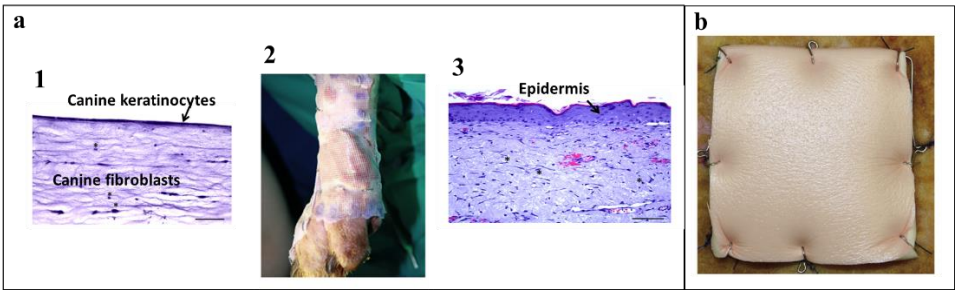

Fig. 1.7 | Skin substitutes in veterinary clinical application. a1) Histology of canine engineerend skin with seeded canine fibroblasts and keratinocytes; a2) Canine skin construct grafted in 2 dogs; a3) Histology of explanted canine engineered skin; b) Grafted ovine autologous skin covered with polyurethane foam dressing (Ramió-Lluch et al., 2017; Niimi, 2020).

Bibliography

Ashrafi M, Baguneid M, Bayat A, 2016. The Role of Neuromediators and Innervation in Cutaneous Wound Healing. Acta Derm Venereol 96: 58 594.

Bacakova M, Pajorova J, Broz A, Hadraba D, Lopot F, Zavadakova A, Vistejnova L, Beno M, Kostic I, Jencova V, Bacakova L, 2019. Int J Nanomedicine 14:5033-5050.

Bentov I, Reed MJ, 2015. The Effect of Aging on the Cutaneous Microvasculature. Microvasc Res. 100, 25–31.

Blake KJ, Jiang XR, Chiu IM, 2019. Neuronal Regulation of Immunity in the Skin and Lungs. Trends Neurosci. 42(8): 537–551.

Boulais N, Misery L, 2008. The epidermis: a sensory tissue. Eur J Dermatol 18 (2): 119-27.

Boyce ST, Kagan RJ, Yakuboff KP, Meyer NA, Rieman MT, Greenhalgh DG, Warden GD, 2002. Cultured skin substitutes reduce donor skin harvesting for closure of excised, full-thickness burns. Ann Surg 235(2):269-79.

Braverman IM, 1989. Ultrastructure and Organization of the Cutaneous Microvasculature in Normal and Pathologic States. J Invest Dermatol 93(2 Suppl):2S-9S.

Burke JF, Yannas IV, Quinby WC, Bondoc CC, Jung WK, 1981. Successful Use of a Physiologically Acceptable Artificial Skin in the Treatment of Extensive Burn Injury. Ann Surg. 194(4): 413–428.

Chang DK, Louis MR, Gimenez A, Reece EM, 2019. The Basics of Integra Dermal Regeneration Template and its Expanding Clinical Applications. Semin Plast Surg 33, 185–189.

Chua AWC, YC Khoo, BK Tan, KC Tan, CL Foo, SJ Chong, 2016. Skin tissue engineering advances in severe burns: review and therapeutic applications. Burns & Trauma 4,1-14.

Clendenning WE, Van Scott EJ, 1965. Skin Autografts and Homografts in Patients with the Lymphoma Mycosis Fungoides. American Association for Cancer Research. 25, 11, 1.

Curran MP, Plosker GL, 2002. Bilayered bioengineered skin substitute (Apligraf): a review of its use in the treatment of venous leg ulcers and diabetic foot ulcers. BioDrugs 16(6):439-55.

D'Avignon LC, Hogan BK, Murray CK, Loo FL, Hospenthal DR, Cancio LC, Kim SH, Renz EM, Barillo D, Holcomb JB, Wade CE, Wolf SE, 2010. Contribution of bacterial and viral infections to attributable mortality in patients with severe burns: An autopsy series. Burns 33, 773-779.

DesJardins-Park HE, Foster DS, Longaker MT, 2018. Fibroblasts and wound healing: an update. Regen Med 13(5):491-495.

Gonzalez SR, Wolter KG, Yuen JC, 2020. Infectious Complications Associated with the Use of Integra: A Systematic Review of the Literature Plast Reconstr Surg Glob Open 8(7): e2869.

Güç E, Briquez PS, Foretay D, Fankhauser MA, Hubbell JA, Kilarski WW, Swartz MA, 2017. Local induction of lymphangiogenesis with engineered fibrin-binding VEGF-C promotes wound healing by increasing immune cell trafficking and matrix remodeling. Biomaterials 131, 160e175.

Halim AS, Khoo TL, Yussof MSJ, 2010. Biologic and synthetic skin substitutes: An overview. Indian J Plast Surg. 43(Suppl): S23–S28.

Han G, Ceilley R, 2017. Chronic Wound Healing: A Review of Current Management and Treatments. Adv Ther 34:599–610.

Hart CE, Loewen-Rodriguez A, Lessem J, 2012. Dermagraft: Use in the Treatment of Chronic Wounds. Adv Wound Care (New Rochelle) 1(3):138-141.

Hickerson WL, Compton C, Fletchall S, Smith R, 1994. Cultured epidermal autografts and allodermis combination for permanent burn wound coverage. Burns 20, 52-56.

Horch RE, Kopp J, Kneser U, Beier J, Bach AD, 2005. Tissue engineering of cultured skin substitutes. J Cell Mol Med 9(3):592-608.

Hsieh ST, Lin WM, Chiang HY, Huang IT, Ko MH, Chang YCh, Chen WP, 1997. Skin Innervation and Its Effects on the Epidermis J Biomed Sci 4(5):264-268. doi: 10.1007/BF02253428.

Hyland EJ, D'Cruz R, Menon S, Harvey JG, La Hei E, Lawrence T, Waddell K, Nash M, Holland AJA, 2018. Biobrane™ versus acticoat™ for the treatment of mid-dermal pediatric burns: a prospective randomized controlled pilot study. Int J Burn Trauma 8(3):63-67.

Jeong S, Yoon S, Kim S, Jung J, Kor M, Shin K, Lim C, Han HS, Lee H, Park K, Kim J, Chung HJ, Kim HJ, 2019. Int J Mol Sci 21(1):73.

Jeschke MJ, van Baar ME, Choudhry MA, Chung KK, Gibran NS, Logsetty S, 2020. Burn injury. Nat Rev Dis Primers 6(1):11.

Kaasi A, Lima-Neto JF, Matiello-Filho JA, Calejo MHS, Jardini AL, Kharmandayan P, 2018. Regenerative collagen biomembrane: Interim results of a Phase I veterinary clinical trial for skin repair. F1000Res 7:729.

Kesler CT, Liao S, Munn LL, Padera TP, 2013. Lymphatic vessels in health and disease. Wiley Interdiscip Rev Syst Biol Med. 5(1): 111–124.

Krzyszczyk P, Schloss R, Palmer A, Berthiaume F, 2018. The Role of Macrophages in Acute and Chronic Wound Healing and Interventions to Promote Pro-wound Healing Phenotypes. Front Physiol 9:419.

Lalan, S, Pomerantseva I, Vacanti, JP, 2001. Tissue Engineering and Its Potential Impact on Surgery World J. Surg. 25, 1458–1466.

Langer A, Rogowski W, 2009. Systematic review of economic evaluations of human cell-derived wound care products for the treatment of venous leg and diabetic foot ulcers. BMC Health Serv Res 9:115.

LeBleu VS, Macdonald B, Kalluri R, 2007. Structure and function of basement membranes. Exp. Biol. Med. (Maywood) 232, 1121–9.

Leigh I, Lane EB; Watt FM, 1995.The keratinocyte handbook.

Levi N, Papismadov N, Solomonov I, Sagi I, Krizhanovsky V, 2020. The ECM path of senescence in aging: components and modifiers. FEBS J 287(13):2636-2646.

Ma W, Gil1 HJ, Liu X, Diebold LP, Morgan MA, Oxendine-Burns MJ, Gao P, Chandel NS, Oliver G, Mitochondrial respiration controls the Prox1-Vegfr3 feedback loop during lymphatic endothelial cell fate specification and maintenance, 2021. Science Advances 7, 18, 7359.

MacNeil S, 2007. Progress and opportunities for tissue-engineered skin. Nature 445.22.

Majewski S, Jablonska S, 1997. Skin Autografts in Epidermodysplasia Verruciformis: Human Papilomavirus associated Cutaneous Changes Need Over 20 Years for Malignant Conversion' Cancer research 57, 4214-4216.

Mann EA, Baun MM, Meininger JC, Wade CE, 2012. Comparison of mortality associated with sepsis in the burn, trauma, and general intensive care unit patient: a systematic review of the literature. Shock 37(1):4-16.

Marino D, Luginbühl J, Scola S, Meuli M, Reichmann E, 2014. Bioengineering: Bioengineering dermo-epidermal skin grafts with blood and lymphatic capillaries. Sci. Transl. Med. 6,221.

Matsumura W, Fujita Y, Shinkuma S, Suzuki S, Yokoshiki S, Goto H, Hayashi H, Ono K, Inoie M, Takashima S, Nakayama C, Nomura T, Nakamura T, Abe R, Sato N, Shimizu H, 2019. Cultured Epidermal Autografts from Clinically Revertant Skin as a Potential Wound Treatment for Recessive Dystrophic Epidermolysis Bullosa. J Invest Dermatol 139(10):2115-2124.e11.

Melotti L, Martinello T, Perazzi A, Iacopetti I, Ferrario C, Sugni M, Sacchetto R, Patruno M, 2021. A Prototype Skin Substitute, Made of

Recycled Marine Collagen, Improves the Skin Regeneration of Sheep. Animals (Basel) 11(5):1219.

Metcalfe AD, Ferguson MWJ 2007. Tissue engineering of replacement skin: the crossroads of biomaterials, wound healing, embryonic development, stem cells and regeneration. J. R. Soc. Interface 4, 413–437.

Meuli M, Hartmann-Fritsch F, Hüging M, Marino D, Saglini M, Hynes S, Neuhaus K, Manuel E, Middelkoop E, Reichmann E, Schiestl C, 2019. A cultured autologous dermo-epidermal skin substitute for full-thickness skin defects: a phase I, open, prospective clinical Trial in children. Plast Reconstr Surg 144(1):188-198.

Min JH, Yun IS, Lew DH, Roh TS, Lee WJ, 2014. The use of matriderm and autologous skin graft in the treatment of full thickness skin defects. Arch Plast Surg 41(4):330-6.

Misery L, 1998. Langerhans cells in the neuro-immuno-cutaneous system. J Neuroimmunol 14;89(1-2):83-7.

Monavarian, M, Kader S, Moeinzadeh S, Jabbari E, 2019. Regenerative Scar-Free Skin Wound Healing. Tissue Eng Part B Rev 25(4):294-311.

Namdar T, Stollwerck PL, Stang FH, Siemers F, Mailänder P, Lange T, 2010. Transdermal fluid loss in severely burned patients. Ger Med Sci.

Nathoo R, Howe N, Cohen G, 2014. Skin Substitutes An Overview of the Key Players in Wound Management. J Clin Aesthet Dermatol 7(10):44-8.

Neubauer-Geryk J, Hoffmann M, Wielicka M, Piec K, Kozera G, Brzeziński M, Bieniaszewski L, 2019. Current methods for the assessment of skin microcirculation: Part 1. Postepy Dermatol Alergol 36(3):247-254.

Nicoli F, Rampinelli I, Godwin Y, 2016. The application of Integra in a challenging contextScars, Burns & Healing 2: 1–6.

Niimi Y, 2020. Polyurethane foam for skin graft fixation in clinical-relevant ovine burn wound model for wound repair and regeneration research. Regen Ther. 14: 341–343.

O'Connor NE, Mulliken JB, Banks-Schlegel S, Kehinde O, Green H, 1981. Grafting of burns with cultured epithelium prepared from autologous epidermal cells. Lancet.

Oualla-Bachiri W, Fernández-González A, Quiñones-Vico MI, Arias-Santiago S, 2020. From Grafts to Human Bioengineered Vascularized Skin Substitutes. Int J Mol Sci 21(21):8197.

Powers JG, Higham C, Broussard K, Phillips TJ, 2016. Wound healing and treating wounds: Chronic wound care and management. J Am Acad Dermatol 74(4):607-25

Przekora A, 2020. A Concise Review on Tissue Engineered Artificial Skin Grafts for Chronic Wound Treatment: Can We Reconstruct Functional Skin Tissue In Vitro? Cells, 9, 1622.

Ramió-Llucha L, Cerratoa S, Brazisa P, Rabanalb RM, Fondevilab D, Puigdemontc A, 2017. Proof of concept of a new autologous skin substitute for the treatment of deep wounds in dogs. The Veterinary Journal 230 36–40.

Reinke JM, Sorg H, 2012. Wound Repair and Regeneration. Eur Surg Res 49:35–43.

Rodrigues M, Kosaric N, Bonham CA, Gurtner GC, 2019. Wound Healing: A Cellular Perspective. Physiol Rev ;99(1):665-706.

Rothe K, Tsokos M, Handrick W, 2015. Animal and Human Bite Wounds. Dtsch. Arztebl. Int. 112, 433–443.

Shimizu R, Nonomura Y, 2018. Preparation of Artificial Skin that Mimics Human Skin Surface and Mechanical Properties. J Oleo Sci 67(1):47-54.

Shook BA, Wasko RR, Rivera Gonzalez GC, Salazar-Gatzimas E, López-Giráldez F, Dash BC, Muñoz-Rojas AR, Aultman KD, Zwick RK, Lei V, Arbiser JL, Miller-Jensen K, Clark DA, Hsia HC, Horsley V, 2018. Myofibroblast proliferation and heterogeneity is supported by macrophages during skin repair. Science 23; 362(6417).

Supp DM, Boyce, 2005. Engineered skin substitutes: practices and potentials. Clinics in Dermatology 23, 403–412.

Taufique ZM, Bhatt N, Zagzag D, Lebowitz RA, Lieberman SM, 2019. Revascularization of AlloDerm Used during Endoscopic Skull Base Surgery. J Neurol Surg B 80:46–50.

Theoret CL, 2005. The pathophysiology of wound repair. Vet. Clin. N. Am. Equine Pract., 21, 1–13.

Tremblay P, Hudon V, Berthod F, Germain L, Auger FA, 2005. Inosculation of tissue-engineered capillaries with the host's vasculature in a reconstructed skin transplanted on mice. Am J Transplant 5(5):1002-10.

Varkey M, Ding J, Tredget EE, 2015. Advances in Skin Substitutes—Potential of Tissue Engineered Skin for Facilitating Anti-Fibrotic Healing. J. Funct. Biomater. 6, 547-563.

Vig K, Chaudhari A, Tripathi S, Dixit S, Sahu R, Pillai R, Dennis VA, Singh SR, 2017. Advances in Skin Regeneration Using Tissue Engineering. Int J Mol Sci 18(4):789.

Werner S, Grose R, 2003. Regulation of Wound Healing by Growth Factors and Cytokines. Physiol Rev 83: 835–870.

Bibliography

World Health Organization. 2018. Burns. Available at: http://www.who.int/en/news-room/fact-sheets/detail/burns.

Zaulyanov L, Kirsner RS, 2007. A review of a bi-layered living cell treatment (Apligraf) in the treatment of venous leg ulcers and diabetic foot ulcers. Clin Interv Aging 2(1):93-8.

Chapter 2

Engineered skin integration with the host tissue
The role of vascularization

2.1 Skin microcirculation

In human adult body microcirculation includes the majority of blood vessels and connects all the arterial and venous networks from both the structural and functional standpoints. Microcirculation mainly includes vessels with a diameter of less than 150 μm, i.e. arterioles, small veins, lymphatic vessels and arteriovenous anastomoses (Neubauer-Geryk et al., 2019). Arterioles and venules can be identified by the internal elastic lamina and a thicker wall without elastic fibers respectively, capillaries can be detected by a thin vascular wall including pericytes (Fig.2.1).

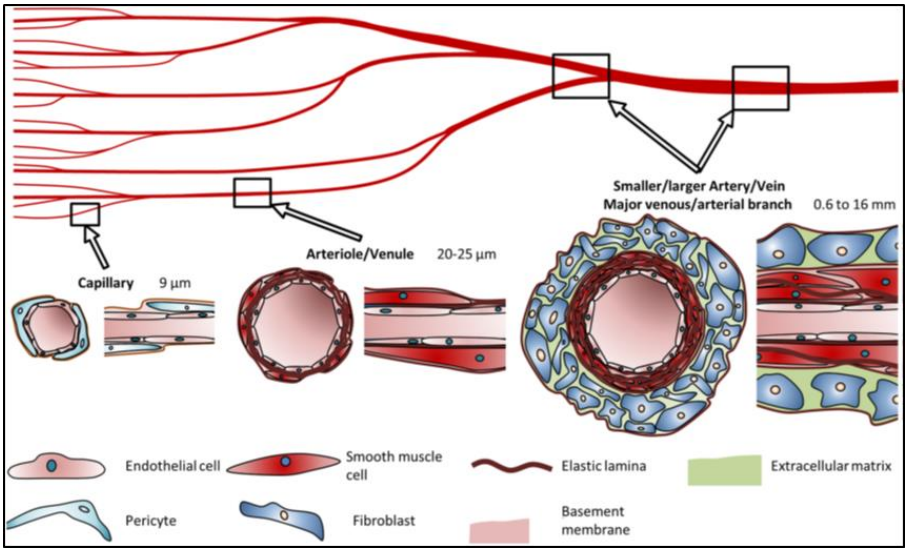

Fig. 2.1 | Vessel wall cell types and organization. Capillaries comprise typical EC lining surrounded by pericytes. Arterioles/venules are surrounded by a small number of SMCs. Arteries and veins consist of a dense SMC layer surrounded- by fibroblasts (Schöneberg et al., 2018).

Microcirculation provides tissue perfusion, fluid homeostasis, and delivery of oxygen and nutrients also contributing to control body temperature and to initiate the inflammatory response (Bentov and Reed, 2015). Cutaneous microcirculation is organized in two different plexuses of arterioles and venules extended in the dermis. The more superficial is at the interface between dermis and subcutaneous tissue at a depth of 400–500 μm from skin surface. The other one is located at 1-1.5 mm below the skin surface (Braverman, 2000) and is formed by perforating vessels deriving from the underlying muscles and subcutaneous fat. From this plexus, arterioles and venules form direct connections with the upper horizontal plexus as well as providing lateral tributary vessels which nourish hair bulbs and sweat glands. The other plexus is located at the surface of dermis, next to the basal epidermis, originating the nutritive capillary loops of the dermal papillae (Fig.2.2 a, b) (Braverman, 1989). Micro-vessels in the papillary dermis vary in diameter from 10 to 35 μm whereas in the lower dermis diameters are wider, reaching a value of about 50 μm. Skin microcirculation can be affected by a variety of pathologies or disorders like allergic shocks, hypoxia, hypoxia-reperfusion injury, clotting phenomena, vasculitis, diabetes mellitus, arterial hypertension, chronic kidney diseases. Therefore, it can be subjected to temperature and blood pressure variations, aging, stress and nutrition status. Currently, several non-invasive techniques are available to feature skin microcirculation such as capillaroscopy and video-capillaroscopy, laser Doppler flowmetry, thermography and transcutaneous oxygen measurement (tcpO2) along with photoplethysmography, orthogonal spectral polarization, near infrared spectroscopy (NIRS) and tissue reflectance spectrophotometry as well as optical coherence tomography (OCT) (Neubauer-Geryk et al., 2019).

Finally, microcirculation is essential to guarantee the exchange of nutrients and metabolites between blood and tissues, to protect these latter from significant fluctuations in hydrostatic pressure in the capillary network and to decrease peripheral vascular resistance (Neubauer-Geryk et al., 2019).

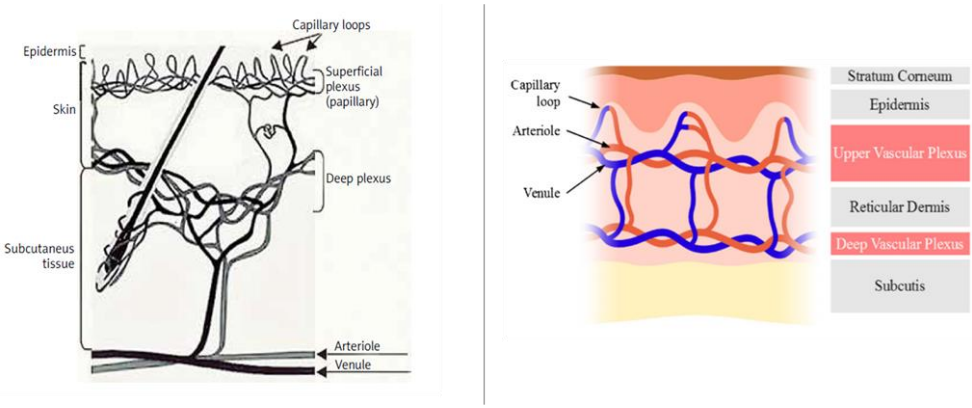

Fig.2.2 | a) Schematic representation of the microvascular organization in human skin. Cutaneous microcirculation is organized in two different plexuses of arterioles and venules extended in the dermis. The more superficial is at the interface between dermis and subcutaneous tissue at a depth of 400–500 μm from skin surface. The other one is located at 1-1.5 mm below the skin surface (Braverman, 1989); b) Simplified scheme of the skin structure with distribution of blood vessels (Zakharov et al., 2011).

2.1.1 Vessel features

The outside diameters of blood vessels in the papillary dermis vary from 10 to 35 μm, but most vessels fall in the range 17- to 22 μm. The outside diameters of the deepest dermal vessels are, in general, 40 to 50 μm, although some can be as large as 100 μm. Endothelial cells form the linings of the blood and lymphatic vessels (Alberts et al., 2002) and contain bundles of 7.5- to 10-nm filaments which are essential to maintain cell morphology, to stabilize the integrity of adhesion junctions and to modulate endothelial permeability. Cells vary in thickness from 0.3 to 1.5μm, except for the spots where the nuclei bulge into the lumen. The arterioles in the papillary dermis vary from 17 to 26 μm in outside diameter and are called terminal arterioles. In the typical terminal arteriole, endothelial cells are surrounded by two layers of smooth muscle cells. The vascular wall includes the basement membrane which completely surrounds elastin and smooth muscle cells. Both smooth muscle cells and endothelial cells send cytoplasmic processes toward each other providing a tight junctional contact (Li et al., 2018). A

terminal arteriole gives rise to the papillary loop in the horizontal plexus. This loop is composed of an ascending limb, an intrapapillary loop having a hairpin structure, and a descending limb that connects with a postcapillary venule in the horizontal plexus (Fig.2.3 a, b, c). The descending venous limb can be 1.5 times as wide as the ascending arterial limb. Each dermal papilla is supplied by a single capillary loop (Braverman, 1989).

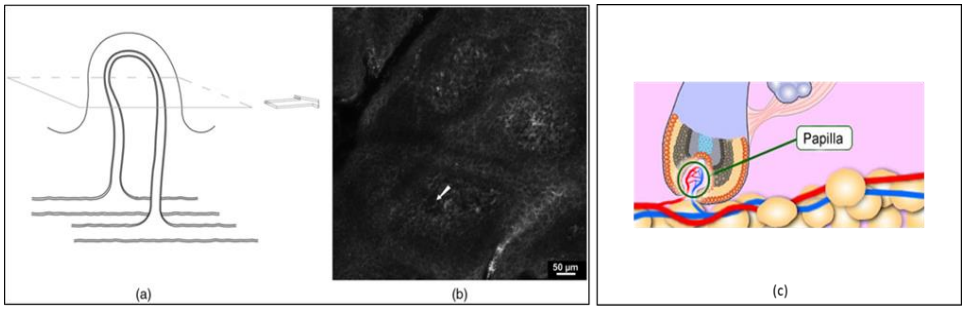

Fig. 2.3 | Capillary loop in healthy skin. (a) Scheme of a healthy dermal papilla supplied by a single capillary loop with simple hairpin structure. (b) Confocal image of a horizontal (en face) section (500 × 500 µm) of a dermal papilla with two surfaces of the capillary loop corresponding to the ascending and descending limb (arrow) (Archid et al., 2012); (c) https://www.ivyroses.com/Define/Papilla_(Hair_Follicle)

2.2 Angiogenesis in wound healing

Wound healing is a very complex process articulated in different phases and involving many types of cells (Takeo et al., 2015). To prevent haemorrhage and to induce the development of an invading matrix useful for the cells, both coagulation and haemostasis are crucial events. The wound healing mechanisms in the acute wound are shifted toward tissue repair. Among the diverse processes in the proliferative phase, angiogenesis and epithelialization f particularly relevant. Endothelial cells play a key role by allowing the growth and survival of newly formed tissue (Velnar and Gradisnik 2018).

2.2.1 Angiogenesis

In wound healing angiogenesis is stimulated by many growth factors (Werner and Grose, 2003; Ishihara et al., 2019) influencing proliferation, survival, differentiation and migration of fibroblasts, endothelial cells, macrophages, neutrophils, mast cells, dendritic cells, and T cells (Krizbai et al., 2000; Rodrigues et al., 2019). The haemostatic protein von Willebrand factor (VWF) which is released by endothelial cells (ECs) in plasma and in the sub-endothelial matrix is a main angiogenesis regulator. All the vessels include in their wall quiescent endothelial cells which are sensitive to angiogenic factors such as fibroblast growth factor (FGF), vascular endothelial growth factor (VEGF), platelet-derived growth factor (PDGF), angiogenin (ANG) and transforming growth factors alpha and beta (TGF-alpha, TGF-beta). Stimuli from these molecules are balanced by those deriving from inhibitor molecules, namely angiotensin and steroids (Oike et al., 2004; Melincovici et al., 2018; Nagaraja et al., 2019) directly inducing endothelial cells proliferation and migration and indirectly stimulating host cells to produce VEGF. Despite the hypoxia featuring the wound healing process, endothelial cell growth is stimulated by specific molecules like VEGF, PDGF and bFGF (Pikula et al., 2015).
In response to hypoxia endothelial cells follow a schematic set of events: I) production of proteases for the degradation of the basal lamina of the pre-existing vessels; II) chemotaxis; III) proliferation; and IV) remodelling and differentiation. FGF and VEGF play a vital regulatory role in all of the processes (Rinke and Sorg, 2012). Endothelial cells forming a new capillary proliferate and migrate into the surrounding tissue and shape capillary like structures allowing blood flow (DeCicco-Skinner et al., 2014). During the formation of new capillaries endothelial cells undergo numerous morphological changes induced by active biomolecules. Endothelial cells are displaced to the site of injury where their differentiation promote the formation of new blood vessels (Velnar and Gradisnik 2018) driven by endothelial cell growth factor (ECGF), vascular endothelial growth factor (VEGF), transforming growth factor- alpha (TGF-alpha), fibrin,

angiopoietin 1, heparin and lipid growth factors (Gianni-Barrera et al., 2018).

Changes in cytoskeletal organization, signal transduction and cell adhesion in the vascular system are regulated by physical and chemical cues. The regulation of these mechanisms involves three types of events: the migration towards the concentration gradient of the chemo-attractive molecule (chemotaxis), the migration in response to a gradient of immobilized ligands (haptotaxis) and the migration induced by mechanical forces (mechanotaxis) (Fig.2.4) (Mañes et al., 2000).

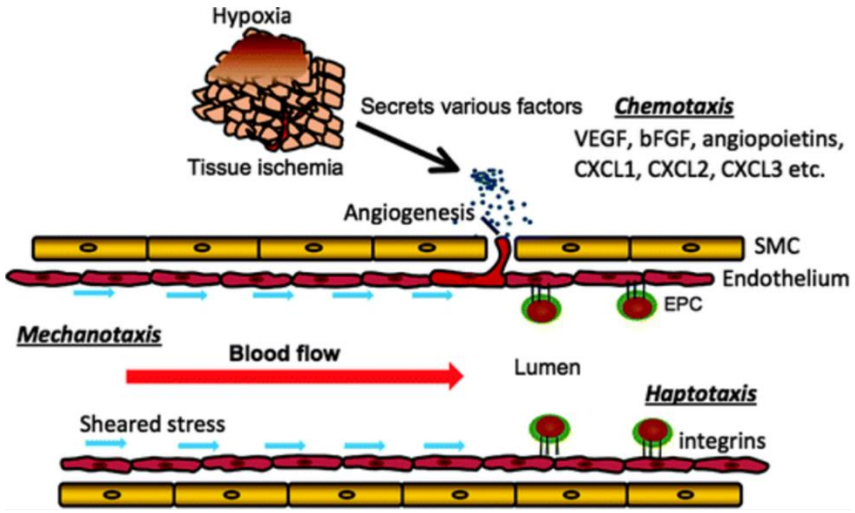

Fig.2.4 | Factors regulating angiogenesis process. Hypoxia, chemokines and cytokines, hypotaxis, and mechanotaxis are the major factors inducing and regulating angiogenesis EPCs endothelial progenitor cells; SMC smooth muscle cells; VEGF vascular endothelial growth factor; bFGF basic fibroblast growth factor; CXCL chemokine (CXC-motif) ligand; MMP matrix metalloproteinases (Lu et al., 2013).

The consequence of chemotaxis is cell migration which plays a key role for the success of angiogenesis. (Li et al., 2005). ECs, representing the inner lining of blood vessels, are subjected to the fluid shear stress, a component

of hemodynamic stresses. The shear stress, applied to the luminal surface of ECs, increases the mechanical-chemical signaling modulating each step of the migration process (Fig.2.5) (Krizbai et al., 2000; Giannone et al., 2004; Li et al., 2005; Wolgemuth et al., 2005).

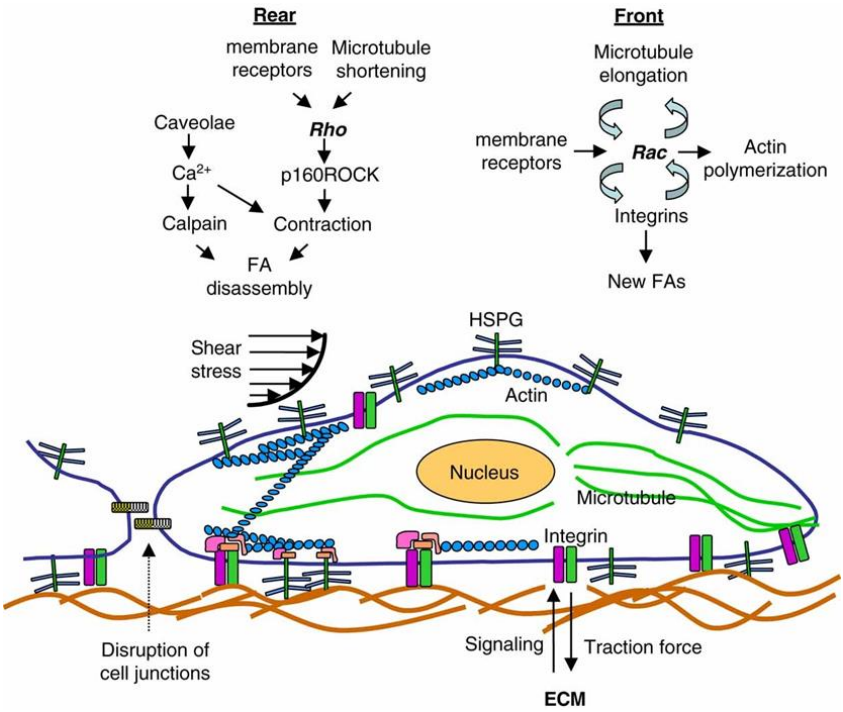

Fig 2.5 | A model of the polarized activation of signalling molecules by shear stress during endothelial cell (EC) migration. Cellular motility requires three distinct events: i) the protrusion of cell leading edge; ii) the formation of new adhesion at the front to attach the actin cytoskeleton to the substratum and, finally, iii) the contraction of the cell and the release of the adhesions at the rear (Li, 2005).

During protrusion, the cytoskeleton provides mechanical support to the cell (Li et al., 2005). The actin network is crucial to coordinate the whole process of cell migration. Therefore, this network is guided by a series of regulatory signals (Giannone et al., 2004; Li et al., 2005). Actin polymerization starts from the leading edge of the cell, guided by the highest concentration of chemo-attractive substance, pushing the plasma membrane outward and developing filopodia. The unidirectional movement of the cell is maintained

through the action of a cyclic assembly and disassembly of actin filaments in front of and behind the leading edge, respectively (Giannone et al., 2007). Then, the second phase is the adhesion to a solid substratum where integrins are involved as primary receptors for extracellular proteins. After the attachment to the extracellular matrix, the cell changes its morphology from oval or spindle-shaped to irregular flattened. These alterations in shape are governed by integrin signalling and depend on integrin contacts with the extracellular matrix in focal complexes, forming initially at the ends of filopodia (Gerhardt et al., 2003). Beyond cell motility, integrins are also involved in signal transduction, regulating, and stimulating cell migration. Immediately after an injury, endothelial cells migrate very fast while afterwards they enter a slower migration rate which is maintained during the healing process (Lee et al., 2018). Finally, the contractile forces generated by the connection between integrins and cytoskeleton force the cell to pull its cytoplasm forward, giving rise to the traction phenomenon. A pulling force in the front and a contraction force at the rear of the cell act during cell migration while the ECM provides the mechanical support through collagen, laminin, fibronectin, vitronectin and fibrinogen (Li et al., 2005; Wu and Bezanilla, 2018).

2.3 Pre vascularized skin substitutes

Many tissue engineering studies are focussed on the development of pre-vascularized skin substitutes for clinical applications aiming to mimic the physiological condition of healthy skin. The re-vascularization of injured skin by the host organism is a very low process when treated by the implant of avascular skin constructs whereas the implantation of pre-vascularized engineered tissues greatly enhances the fast formation of functional anastomosis with the host vasculature by boosting skin graft integration. On the other hand, *in vitro* pre-vascularized tissues provide valuable data to better understand pathological angiogenesis as well as to test drug efficacy (Matei et al., 2019). The first vascularized skin-equivalent model *in vitro* was fabricated in 1998. The tissue was obtained through a co-culture of three types of human cells: fibroblasts, Human Umbilical Vein Endothelial Cells (HUVECs) and epithelial cells seeded onto chitosan/collagen scaffolds. To vascularize an engineered construct, the host tissue can follow two different options: inosculation and neovascularization (Auger et al., 2013). Inosculation implies the anastomoses between the host microvascular network and capillaries already included in the graft (Laschke et al., 2006). This process accelerates vascularization of large 3D tissue-engineered constructs ameliorating graft survival. Neovascularization, instead, correspond to the colonization of the graft by host capillaries.

2.3.1 Cells used to pre-vascularize skin substitutes

Using a pre-vascularized construct leads to a rapid perfusion which, in turn, provides an adequate blood supply to the wounded area, a better collagen type I deposition and dermis and epidermis cell proliferation along with a lower expression of wound healing markers (Klar et al., 2014).
The choice of the cells for the fabrication of a pre-vascularized skin substitute is fundamental but is also interesting to underline the importance of all the factors involved in vascularization. For example, VEGF is the main proangiogenic protein that, by acting with FGF, leads to capillary sprout;

angiotropin is involved in ECs migration and TGF in blood vessels formation.

To date, there are no standard cell culture protocols for engineered tissue pre-vascularization. All the advances are still at the preclinical stage. To pre-vascularize a bioengineered skin substitute, many kinds of cells can be used. ECs accelerate the formation of both lymphatic and blood capillaries after the integration of the graft (Tremblay et al., 2005; Baltazar et al., 2020). However, these cells display a low proliferative activity making difficult to easily obtain a large amount (Laschke et al., 2016). In view of this, a valid alternative to ECs is represented by endothelial progenitor cells (EPCs) (Dai et al., 2018).

First, these cells can be simply obtained from the bone marrow as well as from peripheral blood. If the quantity of cells harvested is too low, for example when the cells are obtained from adults, it is easy to expand the colonies (Peters 2018). Therefore, when EPCs are cultured with fibroblasts, the development of the vascular plexus is encouraged (Vitacolonna et al., 2017). Indeed, the 3D environment is fundamental for the onset of the vascular network but also to mimic the physiological skin conditions of providing oxygen and nutrients. Without mesenchymal cells EC cannot induce the formation of a mature vascular network both *in vitro* and in vivo (Koike et al., 2004). In 2014 Klar and colleagues developed a pre-vascularized model made of both the dermal and the epidermal layer (Klar et al., 2014) pre-vascularizing the construct with the human stromal vascular fraction (SVF). SVF, obtained from human adipose/fat tissue, includes ECs, endothelial precursor cells (EPCs), stromal cells, and pericytes that can contribute to vessel remodelling through the release of angiogenic growth factors (Chiaverina et al., 2019) but also adipose-derived stromal cells (ADSCs) (Bora and Majumdar, 2017). This stromal vascular fraction is easily available for its abundance, and it represents an autologous source of cells avoiding the risk of immune rejection.

ADSCs produce factors like VEGF, promoting EPCs migration and better survival, while EPCs produce PDGF that induce ADSCs to proliferate and migrate. Therefore, the physical interaction between ADSCs and EC support vasculature-like structure formation (Fig.2.6) (Traktuev et al., 2009).

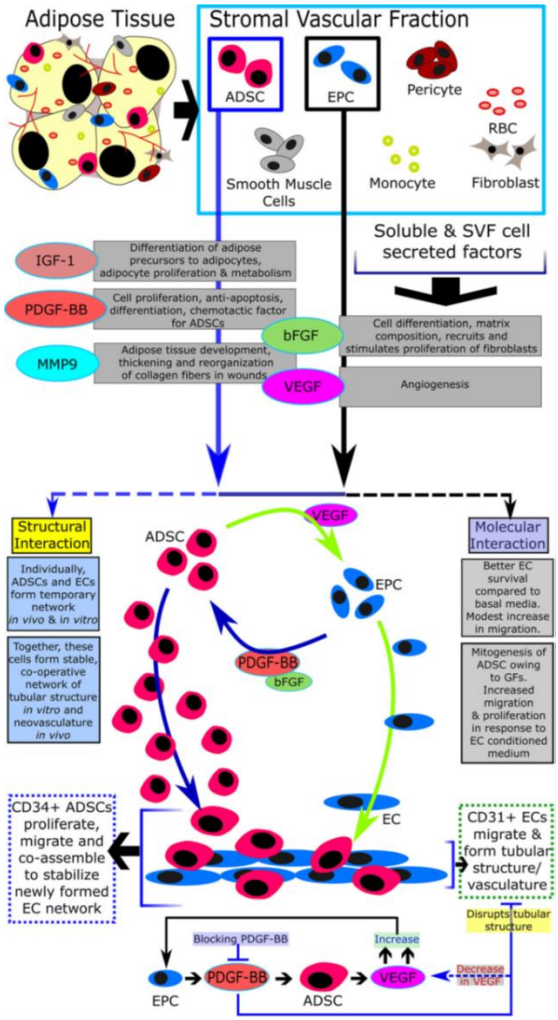

Fig. 2.6 | Potential mechanism of action of ADSCs and ECs present in SVF towards angiogenesis. Breakdown of adipose tissue releases many cell types, which together are termed SVF. ADSCs and EPCs, two important components of SVF, cross-talk via VEGF and PDGF-BB, respectively (among other components), to enable cell proliferation. ADSC adipose-derived stromal cell, bFGF basic fibroblast growth factor, EC endothelial cell, EPC endothelialprogenitor cell, GF growth factor, IGF-1 insulin-like growth factor-1, MMP matrix metalloproteinase, PDGF platelet-derived growth factor, RBC red blood cell, SVF stromal vascular fraction, VEGF vascular endothelial growth factor (Bora and Majumdar, 2017).

Respect to other sources of endothelial cells, like human dermal microvascular endothelial cells (HDMEC) or HUVEC, in culture with fibroblasts, fresh isolated SVF make possible a successful microvessel stabilization because of the capacity to maintain a constant ratio of cells involved (Bi et al., 2019). Other cells able to induce the formation of tubular structures forming a valid vascular network are the adipose-derived stem cells (ASCs) (Klar et al., 2017) thanks to their ability to adopt a proangiogenic phenotype differentiating along the cardiovascular lineage, these cells may be used as a potential source for cardiovascular tissue engineering (Neofytou, 2011).

In addition to cell type, it is also crucial to choose the right biomaterial for scaffold fabrication. Indeed, the chosen biomaterial should be able to sustain cell proliferation and differentiation. 3D-scaffolds are the best representation of ECM encouraging an efficient revascularization in vivo (Wang et al., 2019). Therefore, it has also been shown that both SVF cells and ECs when seeded in a 3D-scaffold, are prone to form a successful capillary-like network thus providing a greater supply of oxygen and nutrients to the engineered tissue. In alternative to the *in vitro* approach, the main application to generate microvascular networks is represented by microfluidic systems (Hasan et al., 2014).

Alberts B, Johnson A, Lewis J, Raff M, Roberts K, Walter P, 2003. Molecular biology of the cell. 4th edn. Ann Bot. 91(3): 401.

Archid R, Patzelt A, Lange-Asschenfeldt B, Ahmad SS, Ulrich M, Stockfleth E, Philipp S, Sterry W, Lademann J, 2012. Confocal laser-scanning microscopy of capillaries in normal and psoriatic skin. J Biomed Opt 17(10):101511.

Auger FA, Gibot L, Lacroix D, 2013. The pivotal role of vascularization in tissue engineering. Annu Rev Biomed Eng 15:177-200.

Baltazar T, Merola J, Catarino C, Xie CB, Kirkiles-Smith NC, Lee V, Hotta S, Dai G, Xu X, Ferreira FC, Saltzman WM, Pober JS, Karande P, 2020. Three Dimensional Bioprinting of a Vascularized and Perfusable Skin Graft Using Human Keratinocytes, Fibroblasts, Pericytes, and Endothelial Cells. Tissue Eng Part A 26(5-6):227-238.

Bentov I, Reed MJ, 2015. The Effect of Aging on the Cutaneous Microvasculature. Microvasc Res. 100, 25–31.

Bi H, Li H, Zhang C, Mao Y, Nie F, Xing Y, Sha W, Wang X, Irwin DM, Tan H, 2019. Stromal vascular fraction promotes migration of fibroblasts and angiogenesis through regulation of extracellular matrix in the skin wound healing process. Stem Cell Res Ther 10(1):302.

Bora P, Majumdar AS, 2017. Adipose tissue-derived stromal vascular fraction in regenerative medicine: a brief review on biology and translation. Stem Cell Res Ther 8(1):145.

Braverman IM, 1989. Ultrastructure and Organization of the Cutaneous Microvasculature in Normal and Pathologic States. J Invest Dermatol 93(2 Suppl):2S-9S.

Braverman IM, 2000. The cutaneous microcirculation. J Investig Dermatol Symp Proc 5(1):3-9.

Chiaverina G, di Blasio L, Monica V, Accardo M, Palmiero M, Peracino B, Vara-Messler M, Puliafito A, Primo L, 2019. Dynamic Interplay between Pericytes and Endothelial Cells during Sprouting Angiogenesis. Cells 8(9):1109.

Dai N, Huang W, Chang F, Wei L, Huang T, Li J, Fu K, Dai L, Hsieh P, Huang N, Wang Y, Chang H, Parungao R, Wang Y, 2018. Development of a Novel Pre-Vascularized Three-Dimensional Skin Substitute Using Blood Plasma Gel Cell Transplant 27(10):1535-1547.

DeCicco-Skinner KL, Henry GH, Cataisson C, Tabib T, Gwilliam JC, Watson NJ, Bullwinkle EM, Falkenburg L, O'Neill RC, Morin A, Wiest JS, 2014. Endothelial cell tube formation assay for the in vitro study of angiogenesis. J Vis Exp (91): e51312.

Gerhardt H, Golding M, Fruttiger M, Ruhrberg C, Lundkvist A, Abramsson A, Jeltsch M, Mitchell C, Alitalo K, Shima D, Betsholtz C, 2003. VEGF guides angiogenic sprouting utilizing endothelial tip cell filopodia. J Cell Biol 161(6):1163-77.

Gianni-Barrera R, Butschkau A, Uccelli A, Certelli A, Valente P Bartolomeo M, Groppa E, Burger MG, Hlushchuk R, Heberer M, Schaefer DJ, Gürke L, Djonov V, Vollmar B, Banfi A, 2018. PDGF-BB regulates splitting angiogenesis in skeletal muscle by limiting VEGF-induced endothelial proliferation. Angiogenesis21:883–900.

Giannone G, Dubin-Thaler BJ, Döbereiner HG, Kieffer N, Bresnick AR, Sheetz MP, 2004. Periodic lamellipodial contractions correlate with rearward actin waves. Cell 116(3):431-43.

Giannone G, Dubin-Thaler BJ, Rossier O, Cai Y, Chaga O, Jiang G, Beaver W, Döbereiner H, Freund Y, Borisy G, Sheetz MP, 2007. Lamellipodial actin mechanically links myosin activity with adhesion-site formation. Cell 128(3):561-75.

Hasan A, Paul A, Vrana NE, Zhao X, Memic A, Hwang Y, Dokmeci MR, Khademhosseini A, 2004. Microfluidic techniques for development of 3D vascularized tissue. Biomaterials 7308e7325.

Ishihara J, Ishihara A, Starke RD, Peghaire CR, Smith KE, McKinnon TAJ, Tabata Y, Sasaki K, White MJW, Fukunaga K, Laffan MA, Lutolf MP, Randi AM, Hubbell JA, 2019. The heparin binding domain of von Willebrand factor binds to growth factors and promotes angiogenesis in wound healing. Blood 133(24):2559-2569.

Klar AS, Güven S, Biedermann T, Luginbühl J, Böttcher-Haberzeth S, Meuli-Simmen C, Meuli M, Martin I, Scherberich A, Reichmann E, 2014. Tissue-engineered dermo-epidermal skin grafts prevascularized with adipose-derived cells. Biomaterials 35(19):5065-78.

Klar AS, Zimoch J, Biedermann T, 2017. Skin Tissue Engineering: Application of Adipose-Derived Stem Cells. Biomed Res Int 2017:9747010.

Koike N, Fukumura D, Gralla O, Au P, Schechner JS, Jain RK, 2004. Tissue engineering: creation of long-lasting blood vessels. Nature 428(6979):138-9.

Krizbai IA, Bauer H, Amberger A, Hennig B, Szabó H, Fuchs R, Bauer HC, 2000. Growth factor-induced morphological, physiological and molecular characteristics in cerebral endothelial cells. Eur J Cell Biol 79(9):594-600.

Laschke MW, Harder Y, Amon M, Martin I, Farhadi J, Ring A, Torio-Padron N, Schramm R, Rücker M, Junker D, Häufel JM, Carvalho C, Heberer M, Germann G, Vollmar B, Menger MD, 2006. Angiogenesis in tissue engineering: breathing life into constructed tissue substitutes. Tissue Eng 12(8):2093-104.

Laschke MW, Menger MD, 2016. Prevascularization in tissue engineering: Current concepts and future directions. Biotechnol Adv 34(2):112-21.

Lee J, Song KH, Kim T, Doh J, 2018. Endothelial Cell Focal Adhesion Regulates Transendothelial Migration and Subendothelial Crawling of T Cells. Front. Immunol. 9:48.

Li M, Qian M, Kyler K, Jian, Xu J, 2018. Endothelial–Vascular Smooth Muscle Cells Interactions in Atherosclerosis. Front Cardiovasc Med 5:151.

Li S, Huang NF, Hsu S, 2005. Mechanotransduction in Endothelial Cell Migration. Journal of Cellular Biochemistry 96:1110–1126.

Lu J, Pompili VJ, Das H, 2013. Neovascularization and hematopoietic stem cells. Cell Biochem Biophys 67(2):235-45.

Mañes S, E Mira E, Gómez-Moutón C, Lacalle RA, Martínez C, 2000. Cells on the move: a dialogue between polarization and motility. IUBMB Life 49(2):89-96.

Matei AE, Chen CW, Kiesewetter L, Györfi AH, Li YN, Trinh-Minh T, Xu X, Tran Manh C, van Kuppevelt T, Hansmann J, Jüngel A, Schett G, Groeber-Becker F, Distler JHW, 2019. Vascularised human skin equivalents as a novel in vitro model of skin fibrosis and platform for testing of antifibrotic drugs. Ann Rheum Dis 78(12):1686-1692.

Melincovici CS, Boşca AB, Şuşman S, Mărginean M, Mihu C, Istrate M, Moldovan IM, Roman AL, Mihu CM, 2018. Vascular endothelial growth factor (VEGF) - key factor in normal and pathological angiogenesis. Rom J Morphol Embryol 59(2):455-467.

Nagaraja S, Chen L, DiPietro LA, Reifman J, Mitrophanov AY, 2019. Predictive Approach Identifies Molecular Targets and Interventions to Restore Angiogenesis in Wounds With Delayed Healing. Front Physiol 10:636.

Neofytou1 EA, Chang E, Patlola B, Joubert L, Rajadas J, Gambhir SS, Cheng Z, Robbins RC, Beygui RE, 2011. Adipose tissue-derived stem cells display a proangiogenic phenotype on 3D scaffolds. J Biomed Mater Res A. 98(3): 383–393.

Neubauer-Geryk J, Hoffmann M, Wielicka M, Piec K, Kozera G, Brzeziński M, Bieniaszewski L, 2019. Current methods for the assessment of skin microcirculation: Part 1. Postepy Dermatol Alergol 36(3):247-254.

Oike Y, Ito Y, Maekawa H, Morisada T, Kubota Y, Akao M, Urano T, Yasunaga K, Suda T, 2004. Angiopoietin-related growth factor (AGF) promotes angiogenesis. Blood 103(10):3760-5.

Peters EB, 2018. Endothelial Progenitor Cells for the Vascularization of Engineered Tissues. Tissue Eng Part B Rev 24(1):1-24.

Pikula M, Langa P, Kosikowska P, Trzonkowski P, 2015. [Stem cells and growth factors in wound healing]. Postepy Hig Med Dosw (Online) 69:874-85.

Reinke JM, Sorg H, 2012. Wound Repair and Regeneration. Eur Surg Res 49:35–43.

Rodrigues M, Kosaric N, Bonham CA, Gurtner GC, 2019. Wound Healing: A Cellular Perspective. Physiol Rev ;99(1):665-706.

Schöneberg J, De Lorenzi F, Theek B, Blaeser A, Rommel D, Kuehne AJC, Kießling F, Fischer H, 2018. Engineering biofunctional in vitro vessel models using a multilayer bioprinting technique. Scientific Reports 8:10430.

Takeo M, Lee W, Ito M, 2015. Wound healing and skin regeneration. Cold Spring Harb Perspect Med 5(1): a023267.

Traktuev DO, Prater DN, Merfeld-Clauss S, Sanjeevaiah AR, Saadatzadeh MR, Murphy M, Johnstone BH, Ingram DA, March KL, 2009. Robust functional vascular network formation in vivo by cooperation of adipose progenitor and endothelial cells. Circ Res 104(12):1410-20.

Tremblay P, Hudon V, Berthod F, Germain L, Auger FA, 2005. Inosculation of tissue-engineered capillaries with the host's vasculature in a reconstructed skin transplanted on mice. Am J Transplant 5(5):1002-10.

Velnar T, Gradisnik L, 2018. Tissue Augmentation in Wound Healing: the Role of Endothelial and Epithelial Cells. Med Arch 72(6):444-448.

Vitacolonna M, Belharazem D, Hohenberger P, Roessner ED, 2017. In-vivo quantification of the revascularization of a human acellular dermis seeded with EPCs and MSCs in co-culture with fibroblasts and pericytes in the dorsal chamber model in pre-irradiated tissue Cell Tissue Bank 18:27–43.

Wang J, Jinying Chen J, Kuo S, Mitchellv GM, Lim SY, Liu G, 2019. Methods for Assessing Scaffold Vascularization In Vivo. Methods Mol Biol 1993:217-226.

Werner S, Grose R, 2003. Regulation of wound healing by growth factors and cytokines. Physiol Rev 83(3):835-70.

Wolgemuth CW, 2005. Lamellipodial contractions during crawling and spreading. Biophys J 89(3):1643-9.

Wu S, Bezanilla M, 2018. Actin and microtubule cross talk mediates persistent polarized growth. J Cell Biol 217(10):3531-3544.

Zakharov P, Dewarrat F, Caduff A, Talary MS, 2011. The effect of blood content on the optical and dielectric skin properties. Physiol. Meas. 32, 131–149.

Chapter 3

Engineered skin integration with the host tissue
The role of the innervation

3.1 Skin innervation

Skin is the centre of perception of numerous stimuli coming from the external environment. From the dorsal root ganglia originate nerve fibers that reach the dermis and then penetrate the basement membrane innervating epidermal cells or remaining as free endings (Boulais and Misery, 2008).
All epidermal cells (keratinocytes, melanocytes, Langerhans cells and Merkel cells) express sensor proteins and neuropeptides regulating the neuro-immuno-cutaneous system. Especially Langerhans cells and mast cells strengthen the communication between neuroendocrine and immune systems (Misery, 1998; Hsieh, 1997; Ashrafi et al., 2016; Blake et al., 2019). More specifically, the cutaneous peripheral nervous system can be divided in two functional units: afferent sensory innervation and efferent autonomic innervation. The first, is sensitive or somatic innervation and is involved in the detection of mechanical, thermal and painful stimuli, whereas the second, defined as autonomous or vegetative innervation, is involved in the endocrine control and in skin thermoregulation (Schulze et al., 1997; Lumpkin and Caterina, 2007; Glatte et al., 2019). Long axons originating from cell bodies in the dorsal root ganglia (DRGs), close to the spinal cord, provide sensory epidermal innervation. DRG cells have a bifurcated axon and are pseudounipolar neurons. These cells link sensory endings in the skin with the synapses in the dorsal horn of the spinal cord (Tandrup, 1995). Nerve fibers into the skin may terminate freely in the epidermis and dermis or around blood vessels, hair follicles, and sweat glands (Hendrix et al., 2008). Autonomic cutaneous nerves, partially exposed from their Schwann-cell sheaths, result in varicosities that enable the non-synaptic release of neurotransmitters and neuropeptides along the axon (Hilarp, 1959; Myers et al., 2013). Peptidergic nerve fibers interact with the main cells of the skin such as dermal fibroblasts, keratinocytes, mast cells, or Langerhans cells (Peters et al., 2006). Sensory neurons release neuropeptides such as calcitonin gene–related peptide (CGRP) and substance P (SP) which bind their specific receptors on skin cells regulating the inflammatory process (Black, 2002; Peters et al., 2006).

Nerves, blood and lymphatic vessels all run through the skin and form vascular-nervous plexuses. In particular, neurovegetative fibres usually arise from paravertebral sympathetic chains and are not myelinated. They innervate the vascular network, hair erector muscles and sweat glands. From these nerve fibers many neurotransmitters are released, like acetylcholine, that is related to some parasympathetic fibers and sympathetic fibers of sweat glands. Numerous myelinated nerve fibres nourish these glands. Instead, sensitive axons are myelinated in the dermis and unmyelinated into the epidermis (Myers et al., 2013). From the anatomical standpoint a plexus of nerve fibers raises from the deep dermis reaching the surface of the dermis and connecting to a second plexus.

Free nerve fibers into the skin are small calibre fibers and transmit noxious stimuli such as thermal ones. These thinly myelinated (Aδ) or unmyelinated (C) fibers pass from the subepidermal neural plexus and end into the dermis or in the dermo-epidermal junction running between keratinocytes (Myers et al., 2013).

Large, myelinated Aβ calibre fibers, innervating cutaneous mechanoreceptors, transmit mechanical sensory signals. Therefore, in hairy skin, Aβ fibers innervate vascular structures like arteriovenous anastomoses (AVAs) and hair follicles that act as mechanical sensory receptors by detecting changes in hair position.

Since in the glabrous skin there is a major quantity of mechanoreceptors, myelinated fibers are principally distributed in this kind of condition (Fig.3.1) (Nolano et al., 2003; Provitera, 2007).

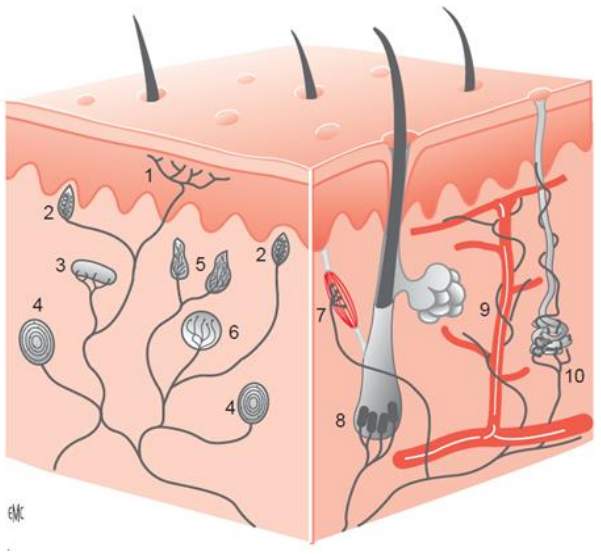

Fig. 3.1 | 1. Intraepidermal free nerve fibers; 2. Merkel corpuscles; 3. Meissner corpuscles; 4. Pacini corpuscles; 5. Ruffini corpuscles; 6. Golgi Mazzoni corpuscles; 7. Hair erector muscle; 8. Perifullicular lanceolate fibers; 9. Perivascular nervous fibers; 10. Nerve fibers of the sweat glands (Misery, 2007).

The principal actors of mechanoperception are Meissener corpuscles (MCs) and Merkel complexes located respectively in the apex and base of dermal papillae immediately below the epidermal basement membrane. Pacinian corpuscles and Ruffini endings are also low-threshold mechanoreceptors located in glabrous skin (Li et al., 2011). Sensory perception is mediated by different cell types in the skin including Merkel cells, terminal Schwann cells, and basal keratinocytes in the epidermis. Merkel cells can be found in the basal layer of the epidermis as well as the root sheath of hair follicles (Boulais et al., 2007).

Merkel cells are transformed epidermal cells with oval-shaped located in the *stratum basale*, immediately above the basement membrane. These cells mediate a sensory perception as mechanoreceptors do for light touch and are linked to keratinocytes by desmosomes while their membranes are associated to the free nerve fibers of the skin. Merkel cells release substance

P (SP) activating keratinocytes to promote proliferation in wound healing (Liu et al., 2006). On the other hand, Merkel cell-derived calcitonin gene-related peptide (CGRP) may inhibit immune cells recruitment and modulate immune function (Feng et al., 2019).

The most abundant cells in the epidermis are basal keratinocytes which have been shown to express vanilloid thermoreceptors like TRPV1,2. Signal transduction is mediated by these receptors when keratinocytes undergo mechanical stress that increases intracellular calcium levels (Nagasawa and Kojima, 2015). Keratinocytes also play a critical role in nerve regeneration, although the mechanism of communication with peripheral dermal nerves is still unknown; thus, direct evidence is still lacking. Melanocytes, which produce photoprotective melanin, are also in close contact with sensory endings (Fig.3.2).

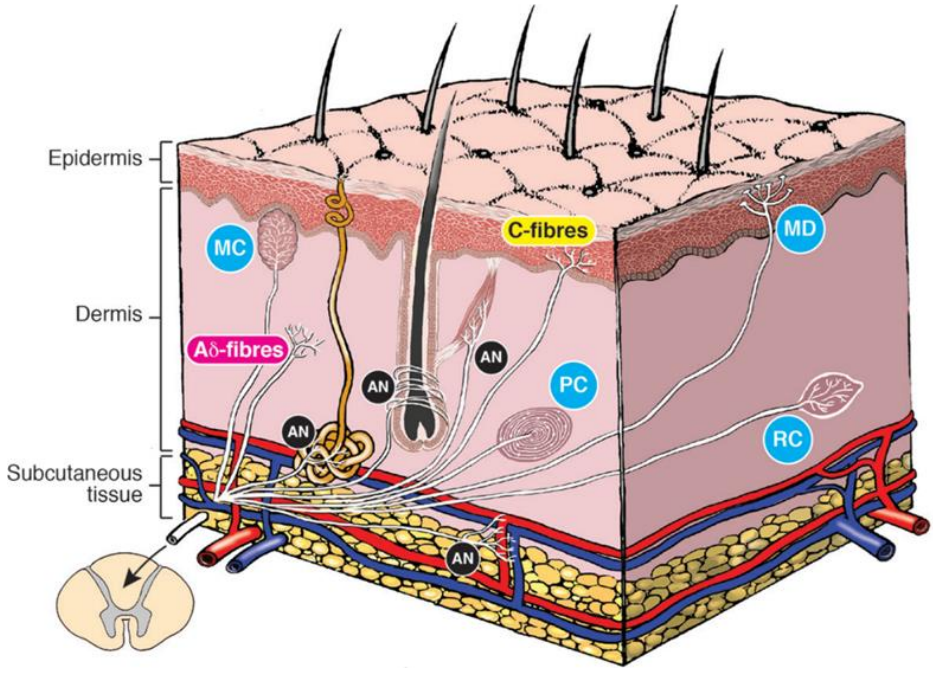

Fig.3.2 | Cross section outlining distribution and morphological features of the different nervous structures involved in skin innervation. MC: Meissner's corpuscles; MD: Merkel disc; PC: Pacinian corpuscle; RC: Ruffini's corpuscle; AN: autonomic nerves (Ashrafi et al., 2016).

3.2 Neurotrophins

Neurotrophins (NTs) belong to a family of growth factors, which control the development, maintenance, and apoptotic death of neurons also fulfilling multiple regulatory functions outside the nervous system. Biological effects induced by NTs strongly depend on the pattern of NT receptor/co-receptors expression in target cells as well as on the set of intracellular adaptor molecules that link NT signalling to distinct biochemical pathways (Richardt, 2006; Khan and Smith, 2015).

NTs are represented by molecules such as nerve growth factor (NGF), brain-derived neurotrophic factor (BDNF), neurotrophin-3 (NT-3), and neurotrophin 4/5 (NT-4/5). They also play a critical role in neuropathic pain and act cardiovascular functions (Khan and Smith, 2015).

Neurotrophins are structurally related dimeric proteins that were originally viewed as neuronal survival factors released from target tissues (Al-Qudah and Al-Dwairi, 2016). These molecules have common chemical and structural properties such as more than 50% sequence homologies in the primary structure, similar molecular weight, 3 disulfide bonds that form a cysteine knot and isoelectric points ranging from 9-10 and exert their biological effects as dimers interacting with specific receptors (Huang and Reichardt, 2001; Skaper, 2012; Bothwel, 2014). The study of the intracellular biosynthesis and sorting of neurotrophins within a cell can be useful to understand how these molecules are released and how they act in both physiological and pathological conditions like synaptic plasticity, memory formation, neurodegenerative disorders, demyelination diseases and inflammation. In general, NTs are produced as precursors, pre-pro-neurotrophins, on the rough endoplasmic reticulum (ER) (Leßmann and Brigadski, 2009). These pre-sequences guide nascent neurotrophins polypeptide synthesis inside the ER where are cleaved off immediately and where the pro-neurotrophins can dimerize into homodimers and to finally to heterodimers. Post-translational take place while the pro-neurotrophins are translocated from Golgi apparatus to the trans-Golgi network (TGN) (Teng and Hempstead, 2004).

After the passage into the TGN NTs are meticulously sorted. At this point NTs secretion could be constitutive or regulated. In the first case small-diameter (50-100 nm) secretory vesicles are involved independently of any triggering stimulus represented by the release of calcium2+ (Ca2+). The second way of secretion involves larger (100-300 nm) secretory vesicles, released by the TGN, and fuse with plasma membrane only in case of an extracellular triggering event in presence of the release of Ca+2 (Fig.3.3) (Leßmann and Brigadski, 2009).

Despite neurotrophins, for a long time, have been considered especially by neuroscientists for their actions on nervous system, during the last decades the attention has fallen also on other relevant functions such as the cardiovascular ones (Caporali and Emanueli, 2009). Indeed, during cardiovascular development, NTs are essential for the formation of the heart and in the postnatal life they are fundamental to control the survival of endothelial cells, vascular smooth muscle cells, and cardiomyocytes as well as to regulate angiogenesis and vasculogenesis by autocrine and paracrine mechanisms. Another important feature related to NTs is the critical role played in the early development of nervous system (Bernd, 2008).

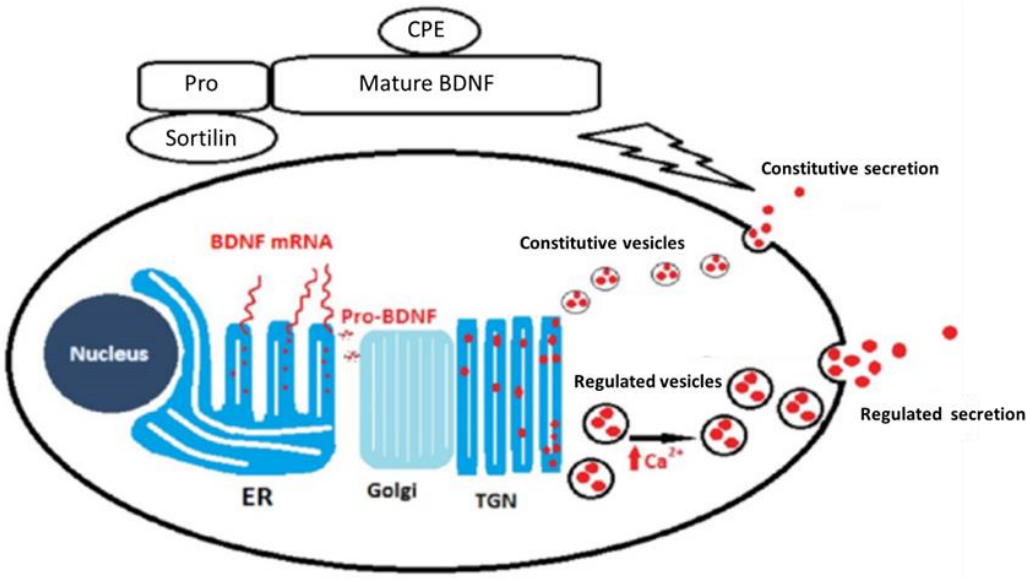

Fig. 3.3 | Neurotrophin synthesis and sorting.
Neurotrophins are synthesized as pre-pro-neurotrophins on the rough endoplasmic reticulum (ER) and then move to the Golgi apparatus to accumulate in the trans-Golgi network (TGN). In the TGN, neurotrophins are sorted to either the constitutive secretory vesicles or the regulated secretory granules. Sortilin and carboxypeptidase E (CPE) are important sorting receptors that mediate neurotrophins targeting to the regulated secretory granules. BDNF - brain derived neurotrophic factor, mRNA - messenger ribonucleic acid (Al-Qudah2016).

3.3 Neurotrophin receptors

High affinity receptors for NTs belong to the tyrosine kinase family: tyrosine kinase receptor A (TrkA) is the high-affinity receptor for NGF, tyrosine kinase receptor B (TrkB) is the high-affinity receptor for BDNF and NT-4, and tyrosine kinase receptor C (TrkC) is the high-affinity receptor for NT-3 (Mitre et al., 2017). However, NT-3 can also bind with low affinity to TrkA and TrkB receptors. All four NTs interact with the low-affinity p75 kDa NT receptor (p75NTR), which is a member of the tumor necrosis factor family of receptors containing the cytoplasmic ‘‘death’’ domain, involved in mediating a number of responses independently or in association with Trk receptors (Roux and Barker, 2002; Makkerh et al., 2005; Reichardt, 2006;

Scott-Solomon and Kuruvilla, 2018). The interaction between NTs and their receptors induces numerous different processes like proliferation, differentiation and survival both for neuronal cells than other kind of cells. All these mechanisms require Trk receptors dimerization,
autophosphorylation and the involvement of different molecules that permit the beginning of three different molecular pathways that involve Ras, phosphatidylinositol 3-kinase, and phospholipase C-γ1(PLC-γ1), and their downstream cascading proteins. Ras activation controls normal survival and differentiation by activating mitogen-activated protein kinase (MAPK) cascades. Phosphatidylinositol 3-kinase governs several neuronal functions such as survival and neurite outgrowth through activation of the protein kinase B commonly known as AKT Lastly, PLC-γ1 activation accounts mainly for the control of activity-dependent synaptic plasticity (Skaper, 2012; Deinhardt and Chao, 2014).
About p75NTR, it performs different functions depending on whether it is associated with Trk receptors or with other growth receptors or if is alone. When linked to Trk receptors p75 increases high-affinity NT binding, enhances Trk ability to discriminate a preferred ligand from the other NTs, and promotes survival effects of the NTs. When p75NTR is co-expressed with sortilin (a non-Gprotein- coupled neurotensin receptor), NT precursor proteins (pro-NTs) interacting with p75NTR–sortilin complex induce apoptotic death (Meeker and Williams, 2015). The co-expression of p75NTR with the Nogo receptor complex results in inducing growth inhibition. When p75NTR is expressed alone on the cell surface, mature NT peptides or selected non-NT ligands are capable of inducing apoptosis (Teng and Hempstead, 2004).
In postnatal mice skin, NTs and their receptors are differentially distributed in distinct cell populations. NGF and NT-4 are expressed in basal epidermal keratinocytes in humans and mice (Tron, 1990).
Nerve growth factor is secreted by several cutaneous cells including keratinocytes, fibroblasts, nerves and adipocytes (Fig. 3.4) (Shi et al., 2013).

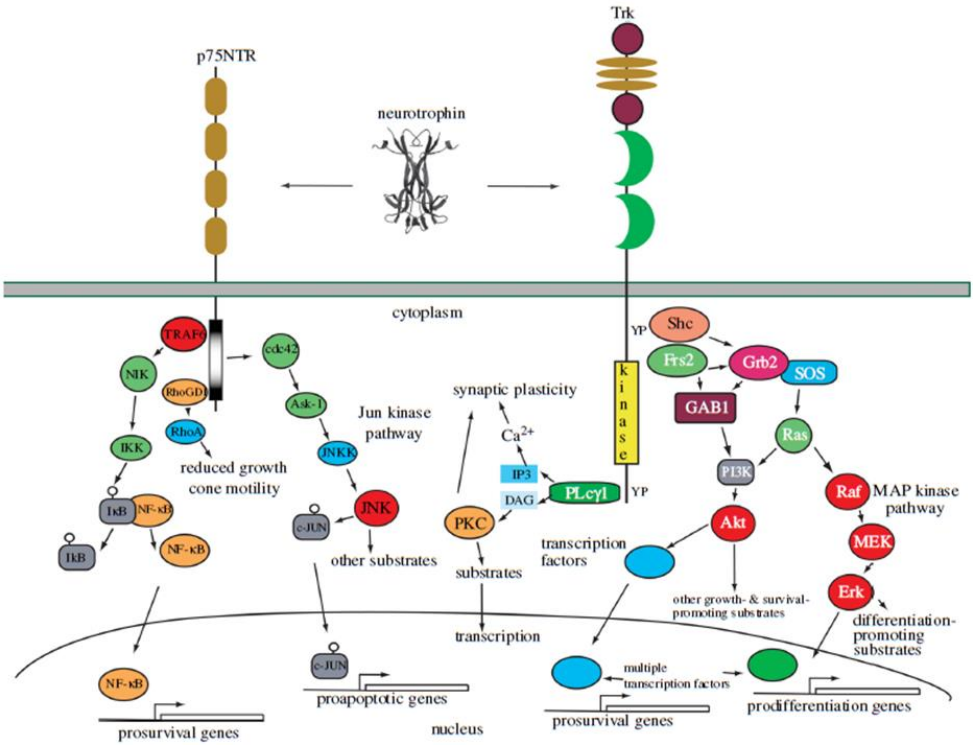

Fig.3.4 | Neurotrophin signalling pathways in particular the interactions of each neurotrophin with Trk and p75NTR receptors and major intracellular signalling pathways activated through each receptor. The p75NTR receptor regulates three major signalling pathways. NF-kB activation results in transcription of multiple genes, including several that promote neuronal survival. Activation of the Jun kinase pathway similarly controls activation of several genes, some of which promote neuronal apoptosis. Ligand engagement of p75NTR also regulates the activity of Rho, which controls growth cone motility. Each Trk receptor also controls three major signalling pathways. Activation of Ras results in activation of the MAP kinase-signalling cascade, which promotes neuronal differentiation including neurite outgrowth. Activation of PI3 kinase through Ras or Gab1 promotes survival and growth of neurons and other cells. Activation of PLC-y1 results in activation of Ca2C- and protein kinase C-regulated pathways that promote synaptic plasticity. Each of these signalling pathways also regulates gene transcription. (Richardt 2006).

3.4 Neurotrophins in the skin

NTs regulate cutaneous sensory innervation. NTs also regulate growth, survival, differentiation, function, and plasticity of neuronal cells but they do much more than this being involved in the growth and survival of skin cells. These molecules accomplish different functions in the skin like homeostasis regulation and angiogenesis promotion. NGF was the first neurotrophic factor identified as a molecule able to induce the synthesis and development of sensory neurons that, in turn, extend their dendrites into the skin, thus playing an essential role in skin innervation (Truzzi et al., 2011). NGF is also linked to the process of angiogenesis especially in the context of skin repair, remodelling, and pathogenesis of some diseases like psoriatic skin (Blais et al., 2013). Besides NGF also other NTs like BDNF are strictly related to the modulation of the dermal microvascular network in a physiological skin tissue as well as in pathological situation like wound healing. Despite the lack of precisely quantification of each neurotrophin in the skin, it was established that these molecules are highly expressed into the skin and are also potent angiogenic factors.

It has been demonstrated that the knock-out condition for genes from the NGF family and their receptors (NTRs) induce the loss/reduction of specific neurons in sensory ganglia. Therefore, cutaneous overexpression of these genes leads to hyperinnervation of the skin (Montaño et al., 2009). NGF is also involved in cutaneous neurogenic inflammation stimulating the release of neuropeptides in the skin. Therefore, in 1994, it has been demonstrated that normal human keratinocytes produce NGF which, once released, acts as a growth factor for these cells (Pincelli et al., 1994). Several studies have therefore shown that NGF and other NTs accomplish numerous functions respect to skin cells.

In addition to NGF, also NT-4 is expressed by basal epidermal in humans and mice (Botchkarev et al., 1999) while keratinocytes also produce BDNF and NT3 (Di Marco et al., 1991; Marconi et al.,2003). It is interesting to highlight that NGF is produced by keratinocytes at highest levels as compared to the other NTs.

UVA induce NT-3 release, whereas NGF expression is downregulated by UVB irradiation (Stefanato et al., 2003). NGF induces human keratinocytes proliferation and stimulates or inhibits murine epidermal and hair follicle keratinocyte proliferation *in situ* (Di Marco et al., 1993). Consequently, human keratinocytes express the high affinity receptors TrkA and TrkC binding respectively, with high affinity, NGF and NT3, but not the functional form of the TrkB that binds with high affinity BDNF (Marconi et al., 2003). NT together with their receptors TrkA and TrkB stimulate mouse keratinocyte proliferation in *ex-vivo* cultured skin explants (Paus et al., 1994).

Since human keratinocytes typically lack TrkB expression, NTs may exert different functions in this system by binding p75NTR alone acting as a proapoptotic receptor.

NGF is mostly expressed and released by stem keratinocytes and blocking TrkA inhibits the proliferation of this keratinocyte subpopulation (Marconi et al., 2003). This seems to indicate that an NGF-TrkA autocrine loop, by acting as both a mitogenic and survival factor, contributes to the maintenance of the so-called “stemness” in keratinocytes.

Dermal fibroblasts and more differentiated myofibroblasts synthetize NTs and their receptors. Especially, p75NTR and TrkB are expressed at higher levels in myofibroblasts, and dermal fibroblasts secrete NGF and NT3 at higher levels than NT4 and BDNF. Therefore, endogenous production of NT is sufficient to normal cell activity and survival. NTs also promote fibroblast differentiation into myofibroblasts, by inducing α-SMA expression, indicating that NT could have a functional role in the fibro-myofibroblast system (Palazzo et al., 2012). It has been demonstrated that all NTs promote fibroblast migration while NGF and BDNF promote their contractile activity.

Therefore, NGF and BDNF, produced by dermal and epidermal cells, could be key regulators of the biomechanical properties of the dermis (Aloe et al., 2008; Sun et al., 2009).

Another fundamental cellular population in the skin are melanocytes which are located in the dermo-epidermal junction and in the hair matrix. NTs are involved in the migration and differentiation of these cells. Normal human

melanocytes also express p75NTR while NGF is implicated in melanocyte survival (Zhai et al., 1996).

NTs are crucial for protection of UV-induced oxidative stress and apoptosis in melanocytes. Moreover, when melanocytes are irradiated with UV, NGF reduces apoptosis via upregulation of the anti-apoptotic Bcl-2 protein (Stefanato et al., 2003). Therefore, when melanocytes are maintained in growth factor-depleted medium, NGF and NT-3 promote melanocyte survival. Human melanocytes also express Trk receptors and the NT low affinity receptor p75NTR (Yaar et al., 1994).

Finally, NTs play a critical role in the process of re-innervation of a damaged tissue, especially NGF mediates re-innervation when released in high concentrations during inflammation.

During cutaneous inflammation, there is NGF-dependent production of SP, CGRP, sodium channels, and other neurotransmitters and neuropeptides or molecules related to nociception.

NTs also regulate the activity of immune cells in normal skin and in numerous pathological conditions including wound healing, inflammation, psoriasis, and atopic dermatitis, as well as in the allergic, autoimmune, and stress induced skin responses. In particular, NGF accomplishes different functions during the inflammatory process and is upregulated in cutaneous nerves following inflammation. Therefore, NGF is a perfect key mediator between nervous and immune systems (Minnone et al., 2017).

In a healthy skin, endothelial cells, mast cells and macrophages express NGF and its high affinity receptor TrkA (Li, 2019). NGF also induce degranulation and cytokine release from skin mast cells thus promoting neurogenic inflammation (Valente et al., 2018).

Moreover, NTs are involved in the control of lymphocyte development and T-lymphocytes can produce NGF and BDNF (Fig.3.5) (Vega et al., 2003).

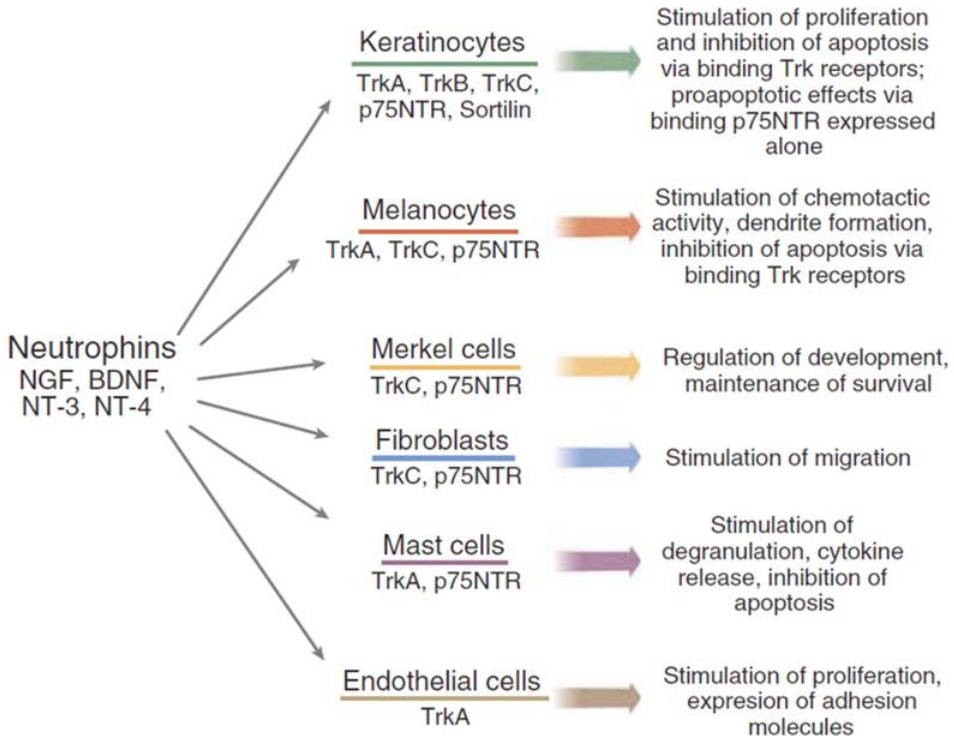

Fig 3.5 | Scheme illustrating the effects of NTs on distinct cell populations in the skin. Note that neurotrophins play different roles respect to the various cells present into the skin. Keratinocytes, express the majority of Trk receptors and p75NTR and are the most involved cells in this communication with neurotrophin (Botchkarev et al., 2006).

Aloe L, Tirassa P, Lambiase A, 2008. The topical application of nerve growth factor as a pharmacological tool for human corneal and skin ulcers. Pharmacological Research 57 253–258.

Al-Qudah MA, Al-Dwairi A, 2016. Mechanisms and regulation of neurotrophin synthesis and secretion. Neurosciences (Riyadh) 21(4):306-313.

Ashrafi M, Baguneid M, Bayat A, 2016. The Role of Neuromediators and Innervation in Cutaneous Wound Healing. Acta Derm Venereol 96: 587 594.

Ashrafi M, Baguneid M, Bayat A, 2016. The Role of Neuromediators and Innervation in Cutaneous Wound Healing. Acta Derm Venereol 96: 587 594.

Bernd P, 2008. The role of neurotrophins during early development Gene Expr 14(4):241-50.

Black PH, 2002. Stress and the inflammatory response: A review of neurogenic inflammation. Brain, Behavior, and Immunity 16, 622–653.

Blais M, Lévesque P, Bellenfant S, Berthod F, 2013. Nerve growth factor, brain-derived neurotrophic factor, neurotrophin-3 and glial-derived neurotrophic factor enhance angiogenesis in a tissue-engineered in vitro model. Tissue Eng Part A 19(15-16):1655-64.

Blake KJ, Jiang XR, Chiu IM, 2019. Neuronal Regulation of Immunity in the Skin and Lungs. Trends Neurosci. 42(8): 537–551.

Botchkarev VA, Metz M, Botchkareva NV, Welker P, Lommatzsch M, Renz H, Paus R, 1999. Brain-derived neurotrophic factor, neurotrophin-3, and neurotrophin-4 act as "epitheliotrophins" in murine skin. Lab Invest 79(5):557-72.

Botchkarev VA, Yaar M, Peters EM, Raychaudhuri SP, Botchkareva NV, Marconi A, Raychaudhuri SK, Paus R, Pincelli C 2006. Neurotrophins in skin biology and pathology. J Invest Dermatol. 126(8):1719-27.

Bothwell M, 2014. The Neurotrophin Family NGF, BDNF, NT3, and NT4. Handbook of Experimental Pharmacology 220.

Boulais N, Misery L, 2008. The epidermis: a sensory tissue. Eur J Dermatol 18 (2): 119-27.

Boulais N, Pereira U, Lebonvallet N, Misery L, 2007. The whole epidermis as the forefront of the sensory system. Exp Dermatol 16(8):634-5.

Caporali A, Emanueli C, 2009. Cardiovascular Actions of Neurotrophins. Physiol Rev. 89(1): 279–308.

Deinhardt K, Chao MV, 2014. Trk Receptors. Handbook of Experimental Pharmacology 220.

Di Marco E, Marchisio PC, Bondanza S, Franzi AT, Cancedda R, De Luca M, 1991. Growth-regulated synthesis and secretion of biologically active nerve growth factor by human keratinocytes. J Biol Chem 266(32):21718-22.

Di Marco E, Mathor M, Bondanza S, Cutuli N, Marchisio PC, Cancedda R, De Luca M, 1993. Nerve growth factor binds to normal human keratinocytes through high and low affinity receptors and stimulates their growth by a novel autocrine loop. J Biol Chem 268(30):22838-46.

Expression and function of neurotrophins and their receptors in cultured human keratinocytes

Feng J, Hu H, 2019. A novel player in the field: Merkel disk in touch, itch, and pain. Exp Dermatol. 28(12): 1412–1415.

Glatte P, Buchmann SJ, Hijazi MM, Illigens BM, Siepmann T, 2019. Architecture of the Cutaneous Autonomic Nervous System. Front. Neurol. 10:970.

Hendrix S, Picker B, Liezmann C, Peters EMJ, 2008. Skin and hair follicle innervation in experimental models: a guide for the exact and reproducible evaluation of neuronal plasticity. Exp Dermatol 17(3):214-27.

Hilarp NA, 1959. The construction and functional organization of the autonomic innevvation apparatus. Acta Physiol Scand Suppl 46: 1–21.

Hsieh ST, Lin WM, Chiang HY, Huang IT, Ko MH, Chang YCh, Chen WP, 1997. Skin Innervation and Its Effects on the Epidermis J Biomed Sci 4(5):264-268. doi: 10.1007/BF02253428.

Huang EJ, Reichardt LF, 2001. Neurotrophins: Roles in Neuronal Development and Function. Annu Rev Neurosci. 24: 677–736.

Khan N, Smith MT, 2015. Neurotrophins and Neuropathic Pain: Role in Pathobiology. Molecules 20, 10657-10688.

Leßmann V, Brigadski T, 2009. Mechanisms, locations, and kinetics of synaptic BDNF secretion: An update. Neuroscience Research 65 11–22.

Li L, Rutlin M, Abraira VE, Cassidy C, Kus L, Gong S, Jankowski MP, Luo W, Heintz N, Koerber HR, Woodbury CJ, Ginty DD, 2011. The functional organization of cutaneous low-threshold mechanosensory neurons. Cell. 147(7): 1615–1627.

Liu JY, Hu JH, Zhu QG, Li FQ, Sun HJ, 2006. Substance P receptor expression in human skin keratinocytes and fibroblasts. Br J Dermatol 155(4):657-62.

Lumpkin EA, Caterina MJ, 2007. Mechanisms of sensory transduction in the skin. Nature Vol 445.

Makkerh JPS, Ceni C, Auld DS, Vaillancourt F, Dorval G, Barker PA, 2005. p75 neurotrophin receptor reduces ligand-induced Trk receptor ubiquitination and delays Trk receptor internalization and degradation. EMBO Rep 6(10):936-41.

Marconi A, Terracina M, Fila C, Franchi J, Bonté F, Romagnoli G, Maurelli R, Failla CM, Dumas M, Pincelli C, 2003. J Invest Dermatol 121(6):1515-21.

Meeker RB, Williams KS, 2015. The p75 neurotrophin receptor: at the crossroad of neural repair and death. Neural Regen Res. 10(5): 721–725.

Minnone G, De Benedetti F, Bracci-Laudiero L, 2017. NGF and Its Receptors in the Regulation of Inflammatory Response. Int J Mol Sci 18(5):1028.

Misery L, 1998. Langerhans cells in the neuro-immuno-cutaneous system. J Neuroimmunol 14;89(1-2):83-7.

Misery L, 2007. Innervazione cutanea. EMC - Medicina Riabilitativa 14, 1-4.

Mitre M, Mariga A, Chao MV, 2017. Neurotrophin signalling: novel insights into mechanisms and pathophysiology. Clin Sci (Lond). 131(1): 13–23.

Montaño JA, Pérez-Piñera P, García-Suárez O, Cobo J, Vega JA, 2010. Development and neuronal dependence of cutaneous sensory nerve formations: Lessons from neurotrophins. Microsc Res Tech 73(5):513-29.

Myers MI, Peltier AC, Li J, 2013. Evaluating dermal myelinated nerve fibers in skin biopsy. Muscle Nerve 47(1): 1–11.

Nagasawa M, Kojima I, 2015. Translocation of TRPV2 channel induced by focal administration of mechanical stress. Physiol Rep, 3 (2), e12296.

Nolano M, Provitera V, Crisci C, Stancanelli A, Wendelschafer-Crabb G, Kennedy WR, Santoro L, 2003. Quantification of Myelinated Endings and Mechanoreceptors in Human Digital Skin. Ann Neurol 54:197–205.

Palazzo E, Marconi A, Truzzi F, Dallaglio K, Petrachi T, Humbert P, Schnebert S, Perrier E, Dumas M, Pincelli C, 2012. Role of neurotrophins on dermal fibroblast survival and differentiation J Cell Physiol 227(3):1017-25. doi: 10.1002/jcp.22811.

Paus R, Lüftl M, Czarnetzki BM, 1994. Nerve growth factor modulates keratinocyte proliferation in murine skin organ culture. Br J Dermatol 130(2):174-80.

Peters EMJ, Ericson ME, Hosoi J, Seiffert K, Hordinsky MK, Ansel JC, Paus R, Scholzen TE, 2006. Neuropeptide Control Mechanisms in

Cutaneous Biology: Physiological and Clinical Significance. Journal of Investigative Dermatology 126, 1937–1947.

Pincelli C, Fantini F, Giannetti A, 1994. Nerve growth factor and the skin. Internation Journal of Dermatology 33:5

Reichardt LF, 2006. Neurotrophin-regulated signalling pathways. Phil. Trans. R. Soc. B 361, 1545–1564.

Roux PP, Barker PA, 2002. Neurotrophin signaling through the p75 neurotrophin receptorProg Neurobiol 67(3):203-33.

Schulze E, Witt M, Fink T, Hofer A, Funk RHW, 1997. Immunohistochemical detection of human skin nerve fibers. Acta histochem. 99, 301-309 (1997).

Scott-Solomon E, Kuruvilla R, 2018. Mechanisms of Neurotrophin Trafficking via Trk Receptors Mol Cell Neurosci. 91: 25–33.

Shi X, Wang L, Clark JD, Kingery WS, 2013. Keratinocytes express cytokines and nerve growth factor in response to neuropeptide activation of the ERK1/2 and JNK MAPK transcription pathways. Regul Pept 186:92-103.

Skaper SD, 2012. Neurotrophic factors. Methods and protocols. Methods in Molecula Biology 846.

Sousa-Valente J, Calvo L, Vacca V, Simeoli R, Arévalo JC, Malcangio M, 2018. Role of TrkA signalling and mast cells in the initiation of osteoarthritis pain in the monoiodoacetate model. Osteoarthritis and Cartilage 26 84e94.

Stefanato CM, Yaar M, Bhawan J, Phillips TJ, Kosmadaki MG, Botchkarev V, Gilchrest BA. Modulations of nerve growth factor and Bcl-2 in ultraviolet-irradiated human epidermis. J Cutan Pathol 30(6):351-7.

Sun W, Lin H, Chen B, Zhao W, Zhao Y, Xiao Z, Dai J, 2009. Collagen scaffolds loaded with collagen-binding NGF-beta accelerate ulcer healing. J Biomed Mater Res A 92(3):887-95.

Tandrup T, 1995. Are the neurons in the dorsal root ganglion pseudounipolar? A comparison of the number of neurons and number of myelinated and unmyelinated fibres in the dorsal root. J Comp Neurol 357(3):341-7.

Teng KK, Hempstead BL, 2004. Neurotrophins and their receptors: signaling trios in complex biological systems. Cell Mol Life Sci 61(1):35-48.

Tron VA, Coughlin MD, Jang DE, Stanisz J, Sauder DN, 1990. Expression and modulation of nerve growth factor in murine keratinocytes (PAM 212). J Clin Invest 85(4):1085-9.

Truzzi F, Marconi A, Pincelli C, 2011. Neurotrophins in healthy and diseased skin. Dermato-Endocrinology 3:1, 32-36.

Vega JA, García-Suárez O, Hannestad J, Pérez-Pérez M, Germanà A, 2003. Neurotrophins and the immune system. J Anat 203(1):1-19.

Vincenzo Provitera V, Maria Nolano M, Angela Pagano A, Giuseppe Caporaso G, Annamaria Stancanelli A, Lucio Santoro L, 2007. Myelinated nerve endings in human skin. Muscle Nerve 35(6):767-75.

Yaar M, Eller MS, DiBenedetto P, Reenstra WR, Zhai S, McQuaid T, Archambault M, Gilchrest BA, 1994. The trk family of receptors mediates nerve growth factor and neurotrophin-3 effects in melanocytes. J Clin Invest 94(4):1550-62.

Zhai S, Yaar M, Doyle SM, Gilchrest BA, 1996. Nerve growth factor rescues pigment cells from ultraviolet-induced apoptosis by upregulating BCL-2 levels. Exp Cell Res 224(2):335-43. doi: 10.1006/excr.1996.0143.

Chapter 4
Aims of the work

4.1 AIMS

In the field of skin tissue engineering numerous advances have been performed over the last decades and many skin substitutes have been launched on the market aiming to overcome skin injuries, burns and pathologies. However, there are still many limitations to their successful use in the clinics due to reduced vascularization, improper scarring, failure to integrate, low mechanical resistance, immune rejection, and loss of sensitivity. One of the main issues of full thickness skin substitute application is the excessively prolonged time of re-vascularization after graft implantation, and, therefore, pre-vascularized constructs may represent an asset.

In this PhD project we investigated a particular pre-vascularized dermis (PVD) produced through a bottom-up technique with the aim of studying how the matrix of this construct encourages both vascularization and innervation after implantation and subsequent integration with the host tissue. We, therefore, aim to demonstrate how and to what extent this construct is suitable to be well integrated with the host tissue after implantation in a full thickness skin defect model.

We chose this model because, respect to the subcutaneous one, it mimics skin physiological conditions, by allowing the replacement of the wound bed and is suitable to be sutured also displaying a significant mechanical resistance.

Wound healing is a key process divided into three different phases: inflammation, proliferation and remodelling. In all these phases many different kinds of cells and molecules are involved. At the beginning of the process platelets are recruited to wound site to arrest bleeding and deposit fibrin that represents a preliminary extracellular matrix. Then, new blood vessels sprout around the wound site while immune cells such as macrophages are recruited to the damaged area. During the first phase of wound healing process macrophages clean the wound from bacteria, over the proliferation phase they promote keratinocytes, fibroblasts, and endothelial cell proliferation while in the remodelling phase they secrete metalloproteinases (MMPs) to remodel the matrix.

Meanwhile, keratinocytes cover the wound bed and fibroblasts produce the extracellular matrix.

In order to investigate the behaviour of our construct in wound healing condition we looked at CD68 to mark macrophages which also play an important role in vascularization by positioning themselves nearby newly forming blood vessels also aiding their stabilization. Finally, we observed the presence and the evolution of the exudate observed in our samples at the time of retrieval at day 3 post-implantation. This wound fluid derives from acute wounds and may have a beneficial effect on wound healing, in contrast with that which can be found in case of chronic wounds, and which may inhibit healing. Changes in the volume and nature of the exudate provide information on the underlying state of the wound and may aldo give an indication of an eventually increasing bacterial load as well as if a wound is likely proceeding to a resolution.

An appreciable integration of a pre-vascularized substitute with the host tissue results in a fast anastomosis between the two vascular networks. However, since integration is a complex process there are other aspects which have to be considered, for example the need the engineered construct to mimic the physiological sensitivity of the host skin.

About vascularization we investigated our samples using lectins such as Griffonia Semplicifolia and Ulex Europeaus Agglutinin to identify murine and human vessels, respectively. The analysis at different timepoints (3,7,14,21 and 42 days after grafting) allowed us to evaluate the evolution of the two vascular networks between the host and the engrafted engineered skin.

In addition, we looked for the quantitative expression of the vascular endothelial growth factor (VEGF) and of hypoxia inducible factor 1-alpha (HIF-1-A) into our samples via RT-PCR.

From the innervation standpoint, to observe the evolution of host nervous fiber invasion of our construct, we focused our attention on different immunofluorescent markers. We investigated Neurofilament-M to identify all the myelinated fibers that eventually re-innervated our construct. Then, we looked at PGP9.5 to identify both myelinated and unmyelinated fibers extending from the host to our construct for two reasons: i) since the

presence of unmyelinated fibers could be representative of a first phase of re-innervation being the newly sprouted nerve fibers unmyelinated, ii) most nociceptive afferents fibers are unmyelinated C fibers.

Neurotrophins act not only as growth and survival molecules for neurons but also for cell type which are constitutive of the skin such as keratinocytes, fibroblasts, melanocytes along with endothelial cells. Therefore, we also investigated the expression of BDNF and NGF and their high affinity receptors TrkB and TrkA in our engineered tissue both pre-implantation and post-retrieval at the different timepoints mentioned above via immunofluorescence analyses.

In addition to a semi-quanttative evaluation, we quantified the expression of BDNF, TrkB and PGP9.5 via RT-PCR.

Finally, since neurotrophins guide fibroblast differentiation into myofibroblasts thus increasing the skin tensile strength we analysed the variation of Young Modulus of our samples via indentation test at 21 and 42 days after implantation.

On the basis of all these analyses we are going to better study the connection between vascularization and innervation during tissue development and maturation.

Chapter 5

Materials and methods

5.1 Pre vascularized human dermis equivalent fabrication

5.1.1 HDFs extraction

Human dermal fibroblasts (HDFs) were extracted from human breast biopsies surplus obtained by "Azienda Ospedaliera di Rilievo Nazionale (AORN) A. Cardarelli/Santobono/Pausillipon (Urology and Biotechnology Units) after approval of the ethical committee. Human skin biopsies were washed in a cool solution of PBS1X + antibiotics (1%penicillin/ streptomycin- Microgem L0022-100- or 5µg/ml gentamicin- SIGMA G1397), PBS1X + antimycotic (1%Amphotericin-SIGMA A2942-) and PBS1X. After rinsing fat was removed and the biopsies were washed again in PBS1X. 3 mm width strips were obtained from cutting skin them and incubation with Dispase (GIBCO 0698) solution 1.8U/mL was performed for 14 h. After epidermis removal, dermal pieces were rinsed in PBS1X, cut in smaller aliquots and put in 2,5 mg/ml collagenase A solution (ROCHE 11088793001) for 40 min at 37 °C. The collagenase was stopped with FBS and then removed by washing the pieces. Afterwards, all the pieces were suspended in a little volume of complete MEM and arranged on a petri dish in order to allow the migration of fibroblasts on the surface of the dish.

5.1.2 Cell culture

After the extraction procedure, human dermal fibroblasts (HDFs) were cultured in enriched MEM composed of: MEM (Microtech L0440-500) with 20% of FBS (Sigma Aldrich), 2% of Non- Essential Aminoacids (EuroClone ECB3054D), 1% of L-Glutamine (Lonza 17-605E) and 1% of penicillin/streptomycin (Microtech L0022- 100), until passage 4/7. HUVECs (GIBCO C0035C) were cultured in supplemented VascuLife®. The final concentrations of the components in the complete kit composed of basal medium along with associated supplements and growth factors were: FGF 5ng/ml, Ascorbic acid 50µg/ml, hydrocortisone hemisuccinate 1µg/ml, FBS 2%, L Glutamine 10mM, IGF-1 105ng/ml, EGF 5ng/ml, VEGF

5ng/ml, Heparin sulfate 0.75U/ml, Gentamicin 30mg/ml and Amphotericin 15µg/ml. Cells were maintained at 37 °C in humidified atmosphere containing 5% CO2.

5.1.3 Micro-scaffold production

Gelatin porous microbeads (GPMs) were prepared according to a modified double emulsion protocol (O/W/O). GPMs were stabilized by crosslinking reaction with glyceraldehyde (GAL) (SIGMA-G5001) in order to make them stable in aqueous environment at 37 °C, as previously described. GAL at 4% w/w of the microbeads was used to perform all the experiments (Imparato et al., 2013).

5.1.4 Micro-tissues production

About 11 HDFs P5/8 were seeded for each bead. Cells were cultured into spinner flask bioreactors (Integra) in continuous agitation (30 rpm) after 6 h of intermitting stirring regime in order to promote cell adhesion (30 min at 0 rpm, 5 min at 30 rpm). The culture medium was enriched MEM supplemented with Ascorbic Acid (2-O-α-D-Glucopyranosiyl-LAscorbic-Acid TCI; Cf: 0.5 mM). µTPs were cultured for 9 days before the assembly phase in order to guarantee the initial collagen synthesis. During this phase human dermal fibroblasts were able to proliferate on the surface and inside the porous gelatin micro-scaffolds forming a thin layer of extracellular matrix (Urciuolo et al., 2016).

5.1.5 Pre-vascularized dermis equivalent model production

µTPs suspension was transferred from the spinner flask to a 50 ml Falcon centrifuge tube and, after settling, transferred by pipetting into the maturation chamber to allow their biosintering. Customized maturation

chambers can be designed depending upon the desired shape and dimension of the final tissue. Rectangular-shaped constructs (7mm x 4 mm of area and 1mm in thickness,) have been used. The assembling chamber was a sandwich-like structure, with a silicon mold in the middle, with empty spaces for μTPs housing. The silicon mold was delimited on both the top and bottom sides by two stainless steel rigid grids characterized by a porous mesh (18 μm). μTPs were inserted in the maturation chamber by using a vacuum pump, the grids retained the μTPs and guaranteed the passage of nutrients and waste products during the culture. The assembling chamber was placed on the bottom of a spinner flask bioreactor (Bellco biotechnology code 1967–00050) and completely surrounded by culture medium. The spinner was run at 60 rpm. The culture medium was enriched MEM plus Ascorbic Acid. After 4/6 weeks of culture the assembling chamber was opened and the biohybrids were collected.

Endothelial cells, HUVECs P4, were seeded as a drop on a surface of the samples, at high density of about 10.000/ 15.000 cells for mm2.Huvec seeding was performed into low attach multiwells in order to avoid cell adhesion on the surface of the petri and to allow it on the dermis equivalent. Cells were suspended in 5/10 μl of medium in order to avoid drop falling. After the seeding, samples were left at 37 °C for 2h enabling endothelial cells adhesion and, afterwards, complete medium was added up to completely cover the sample. During the first 2 h, the samples were monitored to avoid drying and eventually a drop of medium was added on the surface. HUVECs were cultured in supplemented VascuLife® medium. for 1 week (Mazio et al., 2019). The entire process for the production of the Pre-Vascularized Dermis (PVD) model is summarized and described in (Fig. 5.1).

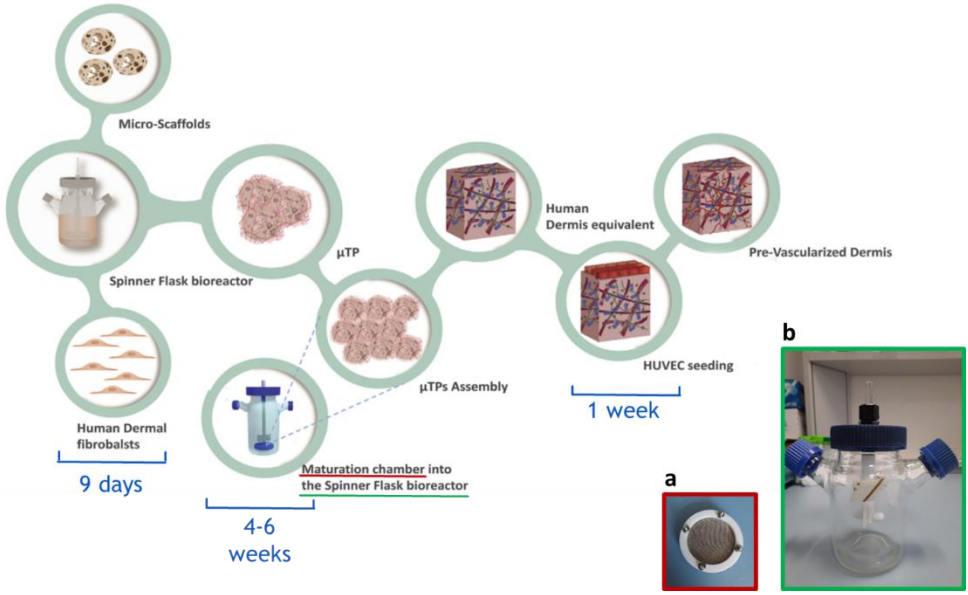

Fig.5.1 | Schematic representation of Pre-vascularized human dermis equivalent production. a) maturation chamber; b) spinner flask bioreactor (Mazio et al., 2019).

5.2 Implantation of PVD in a full thickness skin defect model

Animal studies were performed following the guidelines of the European Communities Council directive (2010/63/EU). Immunodeficient nu/nu mice 6/7 weeks old (Harlan) (n=20) were housed in single cages for 10 days before surgery.

Baytril (2,5%; 25mg/ml) antibiotic solution was subcutaneously administered to the animals the day of surgery and for the following 6 days in drinking water (10mg/Kg).

Mice received deep anaesthesia by intraperitoneal injection of ketamine (75 mg/kg body weight) and xylazine (15 mg/kg body weight). The surgical procedure began when the required anaesthesia level was obtained.

After sanitization with 10% Iodopovidone (Betadine®) a 7mm x 4mm sheet of skin was cut and removed for constructs implantation from the back of the mice, centrally and distally to the shoulder blades. All mice were

implanted with the pre-vascularized dermis model. 3M™ Tegaderm™ Transparent Film was positioned on the implantation area to better preserve the graft and to protect it from any mechanical stress.
Animals were sacrificed in groups of four at different timepoints 3,7,14,21 and 42 days. The retrieved tissues were fixed in formalin and in paraformaldehyde for histological, immunofluorescence and molecular analysis. Only for two timepoints, 21 and 42 days after implantation, 3 samples of each group, before the fixation, immediately after the explant, were analysed for their mechanical resistance via Indentation Test and then appropriately fixed.

5.3 Histological and immunofluorescence analysis

5.3.1 Histology on paraffin sections

Samples were fixed in Formalin 10% (HT501320 Sigma) for 1 h RT and washed in PBS1X (P4417-100TAB Sigma). They were dehydrated in Ethanol from 75% to 100% and treated with Xylene (A9982 ROMIL) before the inclusion in paraffin. Tissue slices thick 7 μm were cut using a microtome (Thermo Scientific HM 355S) and then deparaffinized with xylene. Sections were then hydrated in ethanol from 100% to 75%, washed in water and stained with Hematoxylin/Eosin (Bio Optica W01030708). The sections were mounted with Histomount Mounting Solution (Bio Mount HM 05-BMHM500 Bio-Optica) on coverslips and were observed with a light microscope (Olympus, BX53).

5.3.2 Fluorescent staining of the whole sample

Sigma) in PBS1X for 5 min at RT, washed in PBS1X and put into a 2mg/ml solution of Glycine (G8898-1KG). Samples were then kept in blocking solution with 3%BSA (A9418-100G Sigma) and Glycine in 0,02 %Triton in PBS1X for 1h at RT. Afterwards, samples were stained with 488-Griffonia

Semplicifolia (Lectin from Bandeiraea simplicifolia FITC Conjugate SIGMA L-9381) at a final concentration of 300 µg/ml and Rhodamine Ulex Europaeus Agglutinin I (UEAI Vector Laboratories RL-1062) at a final concentration of 20 µg/ml in blocking solution and kept overnight at 4 °C in the dark. The morning after, samples were washed with PBS1X and the nuclei of all the cells were stained with DAPI (Sigma-Aldrich D9542) for 20 min at RT.

5.3.3 Whole Samples clarification

Stained samples were dehydrated by serial immersions of 30 min each in Methanol 50%, 70%, 80%, 90%, 100%, 100%. BABB solution was prepared containing Benzyl Alcohol (BA) and Benzyl Benzoate (BB) (SIGMA) in 1:2 ratio. Samples were moved into a glass bottle and treated with Methanol and BABB (1:1) for 4 h and then with BABB for 24h at RT. Samples were observed into fluorodishes by Confocal Leica TCS SP5 II microscope. Images and z stack were analyzed using Image J.

5.3.4 Second harmonic generation signal analysis

For SHG imaging samples were fixed for 30 min with 4% paraformaldehyde and investigated by confocal microscopy (TCS SP5 II Leica) combined with a Multiphoton microscopy (MPM) where the NIR femtosecond laser beam was derived from a tunable compact mode-locked titanium: sapphire laser (Chamaleon Compact OPO-Vis, Coherent). Two-photon excited fluorescence was used to induce second harmonic generation (SHG) and obtain high-resolution images of unstained collagen structures. The samples were observed by using λex=840 nm (two photons) and λem=415–425 nm. The SHG images were acquired with a resolution of 12 bit, 1024X1024 pixel by using a 25X water immersion objective (HCX IRAPO L 25.0X0.95 Water, n. a. 0.95).

5.3.5 Fluorescent staining on paraffin sections

Samples retrieved at 14 days were fixed in formalin 10% (Sigma HT501320) for 1h at RT and washed in PBS1X (Sigma P4417-100TAB). They were dehydrated in Ethanol from 75% to 100% and treated with Xylene (A9982 ROMIL) before the inclusion in paraffin. The day after inclusion tissue slices 7 µm thick were cut using a microtome (Thermo Scientific HM 355S) and then deparaffinized using xylene. Sections were hydrated in ethanol from 100% to 30% and washed in water, in PBS1X, in Triton 0,2% for 15 min, finally in PBS1X again. In order to release the epitopes from paraffin, some slices were rinsed in a solution of Buffer Citrate (10X) performing a heat mediated unmasking. Sections were washed in PBS1X, blocked using BSA1% and FBS 5% in PBS1X for 2h at RT and incubated with BDNF (1:100), TrkB (1:100), NGF (1:250), TrkA (1:50) and PGP9.5 (5µg/ml) ON at 4°C in wet condition. The morning after, samples were washed in PBS1X. The samples were then stained with secondary antibodies Alexa Fluor 546 Goat anti-Mouse (1:500) in order to mark and PGP9.5 and Alexa Fluor 488 Goat anti-Rabbit (1:500) in order to mark BDNF, TrkB, NGF and TrkA. Nuclei were stained with DAPI for 20 min and samples were observed by Confocal Leica TCS SP5 II.

Other slices of the same samples retrieved at 14 days, undergone a heat mediated unmasking with TRIS-EDTA (10mM Tris Base, 1mM EDTA Solution, 0.05% Tween 20, pH 9.0) for 30' at 90 °C. the slices were then washed in PBS1X and blocked with a Blocking solution of BSA 1% and FBS 5% in PBS1X for 1h at RT. These slices were incubated with NF-M (1:500) ON at 4°C. The morning after the slices were washed with PBS1X and incubated with Secondary Antibody Alexa fluor 546 Goat anti-Mouse (1:500) for 2h. Nuclei were stained with DAPI for 20 min and samples were observed by Confocal Leica TCS SP5 II.

A heat mediated unmasking with TRIS-EDTA (10mM Tris Base, 1mM EDTA Solution, 0.05% Tween 20, pH 9.0) for 30' at 90 °C was also used for slices of samples at 7, 14, 21 and 42 days incubated with lectins 488-Griffonia Semplicifolia (200µg/ml) and with Rho-UEA I (20µg/ml) ON at 4°C in wet condition. The morning after samples were washed in PBS1X,

stained with Hoescht for 20 min and investigated by Confocal Leica TCS SP5 II.

Slices of samples retrieved at all the timepoints were were rinsed in a solution of Buffer Citrate (10X) for 15 min performing a heat mediated unmasking. Sections were washed in PBS1X, blocked using BSA1% and FBS 5% in PBS1X for 2h at RT and incubated with CD68 (1:50) and PROX-1 (1:200) ON at 4°C in wet condition. The morning after, samples were washed in PBS1X. The samples were then stained with secondary antibodies Alexa Fluor 546 Goat anti-Mouse (1:500) in order to mark CD68 and Alexa Fluor 488 Goat anti-Rabbit (1:500) in order to mark PROX-1. Nuclei were stained with DAPI for 20 min and samples were observed by Confocal Leica TCS SP5 II.

Images and z stack were analyzed using Image J.

NAME	HOST SPECIES	PRODUCT #	COMPANY	DILUITION or FINAL CONC.
BDNF	Rabbit	[EPR1292] ab108319	Abcam	1:100
TrkB	Rabbit	ab18987	Abcam	1:100
NGF	Rabbit	[EP1320Y] ab52918	Abcam	1:250
TrkA	Rabbit	(Y32Ex):sc-80398	Santa Cruz	1:50
NF-M	Mouse	ab7794	Abcam	1:500
PGP9.5	Mouse	[13C4/I3C4] ab8189	Abcam	5µg/ml
CD68	Mouse	ab955	Abcam	1:50
PROX-1	Rabbit	P7124	Sigma	1:200

Table 1 | List of primary antibodies used for immunofluorescence.

NAME	Sugar specificity	PRODUCT #	COMPANY	DILUITION or FINAL CONC.
Griffonia Semplicifolia	α-gal, α-galNAc	L 9381	SIGMA	300µg/ml
***Ulex Europeaus Agglutinin I* (UEA)**	Fucose, Arabinose	RL-1062-2	Vector Laboratories	20µg/ml

Table 2 | List of lectins used for immunofluorescence.

5.4 Quantification of BDNF, TrkB, NGF and TrkA fluorescence signal

After splitting each image with ImageJ software, nuclei channel (blu) was firstly thresholded. The dark background was then removed from this channel and a ROI was choosen to better count nuclei of the green cells in different areas of each image. Nuclei were counted with the plugin Analyze particles. The same ROI was moved to the fluorescent channel (green). This channel was then thresholded and by using the plugin Set Measurements the fluorescence signal area of each ROI was calculated. To quantify the signal the following formula was then used: Number of nuclei (n) / Fluorescent area (μm^2).

5.5 Statistics

All the experiments were performed in triplicate. Data are expressed as mean ± SD. Differences between groups were determined using the statistic test ANOVA with post-hoc Tukey HSD test via KaleidaGraph software. Significance between groups was established with a p value < 0.05.

5.6 Indentation TEST

The mechanical properties of the sample tissue (10 mm diameter and 1mm thickness) were analyzed by Piuma Nano-Indenter (Optics) showed in figure (Fig. 5.2). Indentation is a versatile, quantitative and non-destructive technique for measurements of tissue mechanical behaviour. Based on the indentation of surfaces by using probes with a well-defined geometry, the elastic and viscoelastic constants of the examined materials can be determined by relating indenter geometry and measured load and displacement to parameters which represent stress and deformation

Piuma Nano-Indenter (Optics)is a displacement-controlled nano-indenter machine including a controller, an optical fiber and a spherical probe. The indentation depth was approximately 10 μm during each indentation test performed in 5 different points of each sample. The tip radius was 53.5.

The elastic modulus (E) was obtained as ratio between the indentation stress (σ ind) (3) and strain (ε ind), as described by following formulas.

$E=(\sigma \text{ ind})/(\varepsilon \text{ ind})$

$\sigma \text{ ind}=P/(R\sqrt{hR})$

$\varepsilon \text{ ind}=4h/(3R(1-v^2))$

where P was the load, R the radius of spherical indenter tip, and h the penetration depth.

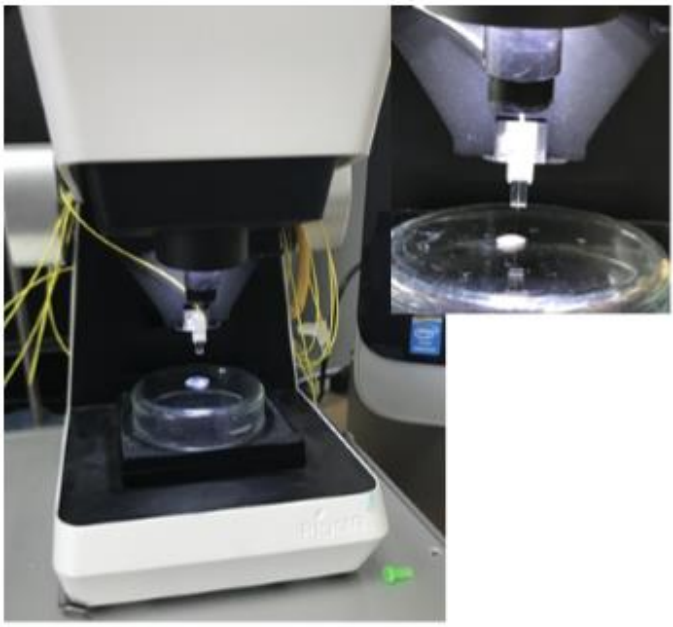

Fig.5.2 | Piuma Nano-Indenter apparatus (Optics).

5.7 Molecular analysis

5.7.1 Purification of total RNA from paraffin-embedded tissue sections

For the quantification of VEGF, HIF-1A, BDNF, TrkB and PGP9.5 the first step was the purification of total RNA from our paraffin embedded tissues. Sections 20 μm thick were cut and placed in a 2 ml microcentrifuge tube. Was added 1ml of Xylene and was centrifuged for 2 min. The supernatant was then removed to add ethanol (96%-100%) for total Xylene removal. To evaporate the residual ethanol, samples were positioned at RT keeping the lid open.
After 10 min were added 280 μl di Buffer solution and then 10 μl di Proteinase K.
Finally, samples were incubated at 56°C for 15 min, then at 80°C for 15 min.

5.7.2 Retro-transcription and Real time –PCR.

For the retrotranscription we analysed 3 samples for each timepoint considering 100 ng of each sample. We used M-MuLV –RH Reverse Transcription Kit that is a complete system for efficient synthesis of first strand cDNA from mRNA or total RNA templates. The kit contains all the necessary components for reverse transcription: M-MuLV –RH reverse transcriptase, two different 5× RT buffers, dNTP mix, DTT solution, random hexaprimer solutions, as well as RNase-free water. Since the sample extracted with our method could be fragmented and missing the tail poly-a (the one to which the oligo dt should bind) we used random hexamers as recommended by literature.
Since the retrotranscription product was ready we performed Real time PCR for BDNF, TrkB, PGP9.5, VEGF and GADPH as housekeeping gene.
Specifically, we used of 10 µl of BlasTaq™ 2X qPCR MM, 0.5 µl of Forward Primer (10 µM), 0.5 µl of Reverse Primer (10 µM) as listed in Table 3, Nuclease-free H2O up to 20 µl. The executed protocol was divided in the following steps: Enzyme Activation at 95°C for 3 min (1 cycle), Denaturation at 95°C for 15 sec (40 cycles), Annealing/Extension at 60°C for 1 min (40 cycles) and finally the melting curve or dissociation analysis (Δ-ΔCT) to validate the specificity of the primers.

PRIMERS	SEQUENCES (5'>3')
GAPDH F	AAATACGGACTGCAGCCCTC
GAPDH R	GTTCACACCGACCTTCACCA
BDNF mus F	CGACATCACTGGCTGACACT
BDNF mus R	CCCGGGAAGTGTACAAGTCC
TrkB mus F	TGCGCCAACTATCACGTTTC
TrkB mus R	TGGCCCCATTGTAGAACCAC
PGP9.5 F	CACAGCTGTCTTCTTGCGTT
PGP9.5 R	AGCAAGGTACGAGACACACA
VEGF F	CTCCGTAGTAGCCGTGGTCT
VEGF R	TTCCTCCCCTCTCTTCTCGG

Table 3 | List of primers for RealTime-PCR.

Imparato G, Urciuolo F, Casale C, Netti PA, 2013. 1994. The role of microscaffold properties in controlling the collagen assembly in 3D dermis equivalent using modular tissue engineering. Biomaterials 34 7851–7861.

Mazio C, Casale C, Imparato G, Urciuolo F, Attanasio C, De Gregorio M, Rescigno F, Netti PA, 2019. Pre-vascularized dermis model for fast and functional anastomosis with host vasculature. Biomaterials 192:159-170.

Urciuolo F, Graziano A, Imparato G, Panzetta V, Fusco S, Casale C, Netti PA, 2016. Biophysical properties of dermal building-blocks affect extra cellular matrix assembly in 3D endogenous macrotissue. Biofabrication 8(1):015010.

Chapter 6

Results

6.1 PVD before grafting: a well-organized matrix with a well distributed vascular network.

In order to confirm the features of our engineered dermis before grafting we performed immunofluorescence staining with UEA to mark the correct development of human vessels inside the engineered dermis along with Ab anti-human-Vimentin to mark the intermediate filaments of human fibroblast cytoskeleton. We also identified the nuclei with DAPI.
The engineered dermis shows a well-organized human vascular network distributed in concomitance with an evident physiological distribution of fibroblast cytoskeletal intermediate filaments into all the tissue extra-cellular matrix (Fig. 6.1a). To better appreciate the organization of the collagen matrix we performed a thorough investigation by Multiphoton microscopy (MMP) using the Second Harmonic Generation (SHG) technique, which is a powerful tool allowing the study of collagen structural organization. We noticed a well-organized collagen matrix revealing that human vessel structures made their way across the holes of the collagen mesh in a physiological manner (Fig. 6.1b).
The figure 6.1(c) acquired by using a higher magnification, shows more clearly the significantly well-organized distribution of the human vascular network into the engineered dermis while in Fig. 6.1(d) the zeta stack representation efficiently highlights the homogeneous distribution of the vessels throughout the tissue being representative of 200 μm thickness sample.

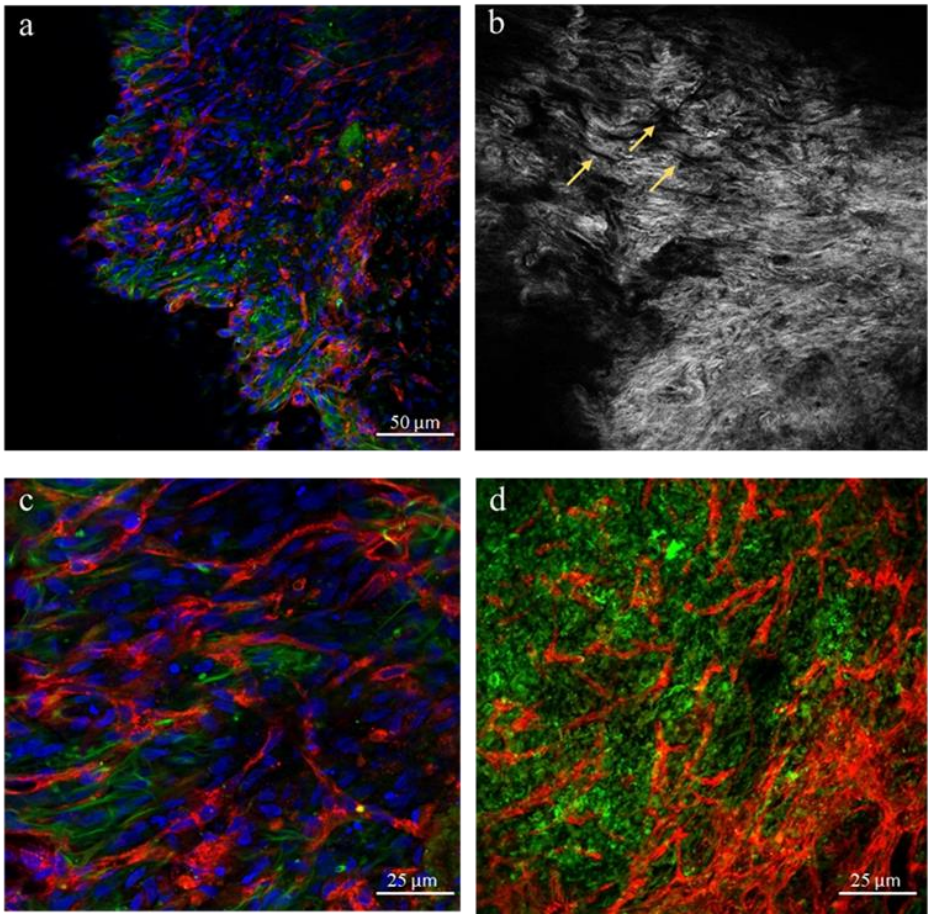

Fig.6.1 | Pre-implanted PVD, whole sample, not clarified. Staining with human-Vimentin (green), Rho-UEA (red) and DAPI. Confocal microscopy analysis, note in a) positive staining for human vessels with UEA (red) and positive staining for anti-human vimentin Ab marking the cytoskeletal structure of human fibroblasts used to produce the original engineered dermis; c) higher magnification to better appreciate the human vascular network developed into the construct; d) zeta stack 200 µm thick of the sample; b) Multiphoton microscopy (MMP) image acquired via Second Harmonic Generation technique to reveal the collagen matrix structure and organization of the tissue before implantation. Note the holes (indicated by the yellow arrows) into the matrix in correspondence of human vessel structures. Objective 25X. N=3.

6.2 PVD integration with the host tissue

In order to characterize the degree of integration of our engineered dermis with the host tissue, after retrieval we performed the histological analysis of the graft explanted after 3, 7 and 14 days via Hematoxylin/Eosin staining on 7μm slices.
The constructs explanted after 3 days showed a good level of integration into the host tissue also displaying several vessel-like structures running inside the construct while we noticed the lack of re-epithelialization of the construct by the host as expected as this early timepoint (Fig. 6.2a-a2). Differently, we detected a successful re-epithelialization, shown in Fig. 6.2 (b-b2), in the samples corresponding to the tissue explanted 7 days post-implantation. At this timepoint we observed, as expected, an improved integration of the engineered dermis with host tissue along with a successful re-epithelialization in comparison to what observed in the tissue retrieved 3 days after implantation. Finally, at 14 days after implantation, in addition to both a good level of integration with host tissue and a successful re-epithelialization, samples show perfused vessel-like structures as well as follicle like-structures (Fig. 6.2 c-c2).

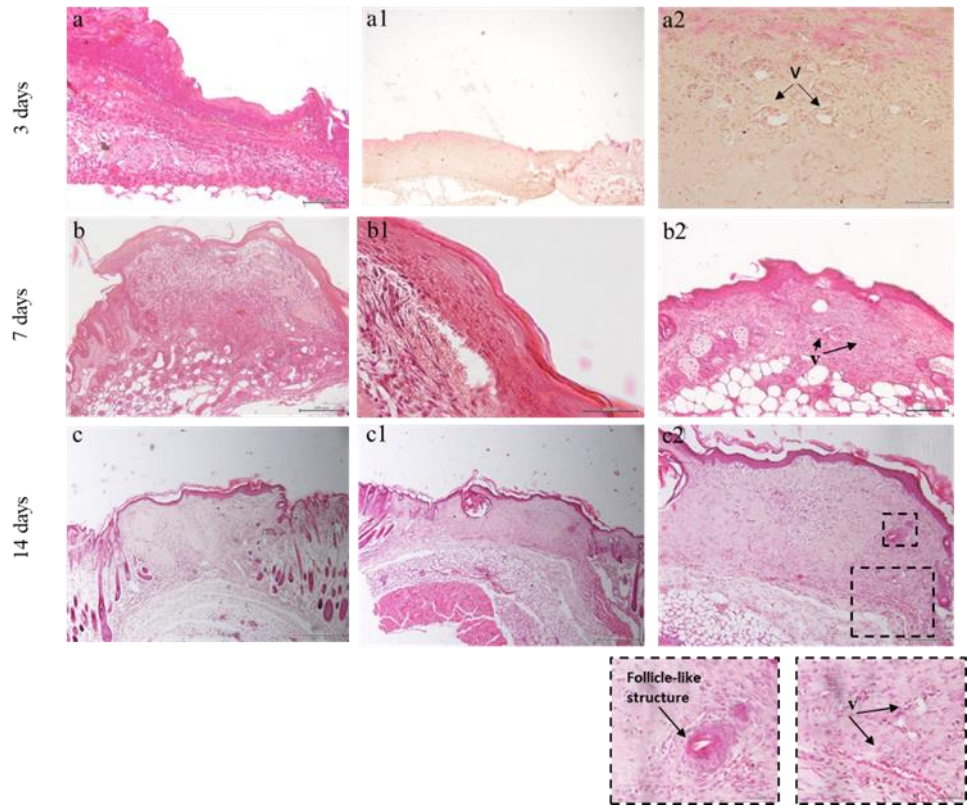

Fig.6.2 Hematoxylin/Eosin staining of the samples corresponding to the engineered dermis explanted at 3,7 and 14 days after implantation. a-a2) tissues harvested 3 days after implantation are well integrated with the host skin, also presenting vessel like-structures (v) but not re-epithelization. ; b-b2) tissues harvested 7 days after implantation show a successful integration with the host as confirmed by vessel-like structures (v) and re-epithelialization which can be observed in b2 and b1 respectively; c-c2) tissues harvested 14 days after implantation are well integrated as confirmed by the presence of perfused vessels (v) and a follicle like-structure. N=3.

6.3 Human and murine vessel interaction into the PVD

To investigate the integration of our engineered dermis with the host tissue from the vascularization standpoint after 14 days of implantation, we performed immunofluorescence with the lectins FITC-*Griffonia Semplicifolia* and Rho-*UEA* to mark murine and human vessels,

respectively. We found an appreciable presence of the human vascular network into our engineered dermis in concomitance with the murine one indicating the good interaction between the two networks (Fig. 6.3a). The higher magnification (Fig. 6.3b) better shows the closeness of two vessels (human and murine) within the construct matrix where human vessels seem to guide the invasion of murine ones into the graft.

Further, by recording zeta stack images throughout a tissue sample of 200µm in thickness, we clearly observed murine vessels invading the graft (Fig. 6.3c).

Also in this case, in tissues retrieved 14 days after grafting, we used SHG technique to appreciate collagen matrix re-organization and remodelling in terms of collagen morphology adequacy in sustaining vessel penetration. More specifically, by merging the images acquired by SHG with those acquired by confocal mode, we observed the newly formed vessels passing through the holes created in the matrix by its remodelling.

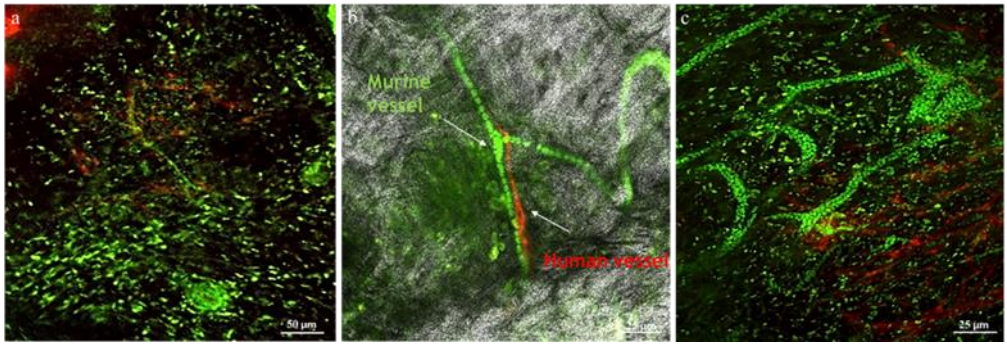

Fig.6.3 | Immunofluorescence analysis on engineered dermis explanted after 14 days. Whole sample clarified with BABB solution. Staining with FITC-Griffonia Semplicifolia (green), Rho-UEA (red). a) human vascular network and murine vessels in the tissue matrix; b) merged image with SHG to identify the holes into the collagen matrix and the vessel structures passing through them; c) 200 µm zeta stack acquisition of the tissue sample performed to observe the closeness of the two vascular networks. Confocal microscopy analysis with objective 25X. N=3.

6.4 Myelinated nerve fibers in the PVD.

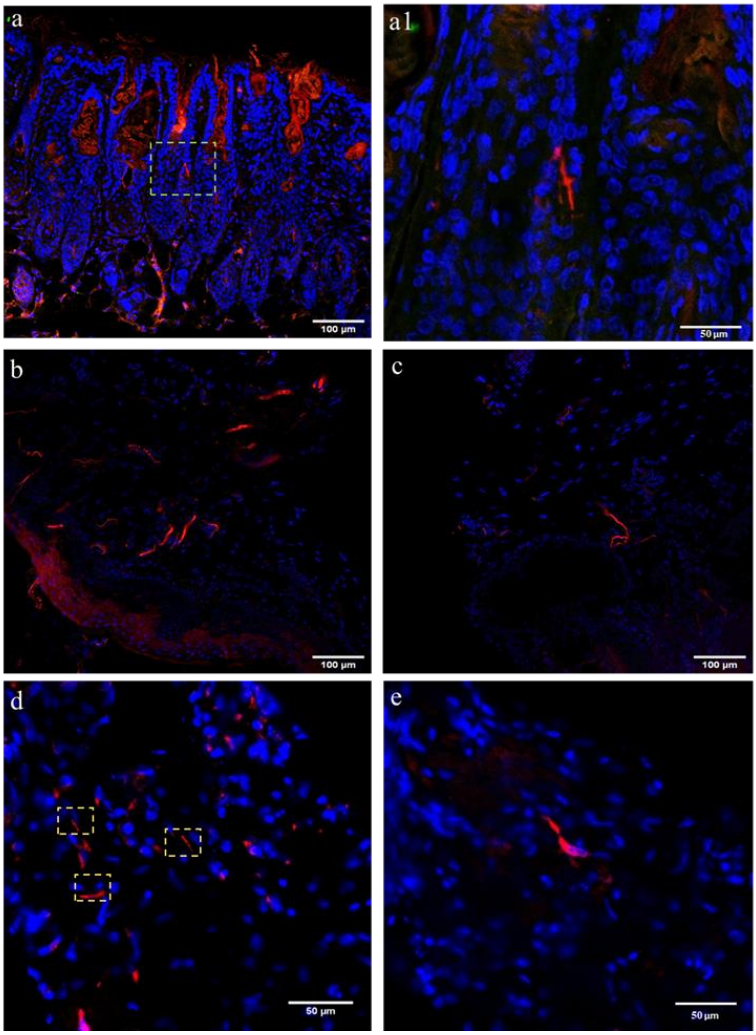

Fig.6.4 | Immunofluorescence analysis on engineered dermis explanted after 14 days. 7µm slices. Staining with NF-M (red) Ab and DAPI (blu). a) Murine tissue retrieved from in the surroundings of the engineered dermis graft after14 days after implantation used as positive control for NF-M staining; a1) higher magnification aiming to highlight the filamentous shape of NF-M; b-c) human foreskin sample also used as positive control for NF-M staining; d) positive staining for NF-M in our engineered tissue explanted at 14 days; e) higher magnification of the filamentous shape of NF-M in our construct. Confocal microscopy analysis with objective 25X. N=3.

To investigate the integration of our engineered dermis with the host tissue from the innervation standpoint after 14 days of implantation, we started performing immunofluorescence analysis with Neurofilament M to mark the neuronal cytoskeletal structure of myelinated fibers.
As positive controls, we showed the positive staining for this cytoskeletal structure into the murine tissue retrieved in the surroundings of the engrafted tissue 14 days after implantation (Fig 6.5a-a1) as well as within a sample of human foreskin since our antibody reacts both with mouse and human fibers (Fig 6.5b-c). We also found this positive staining into our construct after 14 days of implantation (Fig. 6.5d-e). Higher magnifications better show NF-M filamentous shape (Fig. 6.4 a1; e).

6.5 PVD before grafting: neurotrophins and PGP9.5 expression

To deepen the analysis from the innervation standpoint we first performed immunofluorescence staining on our engineered tissue before grafting with markers for the neurotrophins BDNF and NGF along with their high affinity receptors TrkB and TrkA as well as for PGP9.5 to mark both myelinated and unmyelinated fibers.
We observed a high expression of BDNF into the matrix of our tissue (Fig. 6.6a), a lower expression of TrkB respect to BDNF (Fig. 6.6b), a low expression of NGF into the matrix (Fig. 6.6c) and a very low expression of TrkA (Fig. 6.6d). Since we analysed, in this case, the tissue before grafting therefore representative of the dermis alone, these results are in accordance with the literature showing a higher expression of NGF and TrkA into the epidermis.
To better display these results, we reported a graphical representation of the quantitative expression of neurotrophins into the pre-implanted tissue where the different expression of the different neurotrophins along with that of the corresponding receptors is clear. No signal for PGP9.5 was detected as expected at this timepoint, which is too early to detect any innervation pattern.

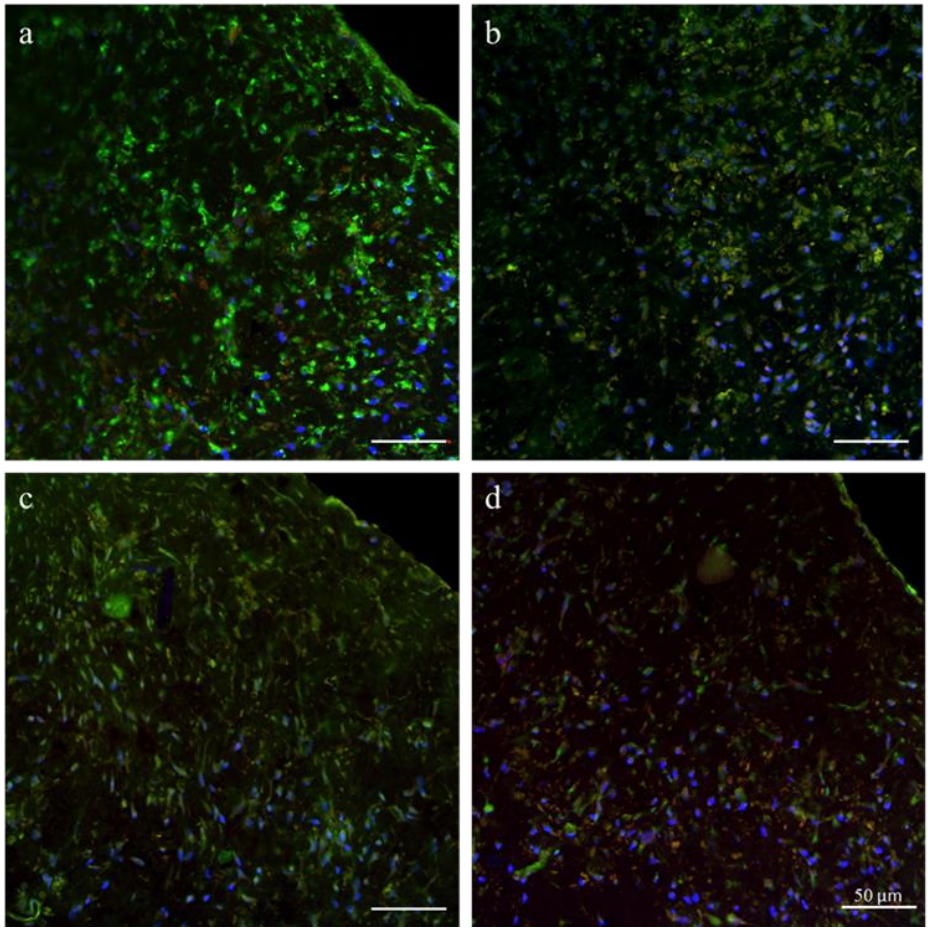

Fig.6.5 | Immunofluorescence on engineered dermis before implantation. 7µm slices. Staining with BDNF, TrkB, NGF, TrkA (green) PGP9.5 (red) and DAPI (blu). a) BDNF (green) displays a high expression into the matrix of our engineered tissue; b) TrkB (green)expression results in a lower signal respect to BDNF into the tissue matrix; c) NGF (green) expression resulting in a low signal into the tissue matrix; d) TrkA (green) expression resulting in a very low signal into the tissue matrix. All the samples were co-stained with PGP9.5 (red) and DAPI. We observed a lack of signal for PGP9.5 as expected. Confocal microscopy analysis with objective 25X. N=3.

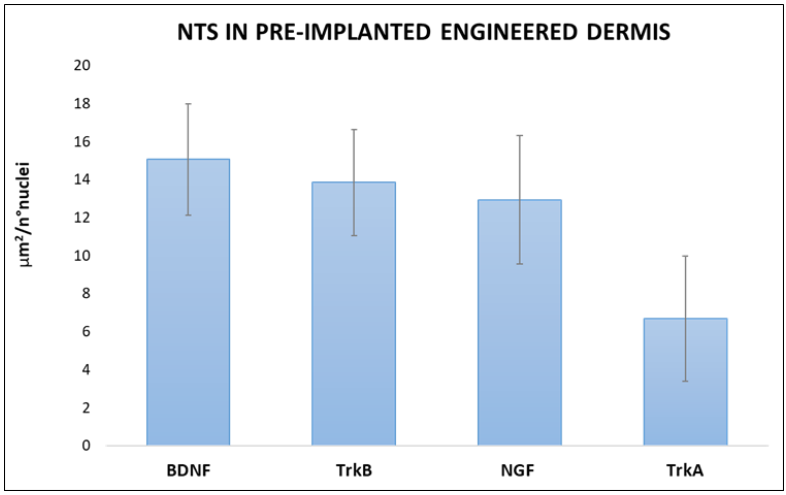

Fig.6.6 | Graphical representation of NT quantitative expression in our engineered tissue before grafting. N=3.

6.6 Neurotrophins and PGP9.5 expression in the PVD

We performed immunofluorescence analysis on the engineered tissue explanted 14 days post-implantation with neurotrophin markers BDNF and NGF and the high affinity receptors for these molecules, TrkB and TrkA as well as for the nervous fiber marker PGP9.5.
We observed a high expression of BDNF and TrkB by the engineered tissue matrix (Fig. 6.8a) (Fig.6.8b), a high expression of NGF immediately below the epidermis and in its basal layer resulting from the re-epithelialization of the engrafted tissue from the host (Fig. 6.8c). Concerning TrkA we found a high expression of this receptor immediately below the epidermis and in the dermal papilla (Fig. 6.8d). According to our results previously reported (Fig. 6.2b-b2) in the histological analysis re-epithelialization appeared as early as 7 days after implantation.

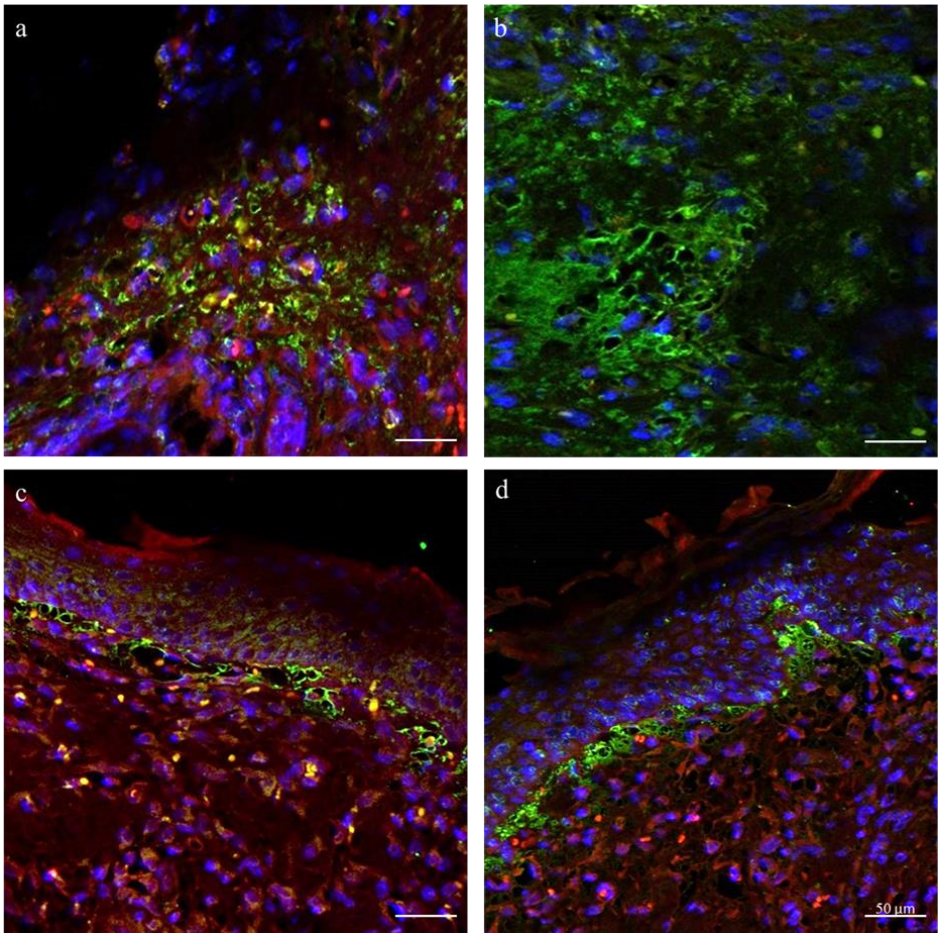

Fig.6.7 | Immunofluorescence on engineered dermis explanted after 14 days. Staining with BDNF, TrkB, NGF, TrkA (green), PGP9.5 (red) and DAPI (blu). a) BDNF (green) result in high expression into the PVD matrix; b) TrkB (green) resulting in a high signal into the PVD matrix; c) NGF (green) resulting in a high signal and into the basal layer of keratinocytes; d) TrkA (green) resulting in a high expression immediately below the epidermis and in the dermal papilla. All these markers were co-stained with PGP9.5 (red) and DAPI. We observed a lack of signal for PGP9.5. Confocal microscopy analysis with objective 25X. N=3.

Therefore, we quantified the expression of neurotrophins and their high affinity receptors in our samples retrieved 14 days after implantation. The

graphical representation (Fig. 6.9) shows the comparison between the expression of NTs and their high affinity receptors into the dermis of our engineered dermis as well as into the re-epithelializing epidermis. According to literature, BDNF and TrkB are the more expressed into the dermis while NGF is the most expressed into the epidermis. No signal for PGP9.5 was detected at this timepoint. We also performed the direct comparison of quantitative expression of NTs and their receptors in our engineered dermis pre-implantation and after retrieval at day 14 post-implantation detecting higher expression levels of BDNF, TrkB, NGF and TrkA into the explanted tissue respect to that analysed after the sole *in vitro* culture (Fig. 6.10).

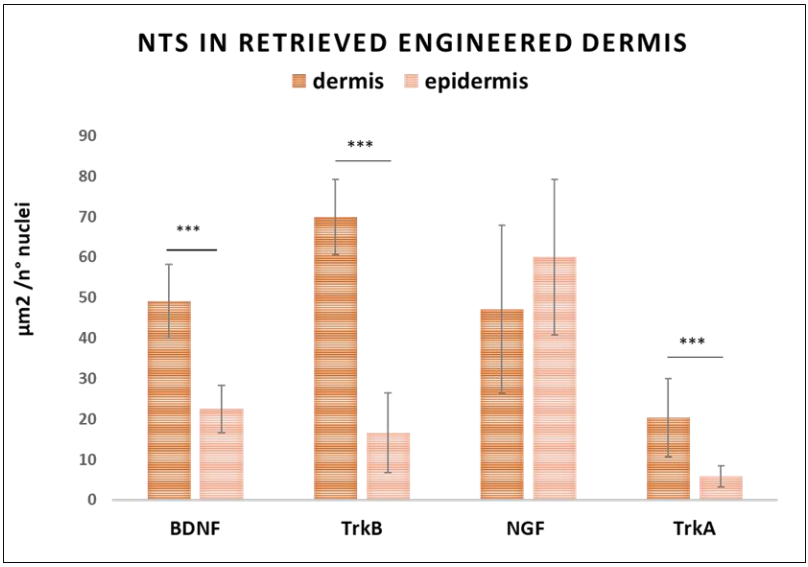

*Fig.6.8 | Graphical representation of NTs quantitative expression in our engineered tissue retrieved 14 days post-implantation. Comparison between dermis and epidermis. N=3; P<0,001***.*

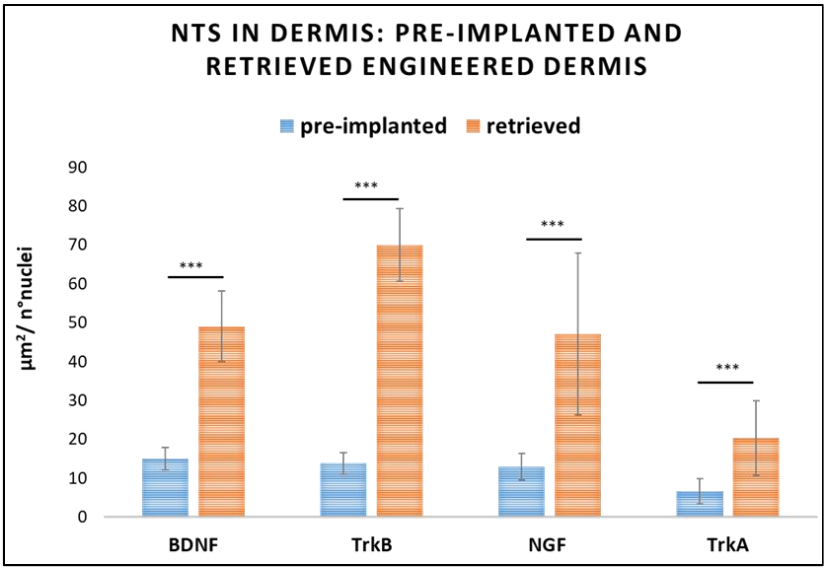

Fig.6.9 | Graphical representation of the comparison between NT quantitative expression in our engineered tissue before grafting and after 14 days of implantation. N=3; P<0,001 ***

6.7 PGP9.5 expression in the PVD

We performed immunofluorescence analysis on our engineered tissue retrieved 42 days post-implantation with markers for TrkA and PGP9.5.
We observed a positive signal for TrkA into the epidermis in accordance with the re-epithelialization of our engineered tissue along with a positive signal for PGP9.5 identifying free nerve fibers extending from the host to our grafted tissue probably starting a re-innervation (Fig. 6.11).

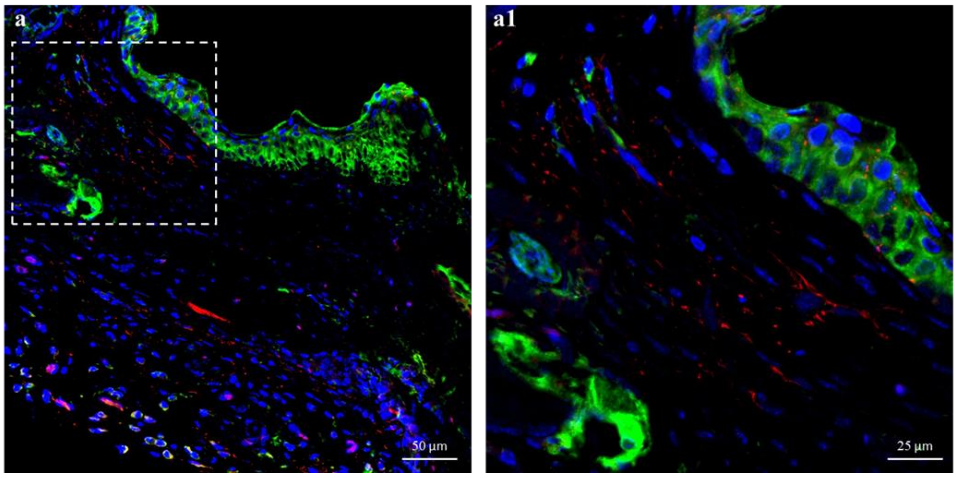

Fig.6.10 | Immunofluorescence on the engineered tissue explanted after 42 days. 7µm slices.
Staining with TrkA (green), PGP9.5 (red) and DAPI (blu). a) Positive signal for TrkA into the epidermis and positive signal for PGP9.5 identifying free nerve fibers that extend from the host to the graft; a1) higher magnification of the white box. Confocal microscopy analysis with objective 40X. N=3.

6.8 Mechanical resistance of the PVD

Since neurotrophins guide fibroblasts differentiation into myofibroblasts, also increasing skin tensile strength, we analysed the variation of the elastic modulus in our engineered tissue via Indentation Test.
We observed that the tissue retrieved 21 days after implantation showed a higher mechanical resistance respect to murine dermis while at 42 days the resistance displayed appears like the one observed in the host dermis. Therefore, we noticed a higher mechanical resistance for both the timepoints respect to the pre-implanted tissue. These results probably suggest that our tissue was well integrated into the host organism by compliantly resembling some of its crucial physiological features such as flexibility and mechanical strength (Fig. 6.11).

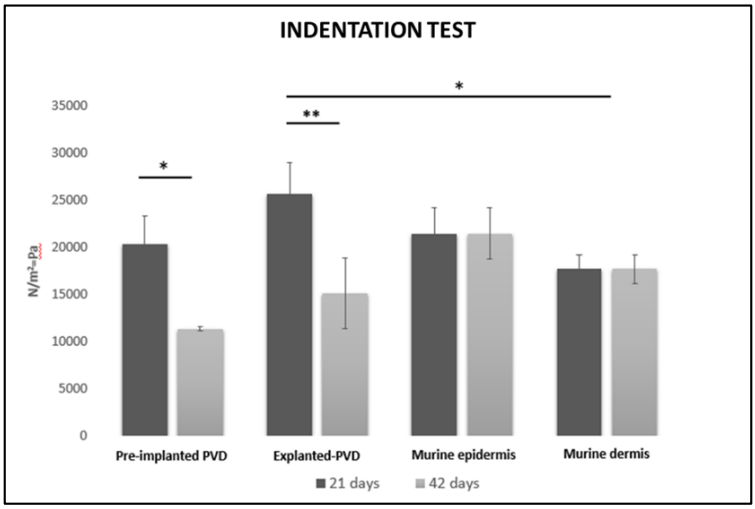

Fig.6.11 | Indentation test on our engineered tissue and on both murine epidermis and dermis before grafting and after retrieval at days 21 and 42 post-implantation. N=3; P<0,05 P<0,01 ***

6.9 Macrophages and lymphatic vessel in the PVD

We performed immunofluorescence analysis on our engineered tissue with anti-CD68 Ab to identify macrophages. We found that 3 days after implantation macrophages were detected as expected according to the first wound healing process phase, the inflammation.

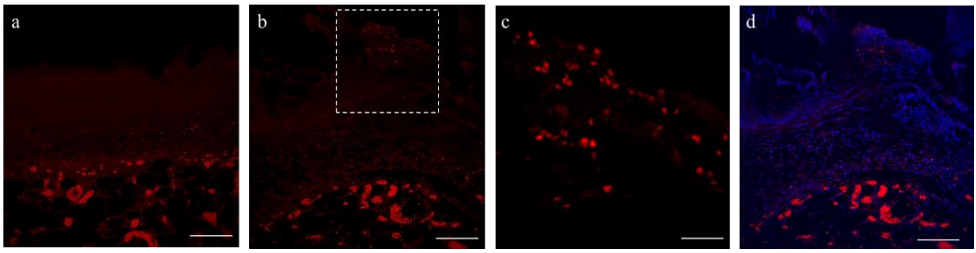

Fig.6.12 | Immunofluorescence on the engineered tissue explanted after 3 days. 7μm slices. Staining with CD68 (red) and DAPI (blu). a) Auto-fluorescence signal that highlight the presence of red blod cells, b) positive signal for macrophages into the engineered dermis; c) higher magnification of the white box; d) CD68 and DAPI. Confocal microscopy analysis with objective 25X. N=3.

We also performed immunofluorescence analysis to mark PROX-1 to observe lymphatic vessel settlement in our engineered tissue and we noticed the presence of host lymphatic vessels at 14 days after implantation. This is a promising result considering that we didn't seed endothelial lymphatic cells in our engineered tissue and since in literature we found that 14 days after implantation is the timepoint when engineered tissues pre-vascularized both with human endothelial and lymphatic cells present anastomosis between the two lymphatic vascular networks, one from the graft and one from the host tissue contributing to improve graft integration and to accelerate healing process.

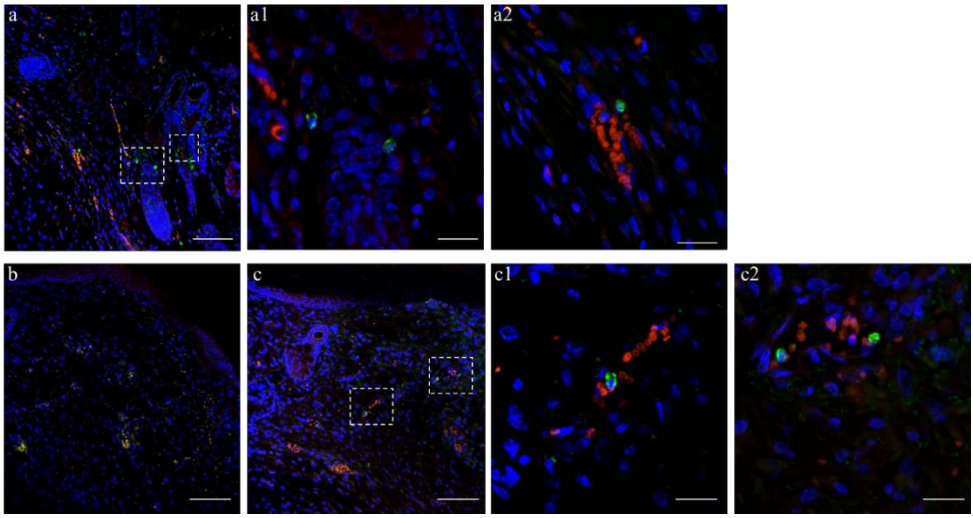

Fig.6.13 | Immunofluorescence on the engineered tissue explanted after 14 days. 7µm slices. Staining with CD68 (red), PROX-1 (green) and DAPI (blu). a) CD68 and PROX-1 in murine surroundingAuto-fluorescence signal that highlight the presence of red blod cells, a1-a2) higher magnifications of white boxes; c) higher magnification of the white box; d) CD68 and DAPI. Confocal microscopy analysis with objective 25X. N=3.

6.10 Molecular expression of murine BDNF, TrkB, PGP9.5 and VEGF in the PVD

We also performed a quantitative analysys through RealTime-PCR on our engineered tissues at 3, 7, 21 and 42 days.
We noticed an increase of BDNF and its high affinity receptor TrkB expression as time progressed suggesting us the successful communication between the host and our engineered tissue as well as the predisposition of our tissue to favour reinnervation. In fact, we also observed the increase of PGP9.5 expression into the engineered tissues explanted at 42 days respect to earlier timepoints, according with the qualitative results obtained through the immunofluorescence analysis (Fig. 6.10).
Finally, from the vascularization standpoint, we observed the highest expression in engineered tissues explanted at 7 days in accordance with the need of the graft to receive oxygen and nutrients at this stage of integration. We also noticed a decrease of VEGF expression at 21 and 42 days

confirming the stabilization and the correct integration with the host tissue of the implanted substitute.

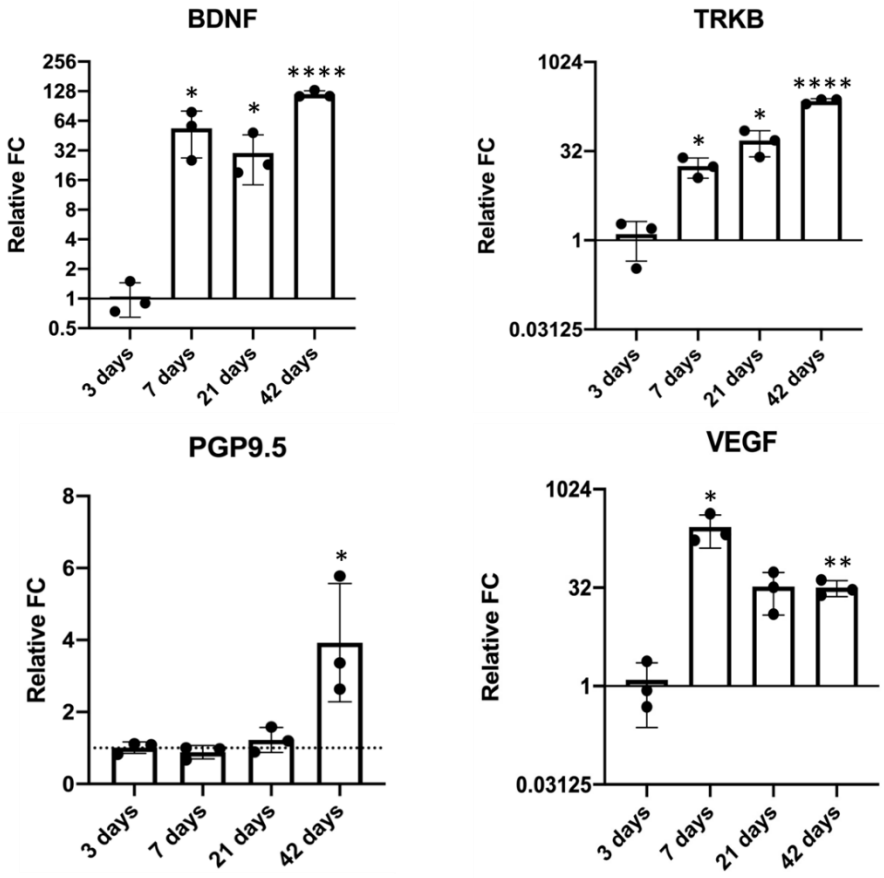

Fig.6.14 |Graphical representation of RealTime-PCR analysis relative to the quantitative expression of murine BDNF, TrkB, PGP9.5 and VEGF into the engineered dermis. BDNF and TrkB increase in time according to a well-established integration and communication with the host, increase of PGP9.5 in tissue explanted at 42 days and decrease of VEGF also confirm the successful integration with host tissue. N=3; P<0,05; P<0,01**; P<0,001***; P<0,0001****(all the P values are related to 3 days sample).*

Chapter 7

Discussion and conclusions

7.1 Discussion

Skin substitutes, which are currently on the market, are of numerous different typologies. For example, they can be acellular or cellular, temporal or permanent, mono-layered, bi-layered or tri-layered, epidermal, dermal or composite (both epidermal and dermal). Despite this many options, some open issues continue to persist probably due to the fact that skin is a very complex organ, which is also the most extensive in the body. The skin plays different critical roles and is composed of different kind of cells along with the vascular and the nervous components. Moreover, in the clinical setting wounded areas which need to be recovered are often of considerable size. Therefore, it is very hard to create a skin substitute suitable to recapitulate all the morpho-functional features of this organ. The main focus of this PhD project was to study the degree of integration of a particular engineered tissue, a pre-vascularized dermis obtained by a bottom-up technique, with host tissue (Casale et al., 2016). Our tissue had been already implanted and characterized in a subcutaneous pocket mouse model showing promising results such as the onset of functional anastomosis between the implanted skin and the host vasculature in a single week. In this project we addressed our efforts to a more physiological preclinical setting by implanting our tissue in a full thickness skin defect model, which better represents the wound healing condition.

When a non prevascularized dermo-epidermal substitute is implanted in a patient it suffers a physiological "crisis" due to impaired nutrition, oxygen, and growth factor supply between 14 and 21 days after transplantation, which is a very long time. Different strategies such as the fabrication of tissues with specific architectures able to guide angiogenesis as well as the administration of growth factors and the production of pre-vascularized tissues have been proposed to overcome the hindrance of the long time needed for re-vascularization (Mastrullo et al., 2020).

It is in this scenario that we fabricated and featured in a preclinical setting our engineered dermis tissue which is characterized by an endogenous collagen-rich matrix, self-produced by the human seeded fibroblasts (Mazio et al., 2019). This aspect is a clear asset for our work respect to other

engineered skin substitutes described in literature and including exogenous matrices because it is a physiological tissue suitable to be re-vascularized and re-innervated sooner compared to its analogues currently available.
At day 14 after implantation in a full thickness skin defect model, in the retrieved tissue, we found perfused vessels into the two vascular networks, human and murine, which were positioned one close to each other. This result suggested us that a good degree of integration took place between our tissue and the host organism. In addition to blood vessels, we consider also lymphatic vessels that are foundamental for the wound healing process expecially for the drenage function. Our engineered dermis displays a vascularization by host lymphatic vessels 14 days after implantation suggesting that this is the ideal time-point when our dermis model is at the peack of its successful integration.
Another crucial issue is the loss of sensitivity in the injured areas along with the difficulty in re-innervation of skin substitutes (Biedermann et al., 2012; Biedermann et al., 2016). The most common hindrance reported in the studies performed over the last decades is the very long time required for innervation, about 6-8 weeks after implantation. In the skin, there are many unmyelinated fibres devoted to the slow conduction of pain signals respect to the myelinated ones devoted to the fast conduction of thermal sensation and mechano-transduction (Julius and Basbaum, 2001).
Numerous attempts have been made *in vitro* to obtain a pre-innervated construct (Roggenkamp et al., 2013; Martorina et al., 2017), however, for in vivo applications significant results have not yet been shown. In our pre-vascularized dermis, we found that a partial re-innervation, revealed by the presence of some myelinated fibers, occurred after 14 days of implantation while a more substantial re-innervation, with the positive staining of both myelinated and unmyelinated fibers, occurred instead 42 days after implantation. This latter result is also confirmed by the quantitave analysis of PGP9.5 perfomed via RealTime-PCR and is an unquestionably very important achievement considering the data so far reported in literature which confirm the long re-innervation time required by skin substitutes.
Since neurotrophins play different critical roles into the skin such as the induction of skin cell proliferation and growth, we looked at the expression

of these molecules and their high affinity receptors respect to the tissue at the end of the *in vitro* culture time. The success of the integration has been also shown through the augmentation of murine BDNF and TrkB into our tissue and the decrease of VEGF at longer time of implantation probably when the engineered dermis is so highly integrated that it does not need anymore an extended blood supply

Moreover, neurothrophins induce the differentiation of fibroblasts into myofibroblasts increasing skin tensile strength. In view of this we performed an Indentation test, by measuring the elastic modulus of our tissue, detecting an increase of the mechanical resistance in the retrieved tissues respect to those tested at the end of the *in vitro* culture time and a very similar value of tensile strength between the tissue retrieved 21 days post-implantation and murine dermis.

The presence of macrophages 3 days post-implantation also confirms a positive reaction expressed from the host respect to the integration of our dermis model into the mouse skin tissue. Moreover, macrophages also play particularly important roles in vascularization by moving nearby the newly forming blood vessels also aiding their stabilization and fusion. The detection of lympathic vessels represents a successful migration of the host lymphatic system into the graft and also the onset of a drenage system of the damaged site, which is a critical aspect for a correct healing process can also contribute to the successfull integration of our engineered dermis into the host organism.

7.2 Conclusions

We investigate the integration of this tissue with the host organism in a full thickness skin defect model and its effective involvement and degree of contribution in the wound healing process.

Considering the results like presence of perfused vessels at 14 days after implantation, macrophages at 3 days after implantation, murine vessels into our tissue at day 14 after grafting we conclude that our engineered tissue displays a well organized matrix, a well distributed vascular network, the

capability to mimic a physiological behaviour and a good degree of integration with host tissue.

From the innervation side, considering both the sporadic presence of some myelinated nerve fibers at 14 days after implantation and a stronger and more convincing re-innervation in the tissue retrieved 42 days after implantation we hypothesize that our pre-vascularized dermis can be used in a future perspective as a valuable and effective skin substitute in the clinical setting.

Since our tissue, explanted after 14 days of implantation, shows an increase in the quantitative expression of neurotrophins and their high affinity receptors respect to *in vitro* starting condition we can also conclude that it is well integrated and in communication with the host and that it has been successfully re-epithelialized by the host at this timepoint.

Moreover, regarding the presence of lymphatic vessel cells 14 days after implantation, we considered to implant the same engineered dermis pre-vascularized both with vascular and lympathic endothelial cells in order to accelerate the replacement of the host damaged tissue.

Despite all these positive features described it is always useful to recognize the weakness points of a certain work, in this case we identified the absence of anastomosis between human and vascular networks at day 7 after implantation, as previously described for the same pre vascularized dermis implanted into the subcutaneous pocket, probably due to the onset of a different process in the two models. Also the lack of a Western blot analysis to make stronger RT-PCR results by confirming the expression of the selected genes at a prost-trascriptional level and the lack of the analysis of neurotrophin expression at all timepoints.

Starting from these interesting results we are currently going to study how we can accelerate the integration process by implanting a pre-vascularized skin composed of dermis and epidermis, which we are fabricating by seeding both fibroblasts and keratinocytes onto our scaffolds. Moreover, we wish to obtain results useful to investigate some aspects of the complex relation between vascularization and innervation, taking into account, for example, the role of neurotrophin secretion by endothelial cells indriving innervation.

Biedermann T, Bo¨ttcher-Haberzeth S, Klar AS, Pontiggia L, Schiestl C, Meuli-Simmen C, Reichmann E, Meuli M, 2013. Rebuild, restore, reinnervate: do human tissue engineered dermo-epidermal skin analogs attract host nerve fibers for innervation? Pediatr Surg Int 29:71–78.

Biedermann T, Klar AS, Bo¨ttcher-Haberzeth S, Reichmann E Meuli M, 2016. Myelinated and unmyelinated nerve fibers reinnervate tissue engineered dermo-epidermal human skin analogs in an in vivo model. Pediatr Surg Int.

Casale C, Imparato G, Urciuolo F, Netti PA, 2016. Endogenous human skin equivalent promotes in vitro morphogenesis of follicle-like structures. Biomaterials 101, 86-95.

Julius D, Basbaum AI, 2001. Molecular mechanisms of nociception. Nature 413(6852):203-10.

Martorina F, Casale C, Urciuolo F, Netti PA, Imparato G, 2017. In vitro activation of the neuro-transduction mechanism in sensitive organotypic human skin model. Biomaterials 113:217-229.

Mastrullo V, Cathery W, Velliou E, Madeddu P, Campagnolo P, 2020. Angiogenesis in Tissue Engineering: As Nature Intended? Front Bioeng Biotechnol. 20; 8:188.

Mazio C, Casale C, Imparato G, Urciuolo F, Attanasio C, De Gregorio M, Rescigno F, Netti PA, 2019. Pre-vascularized dermis model for fast and functional anastomosis with host vasculature. Biomaterials 192:159-170.

Roggenkamp D, Köpnick S, Stäb F, Wenck H, Schmelz M, Neufang G, 2013. Epidermal nerve fibers modulate keratinocyte growth via neuropeptide signaling in an innervated skin modelJ Invest Dermatol. 133(6):1620-8.